1978

Prediction of turbulent jets and plumes in flowing ambients

Shinh-Sing Hwang
Iowa State University

INFORMATION TO USERS

This material was produced from a microfilm copy of the original document. While the most advanced technological means to photograph and reproduce this document have been used, the quality is heavily dependent upon the quality of the original submitted.

The following explanation of techniques is provided to help you understand markings or patterns which may appear on this reproduction.

1. The sign or "target" for pages apparently lacking from the document photographed is "Missing Page(s)". If it was possible to obtain the missing page(s) or section, they are spliced into the film along with adjacent pages. This may have necessitated cutting thru an image and duplicating adjacent pages to insure you complete continuity.

2. When an image on the film is obliterated with a large round black mark, it is an indication that the photographer suspected that the copy may have moved during exposure and thus cause a blurred image. You will find a good image of the page in the adjacent frame.

3. When a map, drawing or chart, etc., was part of the material being photographed the photographer followed a definite method in "sectioning" the material. It is customary to begin photoing at the upper left hand corner of a large sheet and to continue photoing from left to right in equal sections with a small overlap. If necessary, sectioning is continued again — beginning below the first row and continuing on until complete.

4. The majority of users indicate that the textual content is of greatest value, however, a somewhat higher quality reproduction could be made from "photographs" if essential to the understanding of the dissertation. Silver prints of "photographs" may be ordered at additional charge by writing the Order Department, giving the catalog number, title, author and specific pages you wish reproduced.

5. PLEASE NOTE: Some pages may have indistinct print. Filmed as received.

University Microfilms International
300 North Zeeb Road
Ann Arbor, Michigan 48106 USA
St. John's Road, Tyler's Green
High Wycombe, Bucks, England HP10 8HR

Prediction of turbulent jets and plumes in flowing ambients

by

Shinh-Sing Hwang

A Dissertation Submitted to the
Graduate Faculty in Partial Fulfillment of
The Requirements for the Degree of
DOCTOR OF PHILOSOPHY

Major: Mechanical Engineering

Approved:

Signature was redacted for privacy.

In Charge of Major Work

Signature was redacted for privacy.

For the Major Department

Signature was redacted for privacy.

For the Graduate College

Iowa State University
Ames, Iowa

1978

TABLE OF CONTENTS

LIST OF TABLES

LIST OF FIGURES

NOMENCLATURE

Latin Symbols

C_D drag coefficient, equal to 2.4 for all calculations in this study

c_p specific heat at constant pressure

D_{eff} effective diameter of jet, equal to twice $r_{1/2}$

d_o diameter of jet or plume at discharge

F velocity ratio function

Fr local Froude number, dimensionless

Fr_o discharge Froude number, $u_o^2/[g_n d_o(\rho_{\infty,o}-\rho_o)/\rho_o]$

F_D drag force caused by crossflow

$f(r)$ initial velocity distribution

$g(r)$ initial temperature distribution

g_n acceleration of gravity, 9.80665 m/s^2

G curvature Richardson number function

H_b buoyancy Richardson number function

k Thermal conductivity

ℓ mixing length

ℓ_o unmodified mixing length

m ratio of the jet discharge velocity u_o to the crossflow velocity u_∞

n total or effective kinematic viscosity

n_H total or effective thermal diffusivity

p corrected pressure

$\bar{p}$ space-averaged pressure over a cross section

p^* estimated pressure

p' pressure correction

Pr Prandtl number, ν/α

q heat flux due to molecular and turbulent transport

$\bar{R}$ raidus of curvature of jet centerline

Re_o Reynolds number at discharge, $u_o d_o/\nu$, dimensionless

Ri gradient Richardson number

Ri_b gradient Richardson number of buoyancy, $\beta_{th} g_n \frac{\partial t}{\partial r}/(\frac{\partial u}{\partial r})^2$

Ri_c gradient Richardson number of curvature, $2(U/\bar{R})/(\partial u/\partial r)$

r_o radius of jet or plume at discharge

s distance along jet or plume axis

S nondimensional axial distance, or the source term in three-dimensional jet

S_M width of the mixing layer in the initial region

Δs step size in the s-direction

t temperature

T nondimensional temperature, $(t-t_\infty)/(t_c-t_\infty)$

$\bar{T}$ stratification parameter, $(\rho_\infty-\rho_o)/[-r_o(d\rho_\infty/dz)]$

u s-component of time mean velocity

v r-component of time mean velocity

u,v,w velocity components in x-, y- and z-directions, respectively, in three-dimensional flow cases

$\vec{V}$ velocity vector, $u\vec{i} + v\vec{j} + w\vec{k}$

x,y,z Cartesian coordinates

U,V,W nondimensional velocity components of u,v,w

X,Y,Z nondimensional distance in x-, y- and z-directions respectively

y_o half-width of jet or plume at discharge in y-direction

z_o half-width of jet or plume at discharge in z-direction

z_M zero momentum height or maximum height of plume rise

Greek Symbols

α thermal diffusivity, $k/\rho c_p$

β_b, β_c constants in buoyancy and curvature effects

β_{th} isobaric volume expansivity, $-(\frac{1}{\rho})(\partial\rho/\partial t)_p$

γ_f intermittency function, see Equation (3.31)

δ mixing layer thickness

μ viscosity

ν kinematic viscosity, μ/ρ

ρ density

τ total or effective shear stress in s-momentum equation

θ angle between $\vec{i}_s$ and the horizontal

λ degree of ambient stratification, $-dt_\infty/dz$

Subscripts

c evaluated at jet centerline

p evaluated at constant pressure

e evaluated at outer edge of jet

1/2 evaluated at velocity half-width

max maximum value

min minimum value

o value at jet discharge

ref reference value

T turbulent flow quantity

∞ free stream or ambient value

$+$ used in special notation, $\Delta S_+ = (S_{i+1} - S_i)$

Superscripts

$()'$ fluctuating quantities

$\overline{()}$ time mean quantities

$(\rightarrow)$ vector quantities

$\tilde{()}$ space averages over flow cross section

I. INTRODUCTION

The problem of the turbulent jet or plume issuing into a flowing ambient has received considerable attention in recent years. The problem of reducing the pollution of the environment, including water bodies and the atmosphere, is still a serious concern to scientists, engineers and government administrators. This problem is of significance in several areas of engineering, such as cooling water discharged from power plants, gaseous jets from cooling towers or stacks (see Figure 1.1) and exhaust gas from combustion systems of aircraft or spacecraft. In the case of spacecraft, the plume discharges from the nozzles may cause heating and contamination problems for the external instrumentation.

Modern steam electric power plants have thermal efficiencies of 40% or less. Therefore, they waste large amounts of heat which is most conveniently discharged into an adjacent environment, a water body or the atmosphere. The addition of such heated discharges to the environment can cause chemical, biological and physical effects on animals and vegetation in the vicinity of the discharge. Thus, site selection for a power plant is important. A schematic diagram [1] of the cooling process of a power plant using a river as a heat sink is shown in Figure 1.2. Cooling water enters the power plant at temperature t_∞, through an intake structure and passes through the condensers, then returns at a temperature t_o to the receiving water. This is a typical open cycle system. The coolant stream undergoes a temperature rise of about 5° to 18° C depending on the amount of rejected heat and the flow rate of

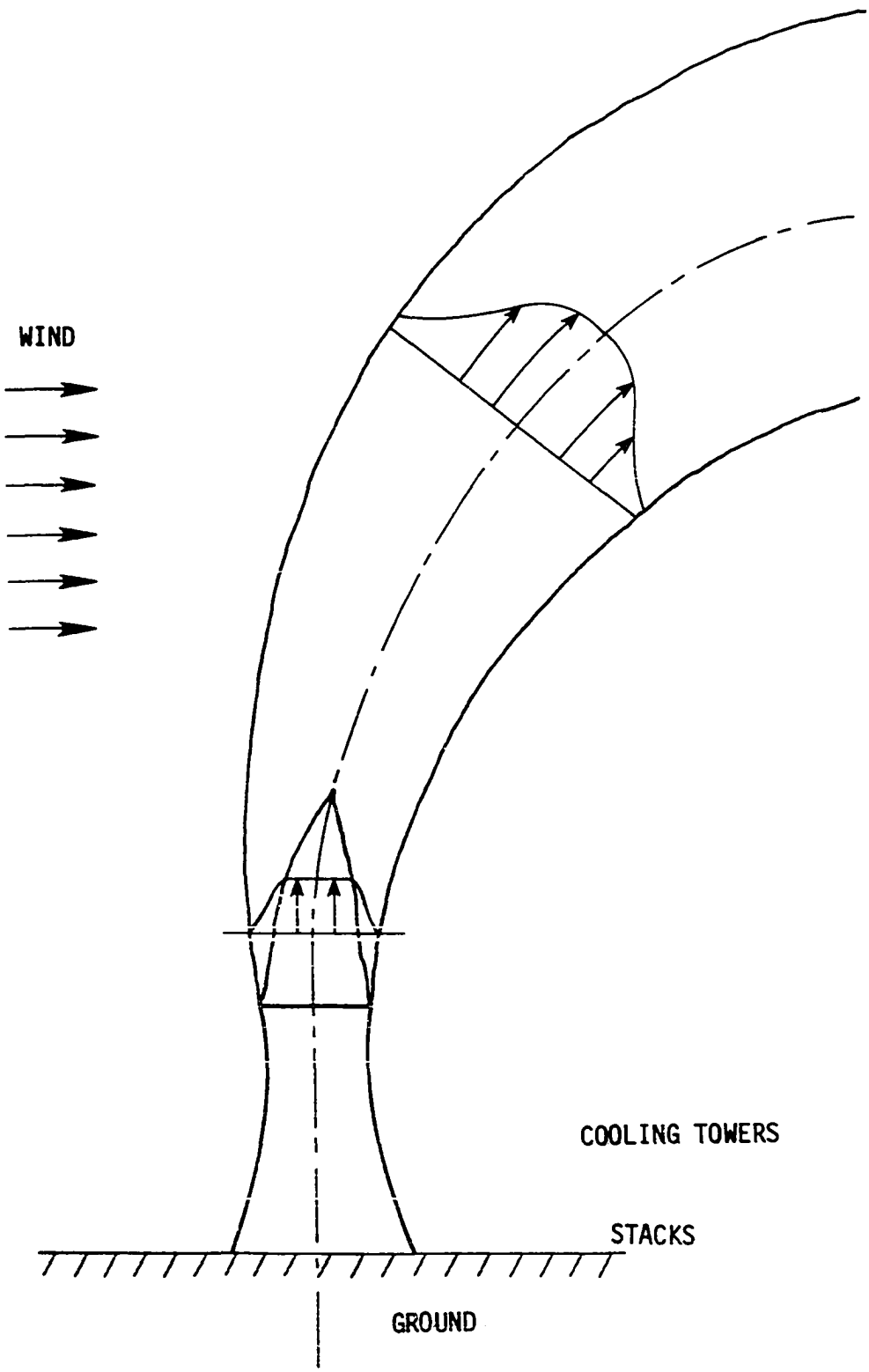

Fig. 1.1. Vertical jet from cooling towers or stacks.

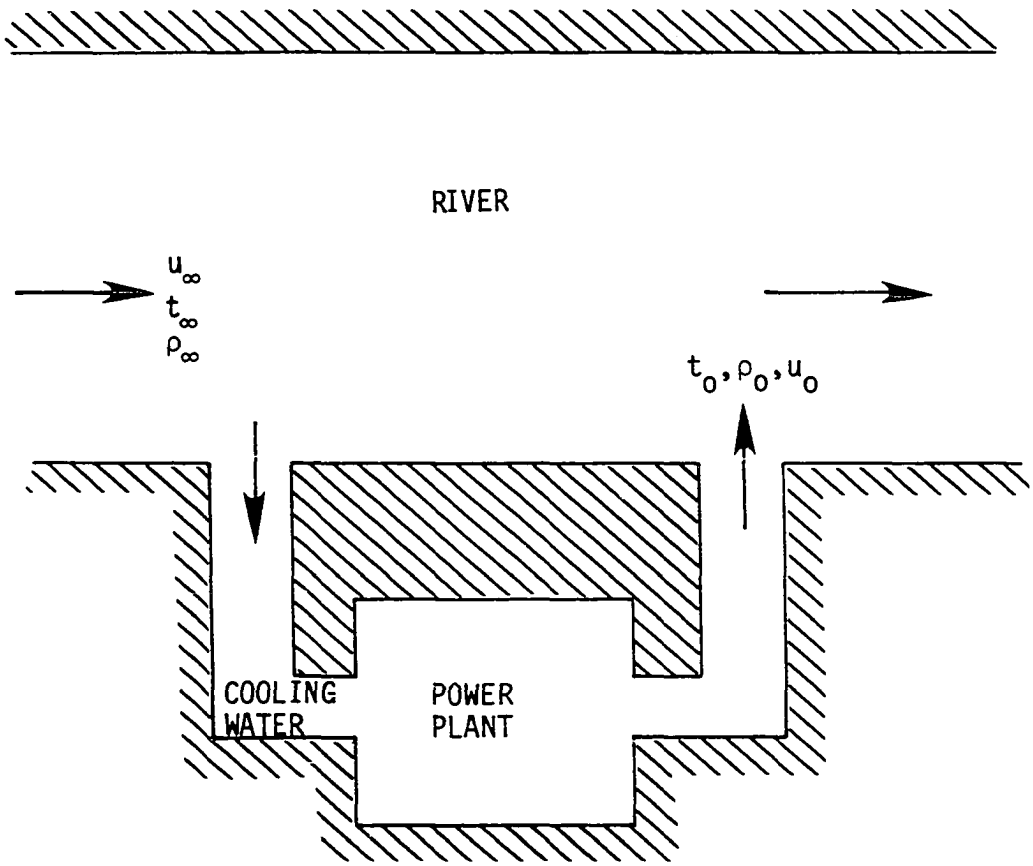

Fig. 1.2 Power plant site near a river.

cooling water.

Figure 1.3 shows a direct thermal cycle [2] of a working fluid, in this case water, in a power plant. The water receives heat from boiler and is converted into high-pressure steam which expands through the turbine to convert part of its thermal energy into electrical energy. The expanded steam from the turbine exhaust then goes through the condenser where it rejects heat to the cooling water and condenses into the liquid phase which is returned to the boiler. This forms a closed cycle. The cooling water receives heat in the condenser and then discharges into the receiving water body, such as a river or water pond.

There is general agreement that water temperature increases which are close to the sub-lethal range of impaired biological activity should be avoided. Indeed, the discharge of fluid wastes from submerged outlets as jets into the receiving fluid bodies is employed more and more commonly by industry as a technique to achieve the maximum amount of mixing or dilution within a minimum distance of travel. These temperature limits have a significant effect on power plant siting and discharge outfall design. If the ecological impact is not acceptable, either an alternative means such as cooling towers must be employed, or the site of the power plant must be changed.

In order to predict the ecological effects of such thermal additions on the environment, knowledge of the changes in physical conditions, such as the temperature and velocity fields caused by the thermal discharge, is required. Similarly, in order to control the pollution for

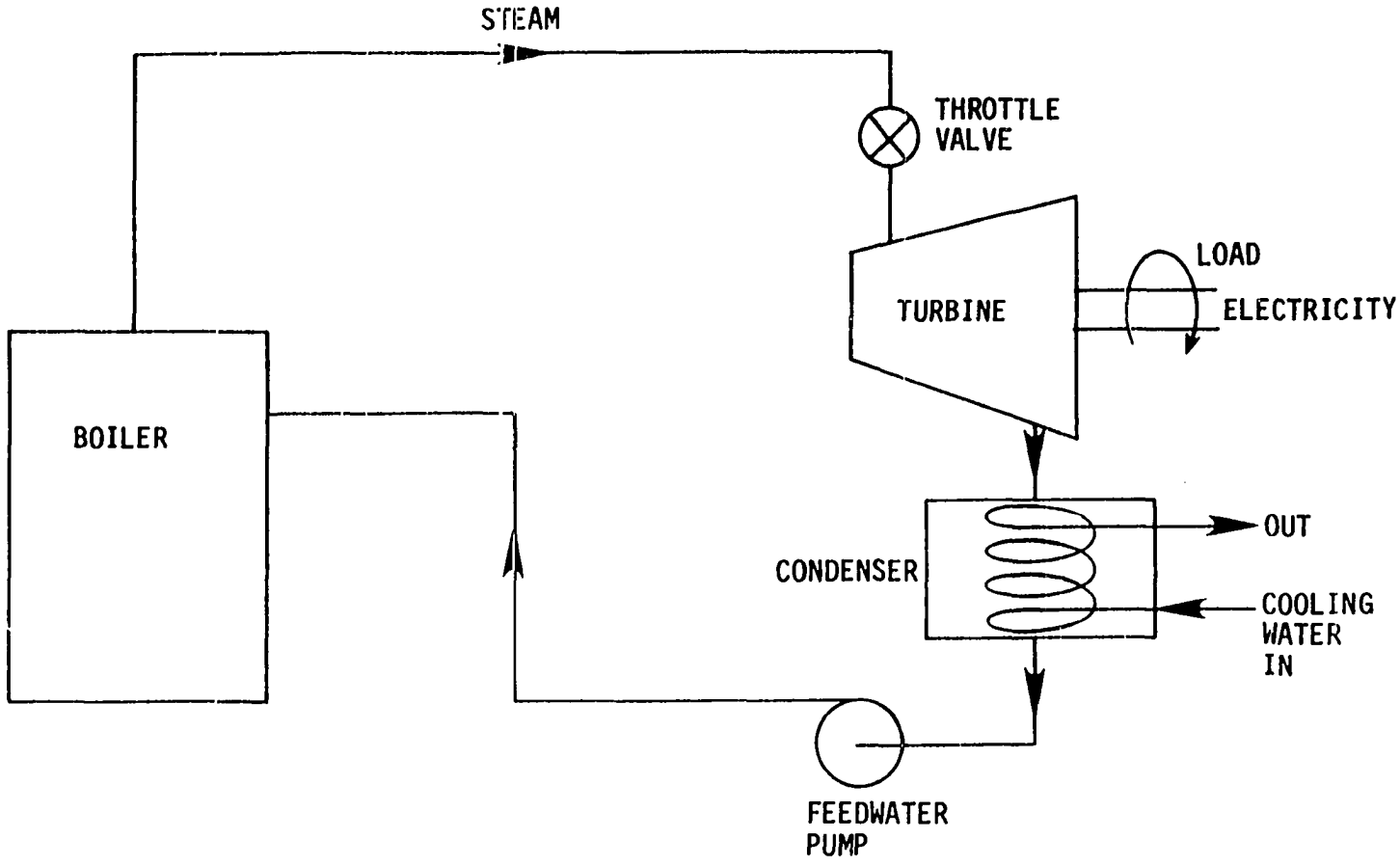

Fig. 1.3 Direct-cycle power plant.

ocean sewage outfalls, knowledge of the concentration and velocity fields caused by the discharge is required. Field studies and experimental work are other excellent ways to gain that knowledge, but mathematical modeling is also useful in making predictions for the discharge design process. It is believed that inexpensive analytical predeterminations of plume problems will be of great assistance in reducing the amount of expensive model testing that is often required for design and for satisfying environmental agency requirements. The present study deals with the prediction of these physical quantities through mathematical modeling [3].

II. BACKGROUND

A. General Information

Jet flows can be divided into several classes according to the trajectory of the jet centerline [4]: (a) straight line trajectories, (b) single plane trajectories, and (c) three-dimensional trajectories. Jet flows could also be classified as two-dimensional or three-dimensional according to the velocity components which are nonzero. A straight line jet discharging from a rectangular orifice will yield a three-dimensional flow even if the trajectory is straight.

The jet passes through several regimes as it moves from the outfall through the ambient. The three flow regimes commonly considered are shown in Figure 2.1.

(1) The initial region, or zone of flow establishment: In this region, the flow is dominated by the discharge conditions. A turbulent shear layer develops at the edge of the jet, and spreads both inward toward the jet centerline, and outward, causing the jet to grow. The axial distance from discharge to the point where mixing has reached the centerline is called starting length.

(2) Main region or zone of established flow: In this region the flow is fully turbulent. The jet is deflected and its motion is governed by its momentum and buoyancy and the free stream conditions, but not by the initial outfall conditions.

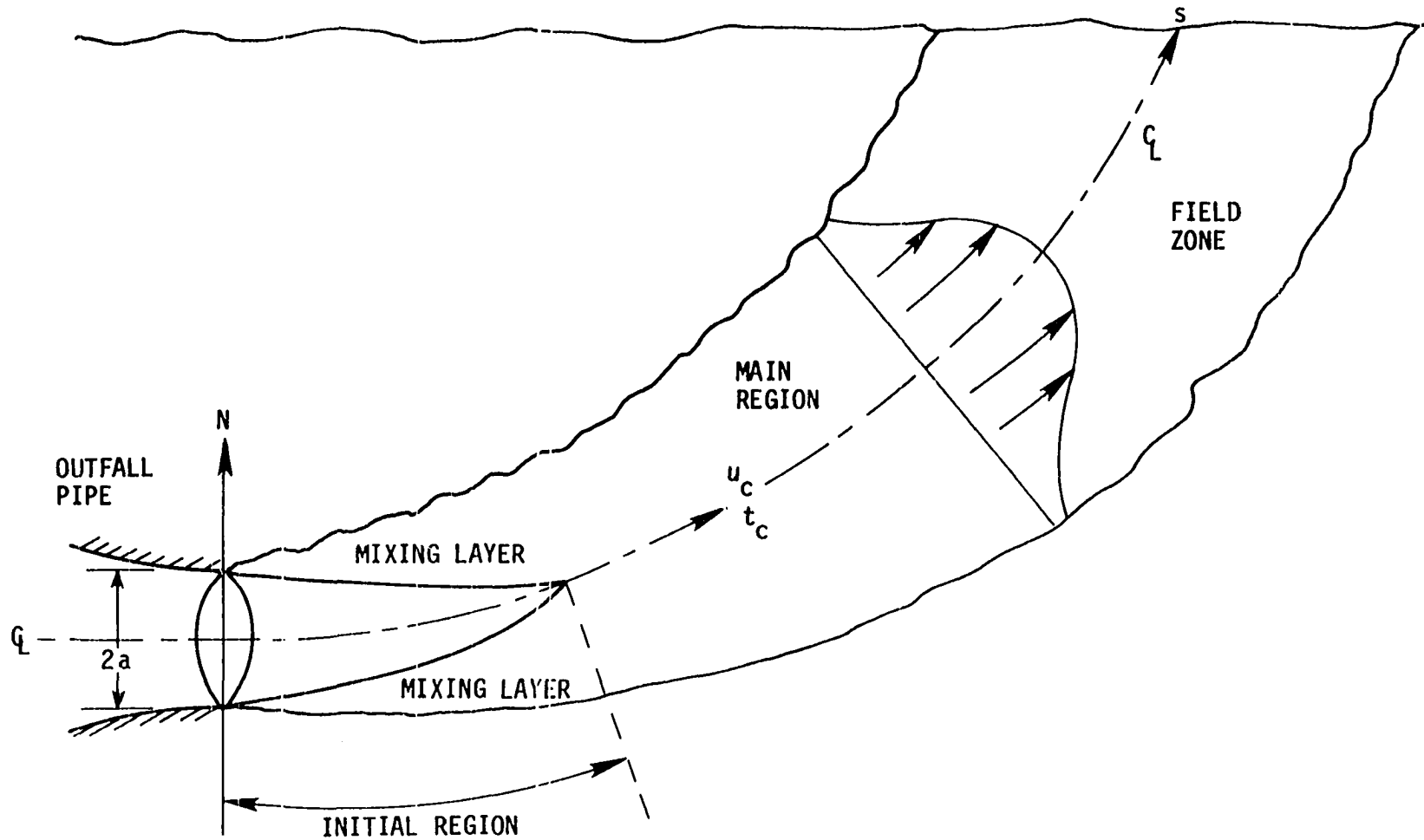

Fig. 2.1. Flow regimes for heated jets.

(3) Field zone or far field region: The jet momentum is depleted and the jet fluid is convected and diffused by the ambient currents and ambient turbulence.

The present analysis is concerned with the near field flow region--the first two regimes, since the jet turbulent mixing and temperature excesses in this region are significant.

B. Literature Survey

For a long period in past years, the prediction of turbulent jet flows was most commonly done by integral methods which utilized assumed velocity and temperature (or concentration) profiles based on similarity assumptions and entrainment approximations. In integral methods, the partial differential equations are then integrated over the whole cross section of jet and converted into a set of simpler ordinary differential equations. Hirst [4] and Schatzmann [5] more recently presented integral methods for jet flows of a fairly general nature.

In recent years, differential methods have become the center of interest for most researchers with the advent of the more advanced and faster digital computers. In differential methods, the partial differential equations of the flow are solved directly using a finite-difference technique without the assumption of profile similarity. Madni and Pletcher [3,6] present more details about differential methods applied to several classes of jet flows. There is an indication of the shift in emphasis from integral toward differential methods. However, the methods most commonly used for plume prediction in waterways, oceans

and the atmosphere, still tend to be integral in nature [4,7,8].

Nonvertical buoyant jets discharged to a uniform quiescent ambient have been studied experimentally by Abraham [9], Frankel and Cumming [10], Anwar [11] and Fan [12], and analytically by Hirst [4] and Madni [6]. Nonbuoyant jets discharged to a crossflow have been investigated experimentally by Gordier [13], Keffer and Baines [14], Pratte and Baines [15], Platten and Keffer [16], and analytically by Hirst [4], Fink [17] and Schatzmann [5]. Buoyant jets discharged vertically into a horizontal crossflow have been extensively studied experimentally by Fan [12], Briggs [18], Hoult et al. [19,20], Fan and Brooks [21], and theoretically by Hirst [4] and Schatzmann [5]. Shirazi and Davis [22] presented a discussion of this classification of submerged discharges. ccording to [22], buoyant submerged jets are classified by the ambient conditions as: (a) discharge into stagnant, nonstratified water, (b) discharge into stagnant, stratified water, (c) discharge into moving, nonstratified water, (d) discharge into moving, stratified water, and (e) vertical discharge into nonstratified, stagnant, shallow water.

For the buoyant jet discharging into a flowing ambient, a few sample calculations for this flow configuration have been reported whereby the Reynolds-averaged Navier-Stokes equations have been solved by finite-difference [23] or finite-element [24] technqiues using a simple algebraic turbulence model. These solutions require considerable computation time and understandably few comparisons have been made with experimental data to establish the validity of the turbulence models

employed for buoyant flows. McGuirk and Spalding [25] have employed a three-dimensional parabolic finite-difference scheme for pressure coupled equations [26] to predict the dispersion of buoyant jets for the special case of discharges into an initially coflowing stream.

A study has been underway in the Department of Mechanical Engineering at Iowa State University for the past several years to develop better methods for predicting thermal diffusion in turbulent jet flows characteristic of those occurring in natural waterways [3,6,27,28,29]. The predictions of these methods which include the initial region where similarity assumptions are definitely not valid, compare favorably with measurements made both in water [30,31] and in the atmosphere [32,33].

In summary, the finite-difference predictions of Madni [3] can be classified in three categories: (a) nonbuoyant jets in a coflowing or quiescent ambient, (b) buoyant vertical jets in a uniform or stratified ambient, (these two cases include only straight line trajectories), (c) horizontal or inclined buoyant jet in a quiescent ambient, (this deals with the curved trajectory caused by the buoyancy force only).

In the present study, it is proposed to extend the finite-difference approach already developed for two-dimensional flows by Madni and Pletcher [3,6,27,34] to include jets and plumes with curved trajectories caused especially by a crossflowing ambient. In this flow, the curvature effect is expected to be important in turbulent mixing.

C. Scope of Investigation

This research contributes to knowledge in the general area of turbulent shear flows as well as contributing to the development of needed prediction methods for applied configurations. The objective of the present investigation is to develop better methods of predicting the development of jets and thermal plumes under conditions which closely simulate the flows found in power plant applications. In the present study, effort was mainly concentrated on the analysis of jets discharged into a uniform or stratified ambient with crossflow. A surprisingly simple mathematical model was found to adequately account for the effect of the crossflow in the r-momentum equation. The curvature effect due to a crossflow on the turbulent mixing was the major development in the present turbulence modeling. The recent work of Trent and Welty [35] suggests that turbulence modeling is the main bottleneck to progress in plume predictions for the more complex configurations and the present study tends to support this view. In addition to the crossflow studies, many test cases were computed for jets in coflowing or quiescent ambients to establish the validity of the turbulence model and to evaluate its range of applicability. These same test cases served to establish the capabilities of the finite-difference method.

The applications of interest in the present study include the thermal plumes from cooling towers and stacks and cooling water discharges into cooling ponds and waterways. The same solution method is applicable to atmospheric discharges also by using the same computer

program with a slight adjustment. Actually, the present analysis can only provide an approximate, but hopefully reasonable, solution to these flows since the ambient flow will be assumed uniform in velocity and temperature which is never quite true in the practical applications. All of the comparisons in the present study are with laboratory rather than field data, not by choice so much as due to the general lack of availability of the latter. However, it is believed that the analysis and calculation procedure in the present study can provide a useful approximation to the true jet and plume flows found in cooling tower and waterway applications.

The procedure followed in the present study is to solve the governing partial differential equations by a finite-difference method, using a turbulence model to calculate the turbulent diffusivities for heat and momentum. The governing equations are of boundary layer form [26], if we assume:

(a) there exists a predominant direction of flow,

(b) the diffusion of momentum, heat and mass is negligible in that direction,

(c) the downstream pressure field has little influence on the upstream flow conditions.

In Chapter III, the basic differential equations governing the development of an axisymmetric buoyant jet in a crossflow are derived in a curvilinear coordinate system which moves with the jet centerline. Approximate initial and boundary conditions are established. Then, the equations are nondimensionalized, and formulated in finite-difference

form.

In Chapter IV the calculation procedure discussed in Chapter III is applied to axisymmetric jets in a coflowing or quiescent ambient. In Chapter V, it is applied to jets in a crossflow. Both chapters include cases of jets in uniform and stratified ambients. Comparisons are made with experimental data and other predictions.

In Chapter VI, the calculation is extended to solve three-dimensional jet problems by the alternating-direction implicit (ADI) finite-difference method. The solution procedure, based on the proposals by Patankar and Spalding [26] and Raithby [36], and modifications made by Zoby [37] and Briley [38], is presented in detail.

Chapter VII states conclusions and provides suggestions for future research.

Copies of computer programs and the printed results from the computer runs to be described in this study can be obtained through the Department of Mechanical Engineering at Iowa State University.

D. Summary of Preliminary Studies

Before an appropriate numerical method was chosen for the present investigation, several methods were tested to solve a simpler boundary layer flow problem. Comparisons were made regarding computer time, step size limitations, stability restrictions, accuracy of results, and convenience of programming. Those numerical methods considered were: the fully implicit method [39], Crank-Nicolson method [40], DuFort-Frankel method [41], alternating-direction explitic (ADE) method by

Saul'yev [42], ADE method by Barakat and Clark (including a modified version) [43] and an ADE method by Larkin [44].

Finally, the fully implicit method was chosen for the calculations of this study. The fully implicit method was not overwhelmingly superior to any of the others but seemed to offer a good compromise between accuracy and convenience. The explanation and finite-difference formulation of these methods are given in Appendix A.

III. ANALYSIS FOR AXISYMMETRIC FLOWS

Figure 3.1 shows the flow configuration and the curvilinear coordinate system used for the analysis of the turbulent jet discharging at an angle θ_o to the horizontal. The ambient is assumed to be uniform in temperature or stratified as characterized by the stratification parameter $\overline{T}$ and flowing with a uniform velocity u_∞ in the x-direction. Although the actual flow conditions do not require that the jet be precisely axisymmetric about the centerline, this assumption, which greatly simplifies the analysis, is used in the present study except as described in Chapter VI. This axisymmetric flow model was observed to be useful for the simpler case of the jet discharging to a quiescent ambient [6] and the merits of the model were thought worth exploring for the present flow configuration before turning to a fully three-dimensional analysis with the associated uncertainties concerning turbulence modeling and with a substantial increase in required computer time.

The flowing ambient will be assumed infinite in extent which precludes the prediction of interactions with a free surface.

A. The Governing Equations

The development of the jet or plume as it moves through the ambient is governed by equations which require the conservation of mass, momentum (one equation for each coordinate direction), energy and perhaps other scalar components (such as salt). These six equations are sufficient to solve for the six unknowns, pressure, three velocity components,

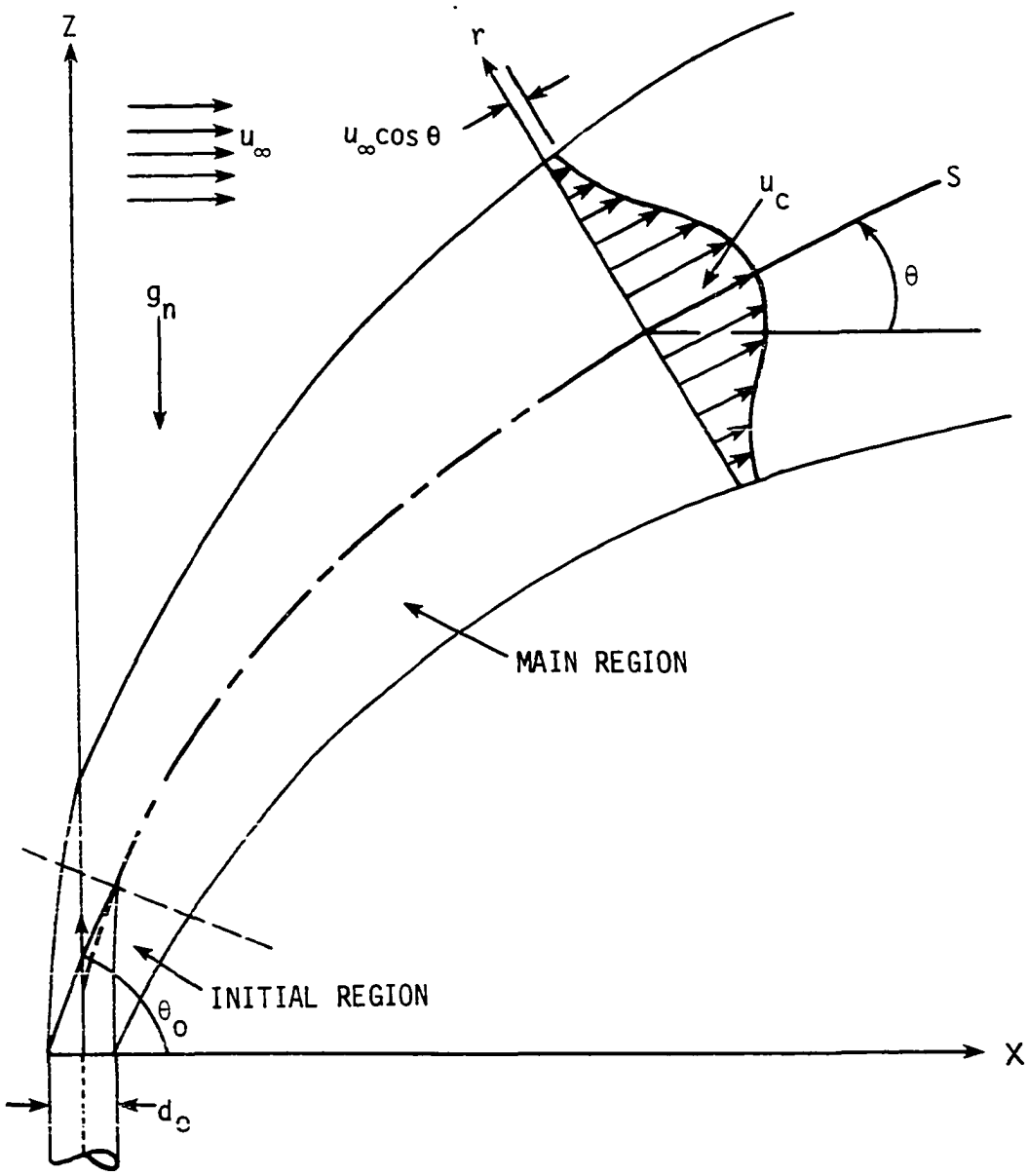

Fig. 3.1. Flow configuration for a buoyant jet into a crossflow.

temperature, and salinity (if considered).

In the present study, the pressure variation is assumed to be purely hydrostatic and will be considered negligible. The flow is assumed to be axisymmetric, and the governing equations can be reduced in accordance with boundary layer assumptions, so only four parameters, namely u, v, θ and t, are of interest along with four basic governing equations; these are s-momentum, r-momentum, continuity and energy equations.

Generally, the fluid was assumed incompressible with density variations accounted for only in the buoyancy force term (Boussinesq approximation). The only exception to this will occur in Chapter 4, Section C, where results of a variable property analysis will be presented.

Viscous dissipation is neglected in the energy equation and the thin shear layer (boundary layer) assumptions have been used to eliminate the second derivatives with respect to the s-direction (see Figure 3.1) from the s-momentum and energy equations. Viscous terms have been neglected entirely in the transverse direction because of the boundary layer assumptions. The resulting equation is a force balance on a stream tube being deflected by the resultant component in the transverse direction of the buoyancy force and the effective drag caused by the crossflowing stream.

This flow model is similar to that used in [6] except for the addition here of the effects of crossflow. More details on the derivation of the equations in the curvilinear coordinate system for the jets in a

coflowing or quiescent ambient can be found in [6] or in Appendix B of [3]. The effective drag force in the transverse direction results from a complex pressure distribution about and within the jet and is being modeled by analogy with a cylinder in crossflow using the component of the crossflow velocity in the r-direction to evaluate the drag force according to

$$F_D = C_D \rho_\infty (u_\infty \sin\theta)^2 \frac{2}{\pi D_{eff}} \tag{3.1}$$

where $C_D = 2.4$ and $D_{eff} = 2\, r_{1/2}$.

With these assumptions, the conservation equations become:

Continuity:

$$\frac{\partial(ru)}{\partial s} + \frac{\partial(rv)}{\partial r} = 0 \tag{3.2}$$

s-momentum:

$$u \frac{\partial u}{\partial s} + v \frac{\partial u}{\partial r} = \frac{1}{\rho_o r} \frac{\partial}{\partial r}(r\tau_s) + \frac{\rho_\infty - \rho}{\rho_o} g_n \sin\theta \tag{3.3}$$

r-momentum:

$$\underbrace{u^2 \frac{d\theta}{ds}} = -C_D (u_\infty \sin\theta)^2 \frac{2}{\pi D_{eff}} \frac{\rho_\infty}{\rho_o} + \underbrace{\frac{\rho_\infty - \rho}{\rho_o}} g_n \cos\theta \tag{3.4}$$

Energy:

$$u \frac{\partial t}{\partial s} + v \frac{\partial t}{\partial r} = \frac{1}{\rho_o c_p r} \frac{\partial}{\partial r}(-rq) \tag{3.5}$$

The terms $\frac{(\rho_\infty - \rho)}{\rho_o} g_n \sin\theta$ and $\frac{(\rho_\infty - \rho)}{\rho_o} g_n \cos\theta$ represent components of the buoyancy force which are generated due to density

differences with the ambient.

An equation for salinity (or concentration) is similar to Equation (3.5). In fact, in a suitable nondimensional form, the equations are identical such that for a uniform ambient (and assuming $Sc_T \simeq 0.7$) a solution to Equation (3.5) can be used to predict the decay of non-dimensional species concentration, also.

The shear stress τ_s in Equation (3.3) includes the viscous and the apparent turbulent contributions [45], thus,

$$\tau_s = \rho\nu \frac{\partial u}{\partial r} - \rho\overline{u'v'} \tag{3.6}$$

Similarly, the heat flux q in the energy equation is due to both molecular and turbulent action. So,

$$q = -k \frac{\partial t}{\partial r} + \rho c_p \overline{v't'} \tag{3.7}$$

In turbulent flow, the number of unknowns usually exceeds the number of independent equations so an additional relationship is required to achieve closure of the mathematical formulation. A turbulence model is provided to play this role.

Assuming a linear equation of state for ρ, the buoyancy terms can be derived and related to the temperature of the fluid through

$$\frac{\rho_\infty - \rho}{\rho_o} = \beta_{th}(t - t_\infty) \tag{3.8}$$

where β_{th}, the isobaric volume expansivity of the fluid, is defined as

$$\beta_{th} = -\frac{1}{\rho_{ref}}\left(\frac{\partial \rho}{\partial t}\right)_p \tag{3.9}$$

Since Equations (3.2) through (3.5) give rise to a parabolic system, marching finite-difference techniques can be applied. The calculation starts at the discharge and is marched in the downstream direction of the jet.

These equations are first order in s, so initial distributions of u, t and θ must be provided at a starting value of s,

$$u(s_o,r) = f(r),\ t(s_o,r) = g(r),\ \theta(s_o) = \theta_o \tag{3.10}$$

Appropriate boundary conditions for Equations (3.2) to (3.5) are

$$\begin{aligned} &\frac{\partial u}{\partial r}(s,o) = \frac{\partial t}{\partial r}(s,o) = 0 \\ &v(s,o) = 0 \\ &\lim_{r\to\infty} u(s,r) = u_\infty \cos\theta \\ &\lim_{r\to\infty} t(s,r) = t_\infty \end{aligned} \tag{3.11}$$

Here, u and t each requires two boundary conditions, while only one is required for v. The initial v's can be computed from the continuity equation. For convenience, initial v's were set equal to zero.

B. Turbulence Model

The Boussinesq concept of apparent turbulent viscosity is used to evaluate τ_s as

$$\tau_s = \rho(\nu+\nu_T)\frac{\partial u}{\partial r} = \rho n \frac{\partial u}{\partial r} \tag{3.12}$$

where ν_T is the turbulent viscosity, and n is the total of effective viscosity. It was assumed that the turbulent diffusivities for heat and momentum are related through

$$\alpha_T = \frac{\nu_T}{Pr_T} \tag{3.13}$$

by the Reynolds analysis where Pr_T is the turbulent Prandtl number which was set equal to a constant value of 0.7 for the calculations in this study, and α_T is the turbulent diffusivity for heat. The heat flux, q, can be expressed as

$$q = -\rho c_p(\alpha + \frac{\nu_T}{Pr_T})\frac{\partial t}{\partial r} = -\rho c_p n_H \frac{\partial t}{\partial r} \tag{3.14}$$

where n_H is the effective thermal diffusivity.

Making use of Prandtl's mixing length hypothesis [46] for the turbulent exchange, the Reynolds' stress term in the momentum equation was evaluated as:

$$-\rho\overline{u'v'} = \rho\ell^2\left|\frac{\partial u}{\partial r}\right|\frac{\partial u}{\partial r} = \rho\nu_T\frac{\partial u}{\partial r}\,, \tag{3.15}$$

where ℓ is the "mixing length", determined by the geometry of the flow system.

This simple mixing length model has some disadvantages [47]. One major shortcoming is the prediction of zero viscosity and thermal diffusivity whenever $\partial u/\partial r = 0$. This would suggest that μ_T and k_T would be zero at the centerline of a pipe, in regions near the mixing of a wall jet with a main stream, and in flow through an annulus or between parallel plates where one wall is heated and the other cooled. Measurements indicate that μ_T and k_T are not zero in these cases. However, for flow such as wall boundary layers in the absence of any unusual geometric or boundary conditions, the simple mixing length model will yield predictions as good as those from the one-equation model and with the use of less computer time. The turbulence model used for the present calculations was based on Equation (3.15), but included some modifications to compensate for the shortcomings of the simple mixing length model for buoyant flows following curved trajectories.

In the previous studies by Madni [6] on the prediction of heated jet discharged horizontally into a quiescent ambient, good predictions for the jet trajectory were noted using the same base-line turbulent model that worked well for nonbuoyant jets. However, the centerline temperature decay was somewhat underpredicted. The influence of buoyancy on mixing was then considered and the mixing length was modified to account for this effect. A good discussion of buoyancy effects on turbulent mixing was presented in [48] by Bradshaw.

The velocity and temperature distributions predicted by Madni were improved by employing the empirical Keyps [49] formula to augment the

effective mixing length due to the effects of buoyancy on the turbulent viscosity. A similar pattern has been observed in the present study with regards to the effects of streamline curvature caused by pressure forces on the effective viscosity in the absence of buoyancy. So, corrections to the effective viscosity are being suggested for the effects of curvature as well as buoyancy. Trajectories can be predicted reasonably accurately without considering the curvature corrections. However, with curvature corrections, the results were improved significantly for profile related parameters such as the decay of centerline temperature and velocity.

The present turbulence model includes both a buoyancy Richardson number function (H_b) and curvature effect (G) due to pressure force from crossflowing ambient. In the initial region, the turbulent viscosity ν_T is calculated as

$$\nu_T = \ell_o^2 \left|\frac{\partial u}{\partial r}\right| H_b G \tag{3.16}$$

where $\ell_o = 0.0762\ S_M$, and S_M is the width of the mixing layer in the initial region.

The effects of buoyancy on the turbulent viscosity are treated through a gradient Richardson number function which is of the same form as Madni [6] used:

$$H_b = (1-\beta_b Ri_b \cos\theta)^{0.5} \tag{3.17}$$

where Ri_b is evaluated on a global basis:

$$Ri_b = \beta_{th} g_n \frac{(t_\infty - t_c)}{(u_c - u_e)^2} S_M \tag{3.18}$$

where β_{th} is the volumetric expansion coefficient, g_n is the acceleration of gravity, with a value of 9.80665 m/s^2.

To account for the effects of pressure induced curvature on the mixing, the following function was found to work well for jets discharging into a flowing ambient.

$$G = (1-\beta_c Ri_c) \tag{3.19}$$

Here G was assumed to be a simple linear function of the gradient curvature Richardson number, and β_c is a constant.

The curvature Richardson number in the present study was evaluated as

$$Ri_c = 2u_c S_M \frac{d\theta}{ds}/(u_c - u_e) \tag{3.20}$$

where $d\theta/ds$ can be recognized as the radius of curvature of the jet centerline and $(u_c-u_e)/S_M$ is a global representation for $\partial u/\partial r$. This equation was derived from

$$Ri_c = 2(U/\bar{R})/(\partial U/\partial r) \tag{3.21}$$

which has been studied and discussed in [50,51].

From Equation (3.21), $\bar{R}$, the radius of curvature, is computed from

$$\frac{1}{\bar{R}} = \frac{d\theta}{ds} \tag{3.22}$$

and

$$\frac{\partial u}{\partial r} = \frac{u_c - u_e}{r_c - r_e} = \frac{u_c - u_e}{S_M} \tag{3.23}$$

Combining Equations (3.22) and (3.23) into Equation (3.21), Equation (3.20) can be derived.

The values of the constants β_b and β_c used for the present calculations are as follows:

β_b = 18 in all calculations

β_c = 1.2 in initial region

= 8.0 in main region

The H_b and G functions represent the influence of buoyancy and pressure forces on the effective turbulent viscosity and thus would represent the influence on the square of the mixing length, i.e.,

$$H_b G = \ell^2/\ell_o^2 \tag{3.24}$$

where ℓ_o is the mixing length without buoyancy and curvature effects and ℓ is the modified mixing length.

The model for the curvature effect due to the crossflow used in the present analysis is one of the major features in this study. If H_b is set equal to one in Equation (3.24), then it follows that

$$\ell^2/\ell_o^2 = G$$

or

$$\ell = \ell_o (G)^{0.5} \tag{3.25}$$

The modified mixing length ℓ is computed from the original mixing length ℓ_o by multiplying a correction factor (CF),

$$\ell = \ell_o \times (CF) \tag{3.26}$$

Comparing Equations (3.25) and (3.26), the correction factor is:

$$CF = (G)^{0.5}$$
$$= (1-\beta_c Ri)^{0.5} \tag{3.27}$$

for the present analysis when neglecting the buoyancy effect ($H_b = 1$).

Two other well-known empirical models are presented here for comparison. The Monin-Oboukhov formula for the modification of the apparent mixing length is given in [49] as

$$\frac{\ell}{\ell_o} = (1-\beta' Ri) \tag{3.28}$$

This gives CF = (1-β' Ri). Where β' is a constant with values from 4.5 to 7 [50] depending on whether the flow conditions are stable or unstable. This formula is valid only for small Richardson numbers. For larger negative Ri, particularly in the range $-0.5 < Ri < 0$, the Keyps formula [49] is commonly used instead of the Monin-Oboukhov formula,

$$\frac{\ell}{\ell_o} = (1-18\ R_i)^{0.25} \tag{3.29}$$

In the present study, negative curvature Richardson numbers as large as 1.8 in magnitude were observed and the Keyps formula seemed to be inadequate for our calculations when Ri exceeded about 0.5 in magnitude. Figure 3.2 shows a comparison of the CF values for negative

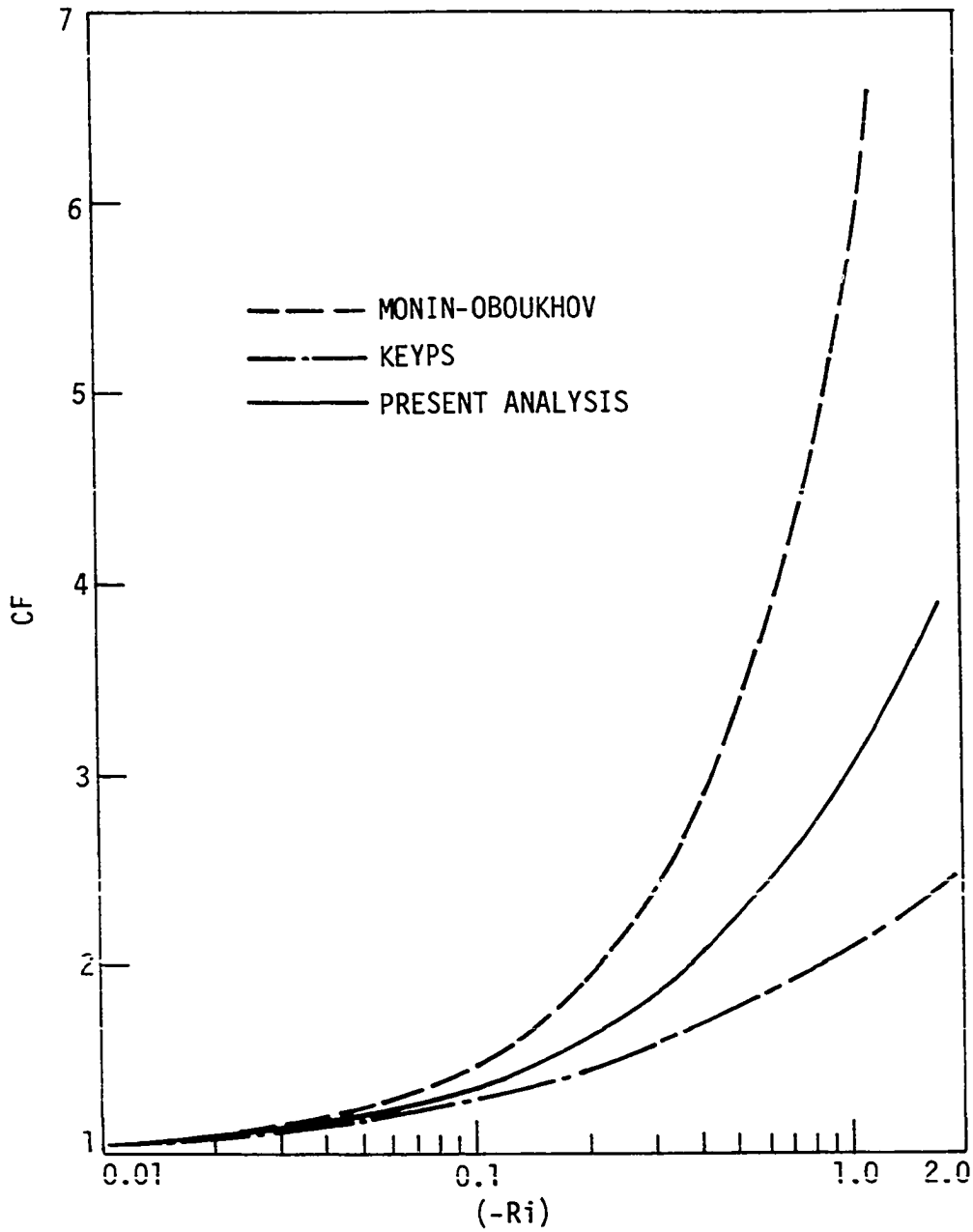

Fig. 3.2. Comparison of the correction factors for three models.

Richardson numbers from 0 to -1.8 for these three models, i.e.,

(a) Monin-Oboukhov formula

$CF = (1-\beta' Ri)$ using $\beta' = 4.5$ which gives the best results for this comparison,

(b) Keyps model

$$CF = (1-18\ Ri)^{0.25}$$

(c) Present model

$$CF = (1-8\ Ri)^{0.5}$$

From Figure 3.2, it can be seen that the CF values computed from these three formulae are very close for very low Richardson number (for $|Ri| < 0.1$). For negative Ri values between 0.1 and 0.5 in magnitude, model (a) is no longer valid, while the present model, model (c), gives CF values from 4% to 25% higher than the Keyps model which is commonly used for Ri in this range. When negative Ri becomes larger in magnitude than 0.5, model (c) still works well. The present correlation formula, which gives corrections intermediate in magnitude to those of the Monin-Oboukhov and Keyps correlations, appears to provide the needed level of correction for Ri large in magnitude and yet reduces values in line with the accepted Monin-Oboukhov correlation for small negative Ri.

The H_b and G functions were used to modify algebraic turbulence models of the same type as used previously for nonbuoyant jets following straight-line trajectories [27,34]. In the initial mixing region, the turbulence model used was

$$\nu_T = \ell_o^2 \left|\frac{\partial u}{\partial r}\right| H_b G \tag{3.30}$$

where $\ell_o = 0.0762\ S_M$.

After mixing penetrated to the jet centerline, i.e., in the main region, the viscosity was evaluated as

$$\nu_T = \gamma_f\ F\ r_{1/2}(u_{max}-u_{min})H_b G \tag{3.31}$$

where γ_f is the intermittency function given by Madni and Pletcher [30] as

$$\begin{aligned} \gamma_f &= 1.0 \qquad 0 \leq \frac{r}{r_{1/2}} \leq 0.8 \\ \gamma_f &= (0.5)^c \quad \frac{r}{r_{1/2}} > 0.8 \quad \text{where } c = \left(\frac{r}{r_{1/2}} - 0.8\right)^{2.5} \end{aligned} \tag{3.32}$$

This intermittency function was introduced to account for the fact that, from the measurements, the turbulent viscosity has an intermittent character near the outer edge of the mixing layer, rather than a constant value. F is the velocity ratio function [27] which was developed from the concept that the mixing of a jet with a flowing ambient must be influenced by the eddy motion characteristic of this ambient. It is assumed that, the greater the velocity ratio (the ratio of stream velocity to jet velocity), the more important this effect would be in the mixing. The following function was suggested [27],

$$F = 0.0246\ (1 + 2.13/m^2) \tag{3.33}$$

The suitability of the H_b function has been demonstrated in

previous work for buoyant jet discharged to quiescent ambients [6].

C. Nondimensional Forms

By using the nondimensional parameters for the governing equations, the variables were nondimensionalized as follows:

$$U = \frac{u}{u_o}, \quad V = \frac{v}{u_o}, \quad T = \frac{t-t_{\infty,o}}{t_o-t_{\infty,o}}$$

$$S = \frac{su_o}{\nu}, \quad R = \frac{ru_o}{\nu}, \tag{3.34}$$

$$N = \frac{n}{\nu}, \quad N_H = \frac{n_H}{\nu}$$

Here, $t_{\infty,o} = t_\infty$ except in stratified ambient where t_∞ is not a constant.

After nondimensionalizing, Equations (3.2) through (3.5) can be rewritten as follows:

Continuity:

$$\frac{\partial(UR)}{\partial S} + \frac{\partial(VR)}{\partial R} = 0 \tag{3.35}$$

s-momentum:

$$U\frac{\partial U}{\partial S} + V\frac{\partial U}{\partial R} = \frac{1}{R}\frac{\partial}{\partial R}(RN\frac{\partial U}{\partial R}) + \frac{\sin\theta}{Re_o Fr_o}(T-T_\infty) \tag{3.36}$$

r-momentum:

$$U\frac{2d\theta}{dS} = -C_D(U_\infty \sin\theta)^2 \frac{2}{\pi D_{eff}}[1-\beta_{th}(T_\infty-T_o)(t_o-t_{\infty,o})] + \frac{\cos\theta}{Re_o Fr_o}(T-T_\infty) \tag{3.37}$$

Energy:

$$U \frac{\partial T}{\partial S} + V \frac{\partial T}{\partial R} = \frac{1}{R} \frac{\partial}{\partial R}(RN_H \frac{\partial T}{\partial R}) \tag{3.38}$$

where

$$Re_o = \frac{u_o d_o}{\nu}$$

and

$$Fr_o = \frac{u_o^2}{d_o g_n \beta_{th}(t_o - t_{\infty,o})}$$

Details on the derivation of these nondimensional forms are given in Appendix B. In Equation (3.37), $(t_o - t_{\infty,o})$ is a constant and $\beta_{th}(t_o - t_{\infty,o})$ is a nondimensional parameter, for simplicity, it is not nondimensionalized individually.

In the stratified ambient cases,

$$T_\infty = \frac{-\lambda \ d_o}{Re_o(t_o - t_{\infty,o})} Z \tag{3.39}$$

where $\lambda = -\frac{dt_\infty}{dz}$, is the ambient temperature stratification, and Z is the nondimensional vertical height.

D. Finite-Difference Formulation

By applying a finite-difference method to the set of Equations (3.35) to (3.38), systems of algebraic equations for the unknowns at each discrete grid point were formulated. The systems of algebraic equations are suitable for high-speed computer solution.

Taylor series expansions were used to obtain finite-difference

approximations for the derivatives. For example, to obtain the finite-difference form for the derivative $(\frac{\partial u}{\partial s})_{i,j}$, as a forward difference, a Taylor series expansion for $u(s_o+\Delta s,r_o)$ about (s_o,r_o) should be employed,

$$u(s_o+\Delta s,r_o) = u(s_o,r_o) + (\frac{\partial u}{\partial s})_{s_o,r_o} \Delta s + (\frac{\partial^2 u}{\partial s^2})_{s_o,r_o} \frac{(\Delta s)^2}{2!} + (\frac{\partial^3 u}{\partial s^3})_{s_o,r_o} \frac{(\Delta s)^3}{3!} + \ldots \quad (3.40)$$

Thus, the forward difference is formed for

$$(\frac{\partial u}{\partial s})_{s_o,r_o} = \frac{u(s_o+\Delta s,r_o)-u(s_o,r_o)}{\Delta s} - (\frac{\partial^2 u}{\partial s^2})_{s_o,r_o} \frac{\Delta s}{2!} - (\frac{\partial^3 u}{\partial s^3})_{s_o,r_o} \frac{(\Delta s)^2}{3!} - O[(\Delta s)^3] \quad (3.41)$$

Switching to the (i,j) notation, and neglecting the higher order terms,

$$(\frac{\partial u}{\partial s})_{i,j} = \frac{u_{i+1,j}-u_{i,j}}{\Delta s} - O[\Delta s] \quad (3.42)$$

Here, $O[\Delta s]$, the truncation error, is of the order of Δs, using the O notation for brevity. In this example, the truncation error is first-order, so the finite-difference formulation in Equation (3.42) is said to be a first-order approximation. More details on truncation errors for finite-difference equations can be found in [52].

The fully implicit formulations of nondimensionalized Equations (3.35) to (3.38) are:

$$\frac{R_{j-1}+R_j}{4(\Delta S_+)}[U_{j-1}^{i+1} + U_j^{i+1} - U_{j-1}^{i} - U_j^{i}] + \frac{(R_j V_j^{i+1} - R_{j-1} V_{j-1}^{i+1})}{\Delta R} = 0 \qquad (3.43)$$

$$\frac{U_j^i}{\Delta S_+}(U_j^{i+1}-U_j^i) + \frac{V_j^i}{2\Delta R}(U_{j+1}^{i+1} - U_{j-1}^{i+1})$$

$$= \frac{1}{4R_j(\Delta R)^2}[(R_{j+1}+R_j)(N_{j+1}^i+N_j^i)(U_{j+1}^{i+1} - U_j^{i+1})$$

$$- (R_j + R_{j-1})(N_j^i + N_{j-1}^i)(U_j^{i+1} - U_{j-1}^{i+1})]$$

$$+ \frac{\sin(\theta^i)}{Re_o Fr_o}(T_j^i - T_\infty^i) \qquad (3.44)$$

Here, the values at the previous step (i) were used to evaluate the viscosity N and the coefficients of the convective terms, u and v, in s-momentum equation.

$$\frac{(U_j^i)^2}{\Delta S_+}(\theta^{i+1}-\theta^i) = \frac{\cos(\theta^i)}{Re_c Fr_c}(T_j^i - T_\infty^i)$$

$$-C_D[U_\infty^i \sin(\theta^i)]^2 \frac{2}{\pi D_{eff}^i}[1-\beta_j^i(T_\infty^i - T_o)Tc_2] \qquad (3.45)$$

where $Tc_2 = t_o - t_{\infty,o}$ before nondimensionalization, so, $\beta_j^i Tc_2$ is nondimensional.

$$\frac{U_j^i}{\Delta S_+}(T_j^{i+1} - T_j^i) + \frac{V_j^i}{2\Delta R}(T_{j+1}^{i+1} - T_{j-1}^{i+1})$$

$$= \frac{1}{4R_j(\Delta R)^2}[(R_{j+1} + R_j)(N_{H_{j+1}}^i + N_{H_j}^i)(T_{j+1}^{i+1} - T_j^{i+1})$$

$$- (R_j + R_{j-1})(N_{H_j}^i + N_{H_{j-1}}^i)(T_j^{i+1} - T_{j-1}^{i+1})] \qquad (3.46)$$

E. Solution Method

A fully implicit finite difference scheme was used to solve the conservation equations which are parabolic in character, thus permitting the solution to be marched in the s-direction. The marching started with an initial distributions of velocity and temperature and an initial flow angle. The new streamwise step size Δs_+ was first established. This step size was usually set as ten percent of the local width of the jet although steps as large as fifty percent of the local width appear possible according to tests to date. Most calculations were made by dividing the discharge radius into twenty increments although more increments were used for sample cases to verify convergence of the procedure.

The s-momentum equation was then solved to obtain the u velocity distribution at i+1st station. After each streamwise step, the r-momentum equation was solved for the new flow angle θ_{i+1}. Here the flow angle is the angle between the jet centerline and the horizontal. Then, the transverse velocity $v_{i+1,j}$ and temperature distribution at new

station were calculated from the continuity and energy equations respectively. Finally, the viscosity and thermal diffusivity were computed by using the new data just calculated, such as $u_{i+1,j}$ and θ_{i+1}.

Many implicit formulations of partial differential equations for initial value problems result in systems of simultaneous algebraic equations which have a tri-diagonal matrix of coefficients. The equations are of the form:

$$b u_{j-1}^{n+1} + d u_j^{n+1} + a u_{j+1}^{n+1} = c \tag{3.47}$$

Where b, d and a are coefficients, and c is a known source term.

Because of the boundary conditions, the first and the last equations each has two unknowns, while the others in the systems have three unknowns. All known u's are merged into the c term. In a matrix form, the systems of equations look like

$$\begin{bmatrix} d_1 & a_1 & 0 & 0 & \cdots & 0 & 0 \\ b_2 & d_2 & a_2 & 0 & \cdots & 0 & 0 \\ 0 & b_3 & d_3 & a_3 & \cdots & 0 & 0 \\ & \cdots & \cdots & \cdots & \cdots & \cdots & \\ 0 & 0 & 0 & 0 & \cdots & b_m & d_m \end{bmatrix} \begin{bmatrix} u_1^{n+1} \\ u_2^{n+1} \\ u_3^{n+1} \\ \\ u_m^{n+1} \end{bmatrix} = \begin{bmatrix} c_1 \\ c_2 \\ c_3 \\ \cdot \\ \cdot \\ \cdot \\ c_m \end{bmatrix} \tag{3.48}$$

The Thomas algorithm [53] provides a very efficient procedure for evaluating the unknowns.

Referring to the tri-diagonal matrix algorithm (TDMA), the system is put into an upper triangular form [54] by computing the new d_i by

$$d_i' = d_i - (b_i/d_{i-1})a_{i-1}, \quad i = 2,3,\ldots m$$

then, (3.49)

$$c_i' = c_i - (b_i/d_{i-1})c_{i-1}, \quad i = 2,3,\ldots m$$

then computing the unknowns from back substitution [52,55].

$$u_m = c_m'/d_m' \tag{3.50}$$

then

$$u_j = \frac{c_j' - a_j u_{j+1}}{d_j'}, \quad j = m-1,m-2,\ldots 1 \tag{3.51}$$

Hirsch and Rudy [56] suggested that errors may grow in the use of the Thomas algorithm unless diagonal dominance is maintained in the system of equations. A sufficient condition for this diagonal dominance to be maintained is $|d| \geq |b| + |a|$, with ">" holding for one equation [57]. If this condition does not hold, even if the stability analysis, such as Von Newmann stability analysis, indicates that the difference scheme is stable, errors might grow in the Thomas algorithm. In terms of the present system of equations, this requires that:

$$\frac{v_j^i \Delta r}{\nu_j^i} \leq 2 \tag{3.52}$$

Physically, $v_j^i \Delta r/\nu_j^i$ can be viewed as a mesh Reynolds number. This is

equivalent to a stability constraint caused by the differencing of the convective derivative term, $v \frac{\partial u}{\partial r}$. An alternative formulation for $v \frac{\partial u}{\partial r}$ can be expressed as

$$v_j^i \frac{(u_j^{i+1} - u_{j-1}^{i+1})}{\Delta r} \quad \text{when } v_j^i > 0 \tag{3.53}$$

and

$$v_j^i \frac{(u_{j+1}^{i+1} - u_j^{i+1})}{\Delta r} \quad \text{when } v_j^i < 0 \tag{3.54}$$

These alternative forms to be used when $v_j^i \Delta r/\nu_j^i > 2$ are included in the present version of the computer program.

Most two-dimensional calculations reported in this study have required less than one minute and none more than two minutes of computation time on the IBM 360/65 computer.

IV. THE AXISYMMETRIC JET IN A COFLOWING OR QUIESCENT AMBIENT

The finite-difference method and calculation procedure described in Chapter III is applied in this chapter to the axisymmetric jet in a coflowing or quiescent ambient as a first step to verify the turbulence model and computational technique. The calculations include first non-buoyant and buoyant jets in a uniform ambient, then buoyant jets in a stratified ambient. Finally, two test cases are presented for the compressible buoyant jet in uniform ambient for a verification study of the "Boussinesq approximation" [58].

Figure 4.1 shows the jet configuration with finite-difference grid points superimposed on the flow field. The main flow direction, s, is the marching direction of the computational technique. The grid sizes Δs and Δr can be varied.

A. Buoyant Horizontal Jet in a Uniform Ambient

For the buoyant jet in a quiescent ambient, the turning of the jet is due to buoyancy force only, so the drag force term in the r-momentum equation, Equation (3.4), can be neglected. For the buoyant jet in a coflowing ambient, after the jet turns, the centerline of the jet makes an angle θ with the ambient flow direction, so there is still a drag force exerted on the jet flow by the ambient fluid. Both drag and buoyancy force terms must be considered in the r-momentum equation in this coflowing ambient case.

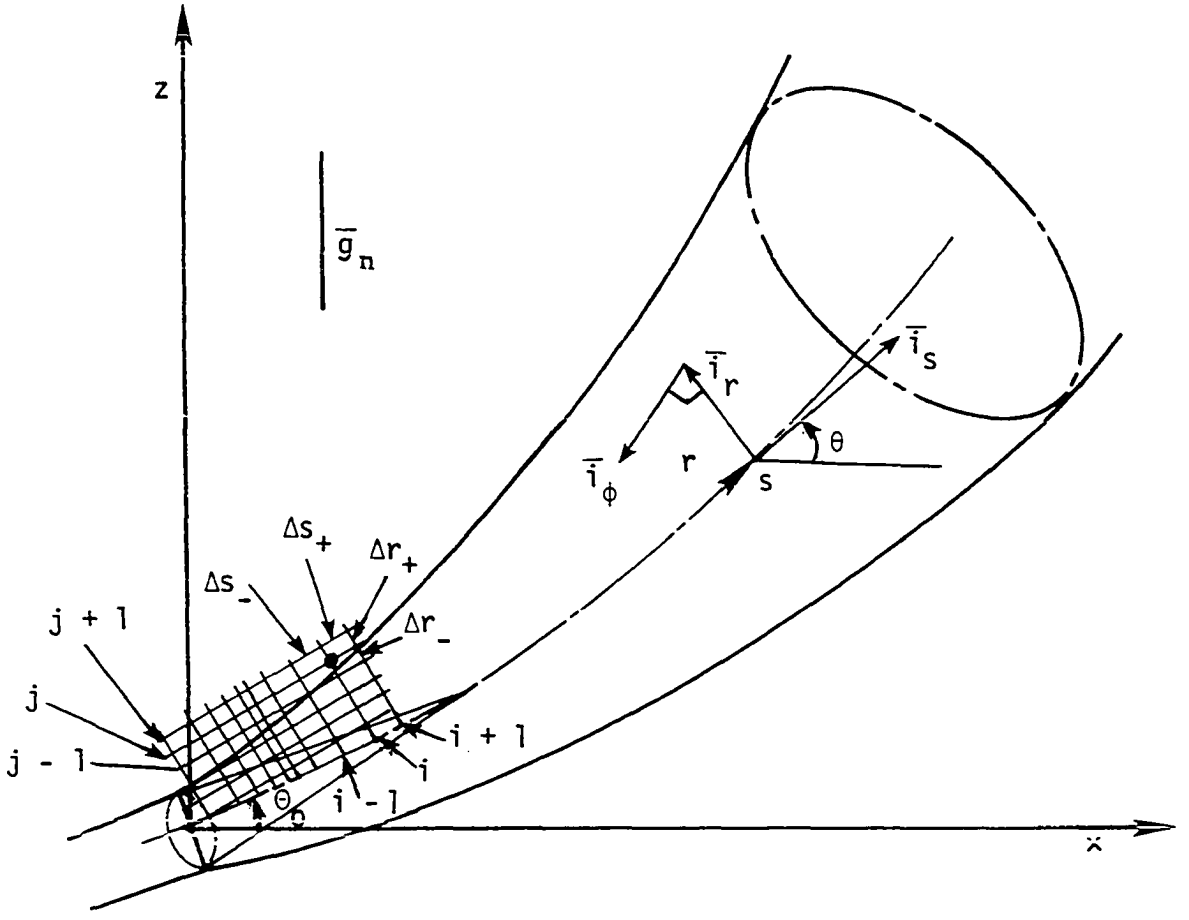

Fig. 4.1. Finite-difference grid for a curved jet analysis.

In Figures 4.2 to 4.5, the predicted trajectories and centerline temperature decay for buoyant jets discharged horizontally into a uniform, quiescent ambient at Fr_o = 16 and 64 are compared to the measurements of Ryskiewich and Hafetz [30], and the prediction of Madni [3], Hirst [4], Fan and Brooks [21], and Abraham [59]. The predictions of the present analysis appear to provide about the best agreement with the experimental data.

In Figure 4.6, trajectories predicted by the present two-dimensional analysis and the three-dimensional calculations of McGuirk and Spalding [25] using the k-ε turbulence model [60] are compared with the measurements of Ayoub [61] for "downward buoyant" jets, or dense jets, discharging horizontally into a coflowing ambient at three different velocity ratios, m = 20, 10 and 5, for Fr_o = 225. A similar comparison with Ayoub's measurements is shown in Figure 4.7 for the centerline temperature decay for a jet with m = 10 and Fr_o = 900. The predictions of the present two-dimensional analysis and algebraic turbulence model is seen to agree about as well with the experimental data as the more complex McGuirk-Spalding [25] three-dimensional predictions with the k-ε two-equation model of turbulence.

Figure 4.8 shows the effect of Froude number on plume trajectory by comparing the trajectory of the jets discharging at a velocity ratio m = 20 for three different Froude numbers, Fr_o = 225, 900 and 3600. Of course, the smaller Froude number is associated with larger relative buoyancy forces, and the trajectory turns faster. In Figure 4.9, predicted temperature profiles are compared with the measurements of

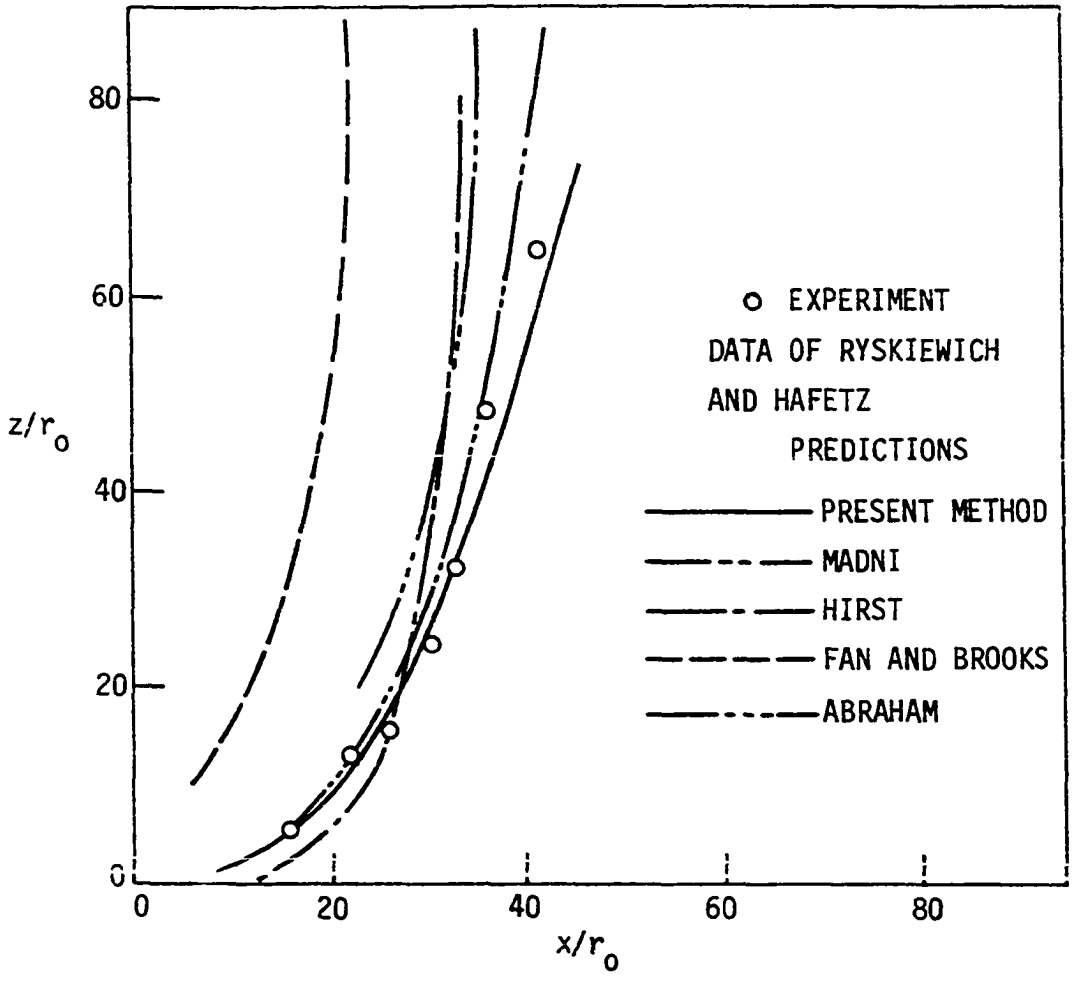

Fig. 4.2. Trajectory for buoyant jet with $Fr_o = 16$ discharged horizontally to a uniform ambient.

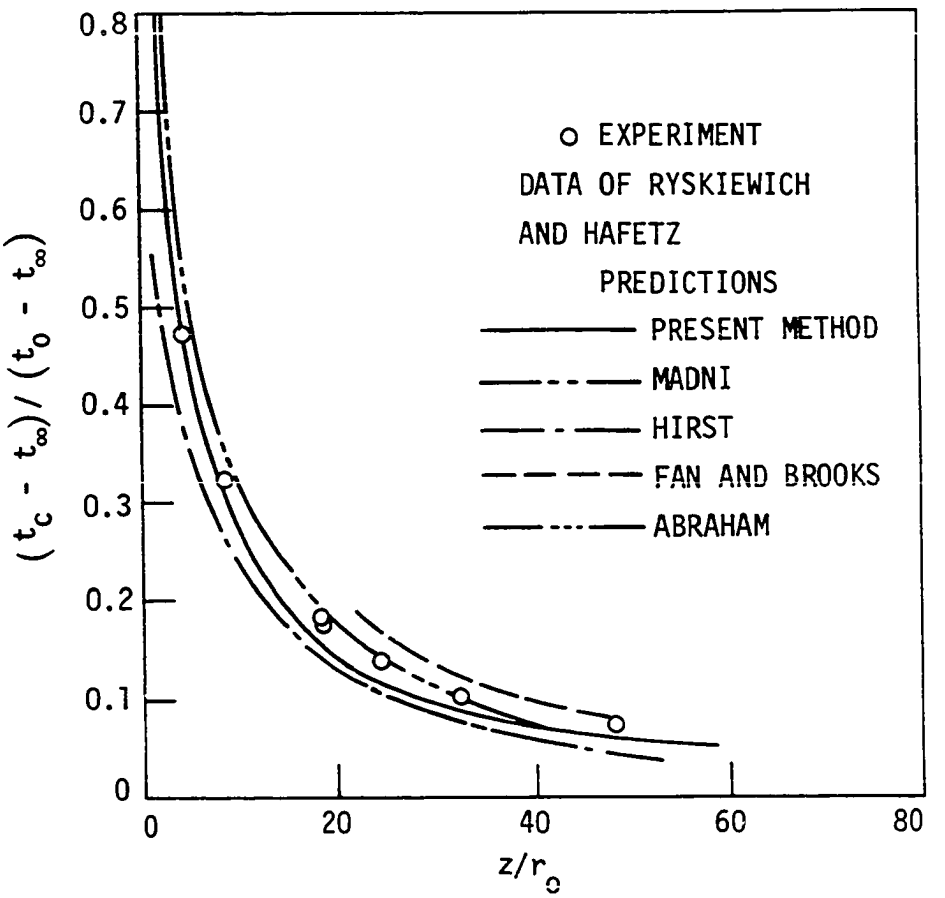

Fig. 4.3. Decay of centerline temperature for buoyant jet with $Fr_o = 16$ discharged horizontally to a uniform ambient.

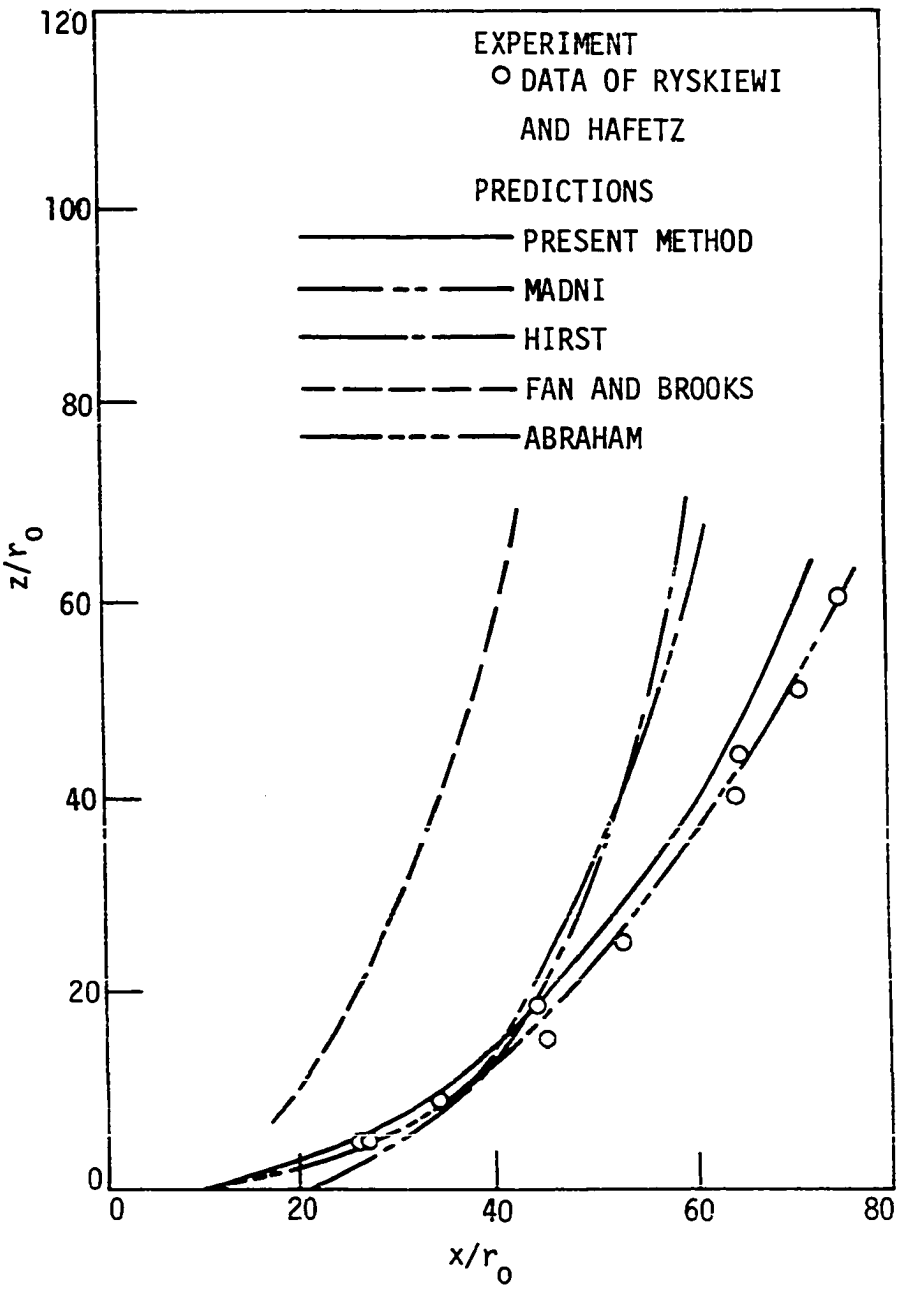

Fig. 4.4 Trajectory for buoyant jet with Fr_o = 64 discharged horizontally to a uniform ambient.

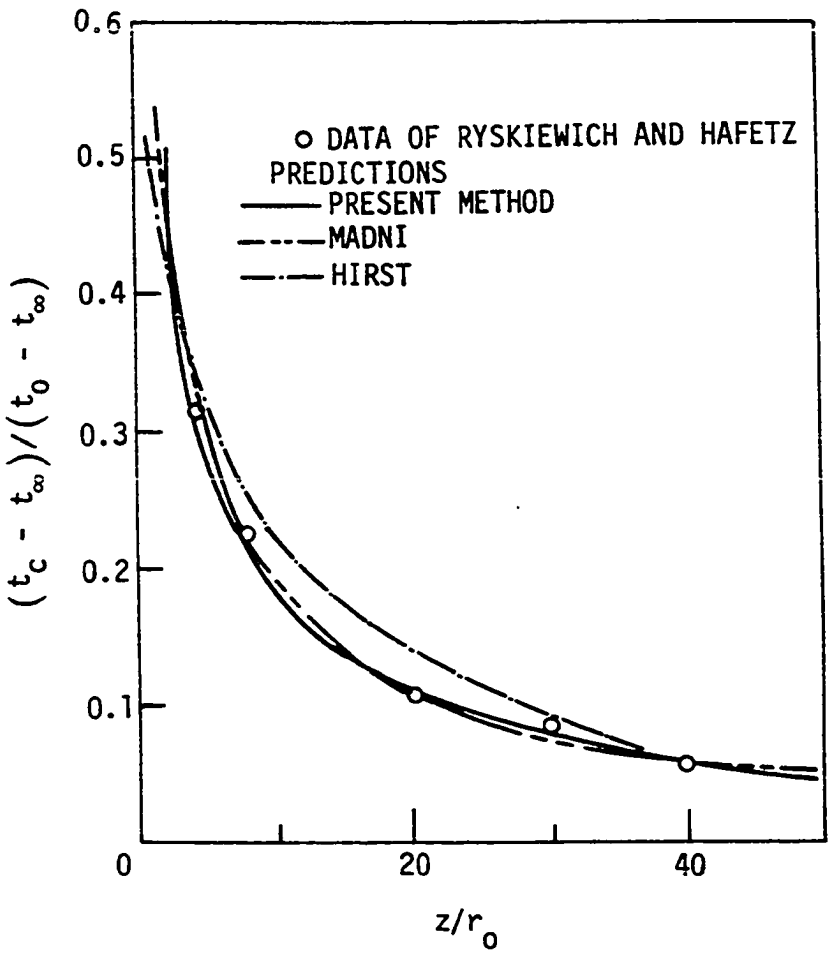

Fig. 4.5. Decay of centerline temperature for buoyant jet with $Fr_o = 64$ discharged horizontally to a uniform ambient.

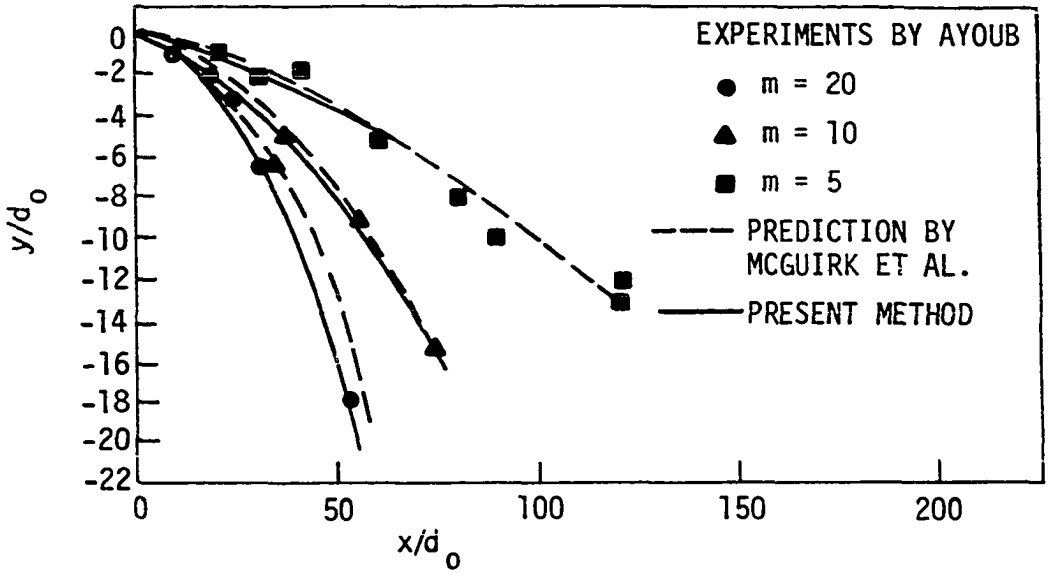

Fig. 4.6. Trajectories for horizontal buoyant jets with Fr_o = 225 discharged into coflowing ambients.

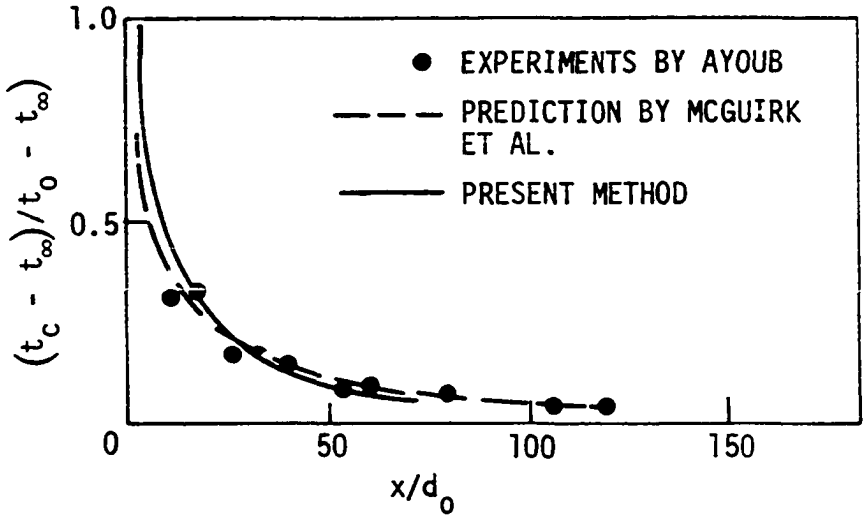

Fig. 4.7. Centerline temperature decay for a horizontal buoyant jet with Fr_o = 900, m = 10 discharged into a coflowing ambient.

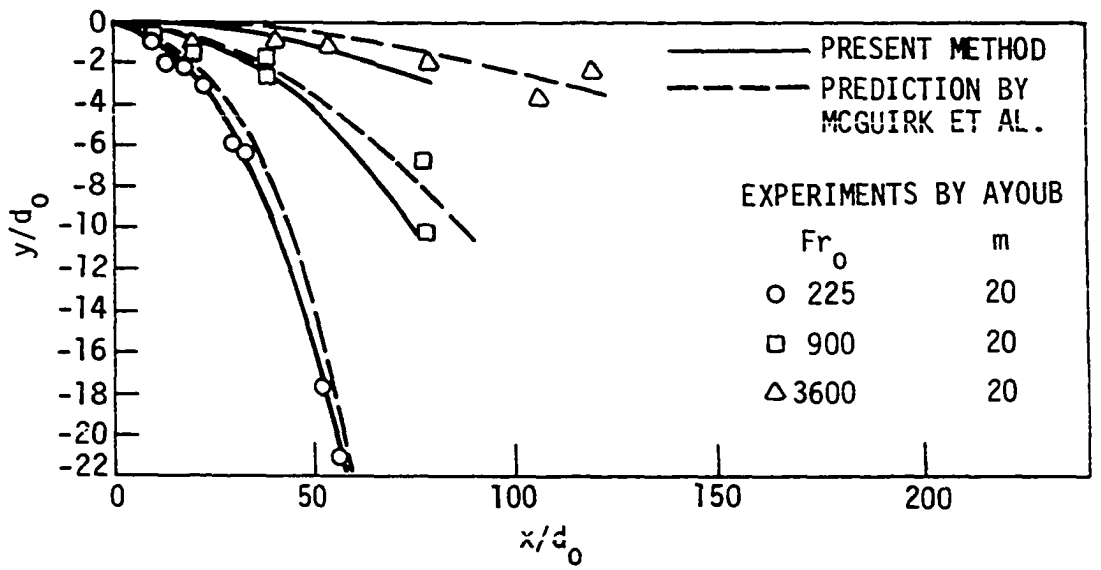

Fig. 4.8. Effect of Froude number on plume trajectory.

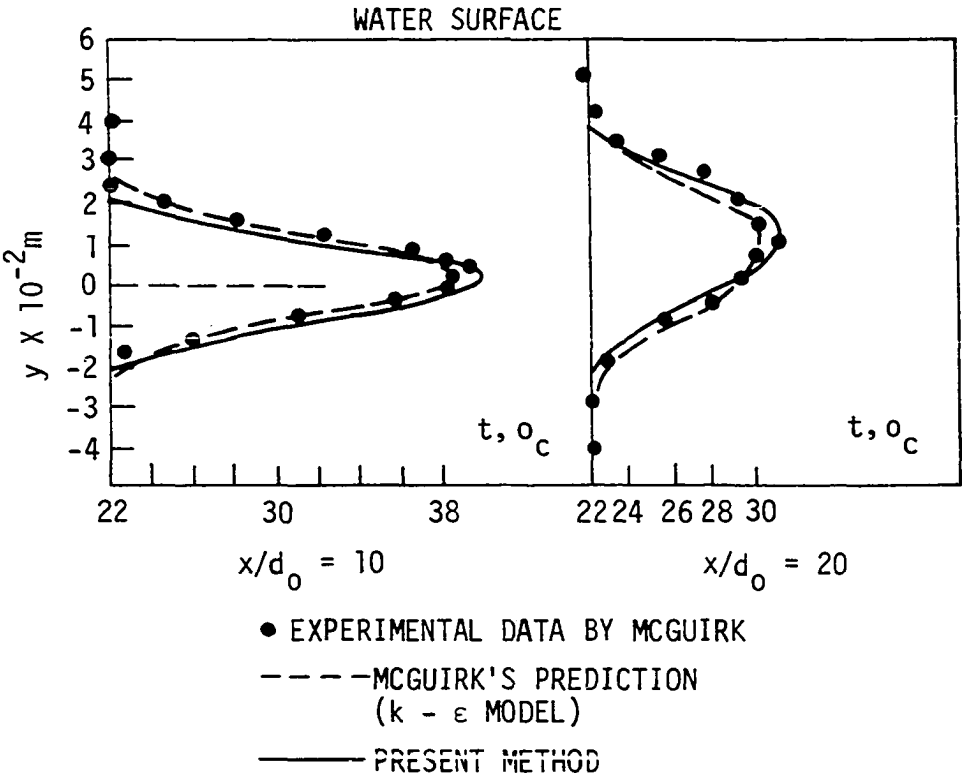

Fig. 4.9. Centerline temperature profiles for a horizontal buoyant jet in a coflowing ambient; d_o = 0.01 m, Fr_o = 225, m = 6.

McGuirk [62] for the buoyant jet discharged into a coflowing ambient for $Fr_o = 225$ and $m = 6$ at two stations, $x/d_o = 10$ and $x/d_o = 20$. McGuirk's three-dimensional predictions using the k-ε model are also shown in the figure. These profile measurements and others by McGuirk [62] tend to support the view that for round buoyant discharges into coflowing streams, the flow remains nearly axisymmetric until distorted by interactions with the free surface. Prior to these interactions, the present two-dimensional analysis should provide a good approximation to the temperature distribution as well as the jet trajectory.

B. Buoyant Jet in a Stratified Ambient

The same turbulence model was used for the stratified ambient analysis as was used for the uniform ambient case. Again, because the ambient is at rest, the drag force term in the r-momentum was omitted. In this case, due to the stratification, the ambient temperature varied and provided a variable boundary condition for energy equation.

$$T_\infty = \frac{-\lambda\, d_o}{Re_o (t_o - t_{\infty,o})} Z \tag{4.1}$$

where $\lambda = -dt_\infty/dz$ has units °C/m, and Z is the nondimensional vertical height. $\bar{T}$, a stratification parameter, which is nondimensional, is defined mathematically as

$$\bar{T} = \frac{(\rho_\infty - \rho_o)}{-r_o \left(\frac{d\rho_\infty}{dz}\right)} \tag{4.2}$$

From Appendix B, it is found that

$$\frac{d\rho}{dz} = -\beta_{th}\rho_{ref}\frac{dt}{dz} \tag{4.3}$$

and

$$(\rho_\infty - \rho_o) = \beta_{th}\rho_o(t_o - t_{\infty,o}) \tag{4.4}$$

By inserting Equations (4.3) and (4.4) into Equation (4.2), the stratification parameter can be expressed in terms of temperature as a more practical form of Equation (4.2),

$$\overline{T} = \frac{(t_o - t_{\infty,o})}{r_o\left(\frac{dt_\infty}{dz}\right)} \tag{4.5}$$

where $dt_\infty/dz = |\lambda|$, the degree of stratification.

Figure 4.10 shows the trajectories for buoyant jets discharged horizontally into a quiescent, stratified ambient with three cases: (1) $Fr_o = 676$, $\overline{T} = 2454$, (2) $Fr_o = 1600$, $\overline{T} = 10997$, and (3) $Fr_o = 3600$, $\overline{T} = 1030$. The results of present analysis are compared with the Hirst prediction [4] and the experimental data by Fan [12]. From this comparison, it can be seen that the present and the Hirst predictions agree fairly well, but neither one is in good agreement with the experimental results of Fan.

Table 4.1 lists the predicted results for maximum height of rise of plumes discharging vertically into stratified quiescent ambients. The predictions are compared to the experimental data of Abraham and Eysink (cited in [7]). The agreement of the present predictions is favorable. Some discussions on the discrepancy between the Fox theory [32,33], and

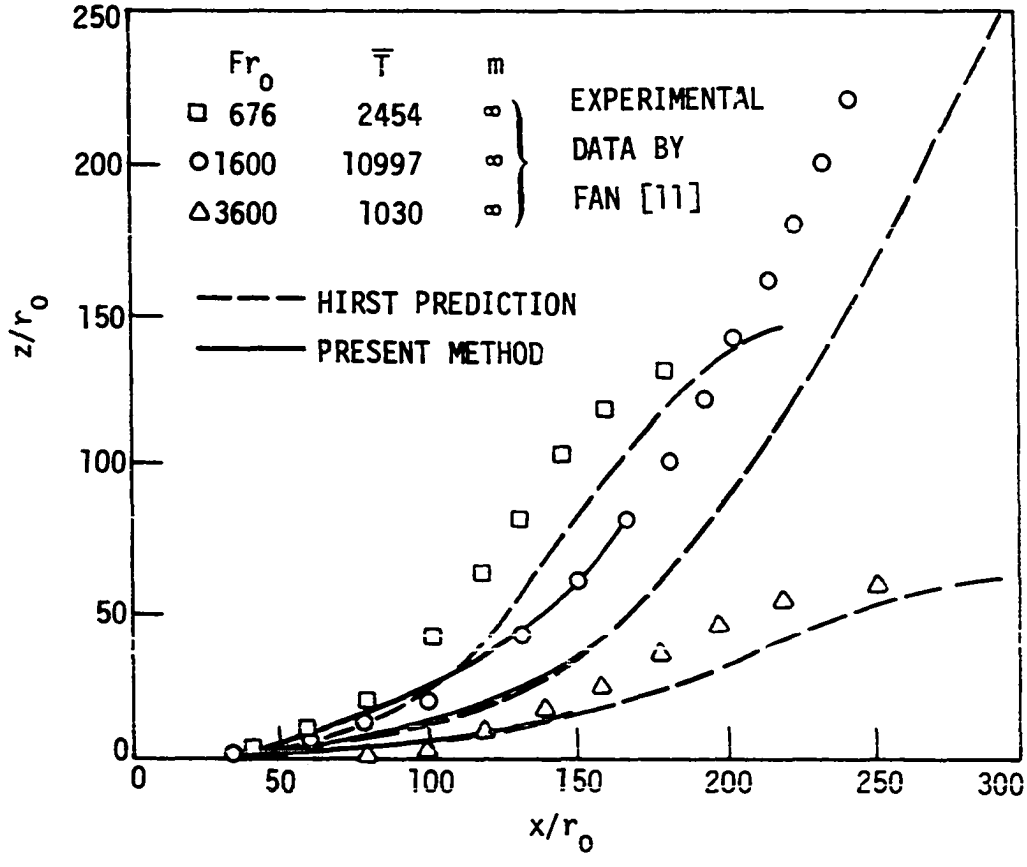

Fig. 4.10. Trajectories for buoyant jets discharged horizontally to a stratified quiescent ambient.

Table 4.1. Maximum height of rise for vertical plumes discharged into stratified quiescent ambients

Case No.	Discharge Froude Number, Fr_o	Stratification Parameter, $\bar{T}$	z_m/r_o Measured by Abraham and Eysink	z_m/r_o Predicted		
				Present Method	Madni	Fox Theory
1	60.5	134	68	70	72.5	49
2	63.0	94	64	62.6	65	44

experimental results of Abraham and Eysink can be found in [3].

C. Horizontal Buoyant Jet with Variable Properties

For the variable property buoyant jet, the governing equations become:

Continuity:

$$\frac{\partial(\rho r u)}{\partial s} + \frac{\partial(\rho r v)}{\partial r} = 0 \tag{4.6}$$

s-momentum:

$$u \frac{\partial u}{\partial s} + v \frac{\partial u}{\partial r} = \frac{1}{\rho r} \frac{\partial}{\partial r}(r \tau_s) + \frac{\rho_\infty - \rho}{\rho} g_n \sin\theta \tag{4.7}$$

r-momentum:

$$u^2 \frac{d\theta}{ds} = -C_D(u_\infty \sin\theta)^2 \frac{2}{\pi D_{eff}} \frac{\rho_\infty}{\rho} + \frac{\rho_\infty - \rho}{\rho} g_n \cos\theta \tag{4.8}$$

Energy:

$$u \frac{\partial t}{\partial s} + v \frac{\partial t}{\partial r} = \frac{1}{\rho c_p r} \frac{\partial}{\partial r}(-rq) \tag{4.9}$$

Here ρ is a variable and changes with temperature. The viscosity μ, thermal diffusivity α, and thermal expansion coefficient β_{th} also varied with temperature. The temperature dependence functions of these properties presented by Hong [63] were used in this case.

Comparisons are made in Figures 4.11 through 4.14 for the trajectory and decay of centerline temperature for the buoyant horizontal jet with $Fr_o = 16$ and $Fr_o = 64$ discharged into a uniform ambient. For these cases, $t_\infty = 10°C$ and $t_o = 26.7°C$. Over this temperature range,

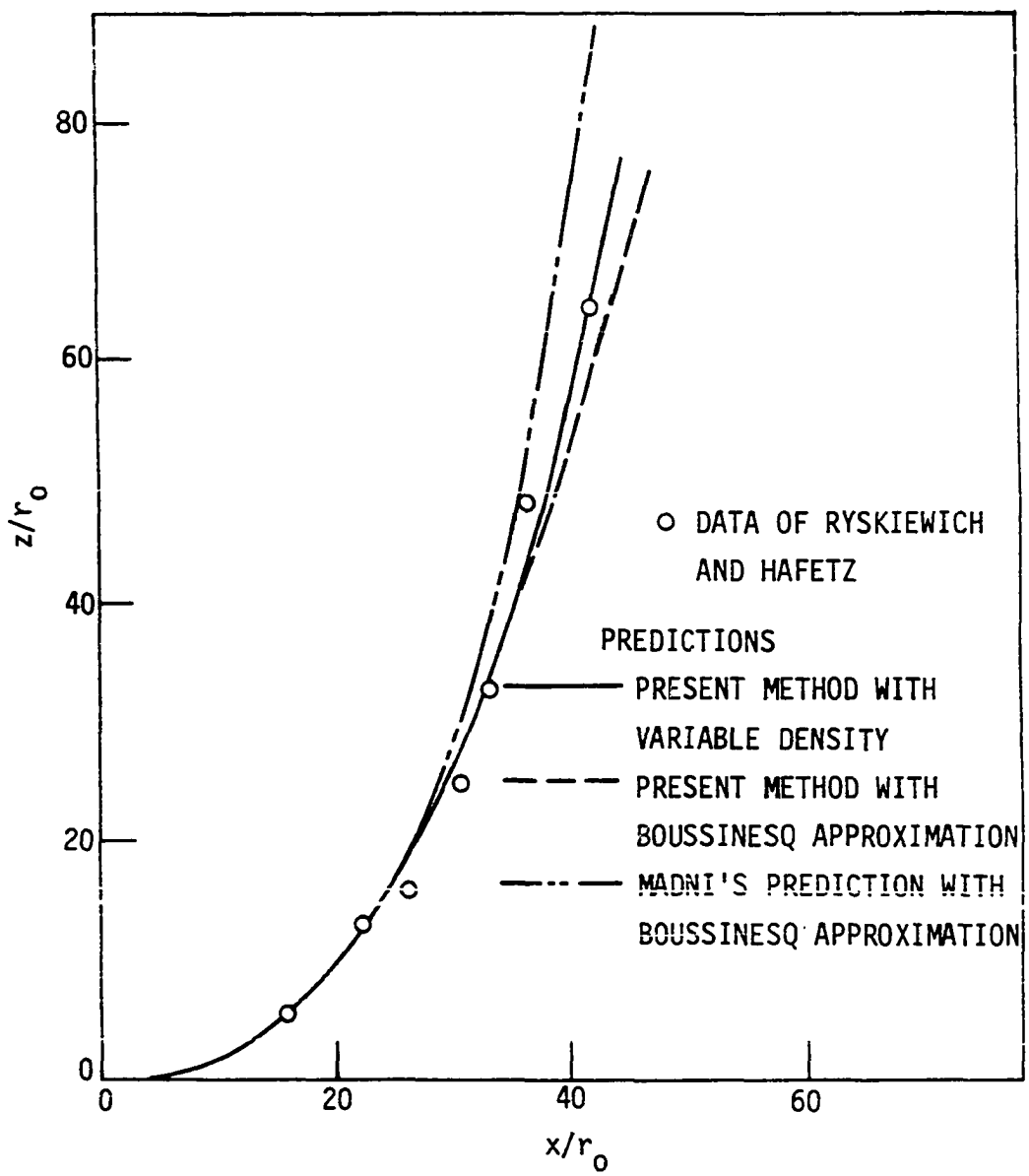

Fig. 4.11. Predicted trajectory for buoyant jet with Fr_o = 16 discharged horizontally to a uniform ambient.

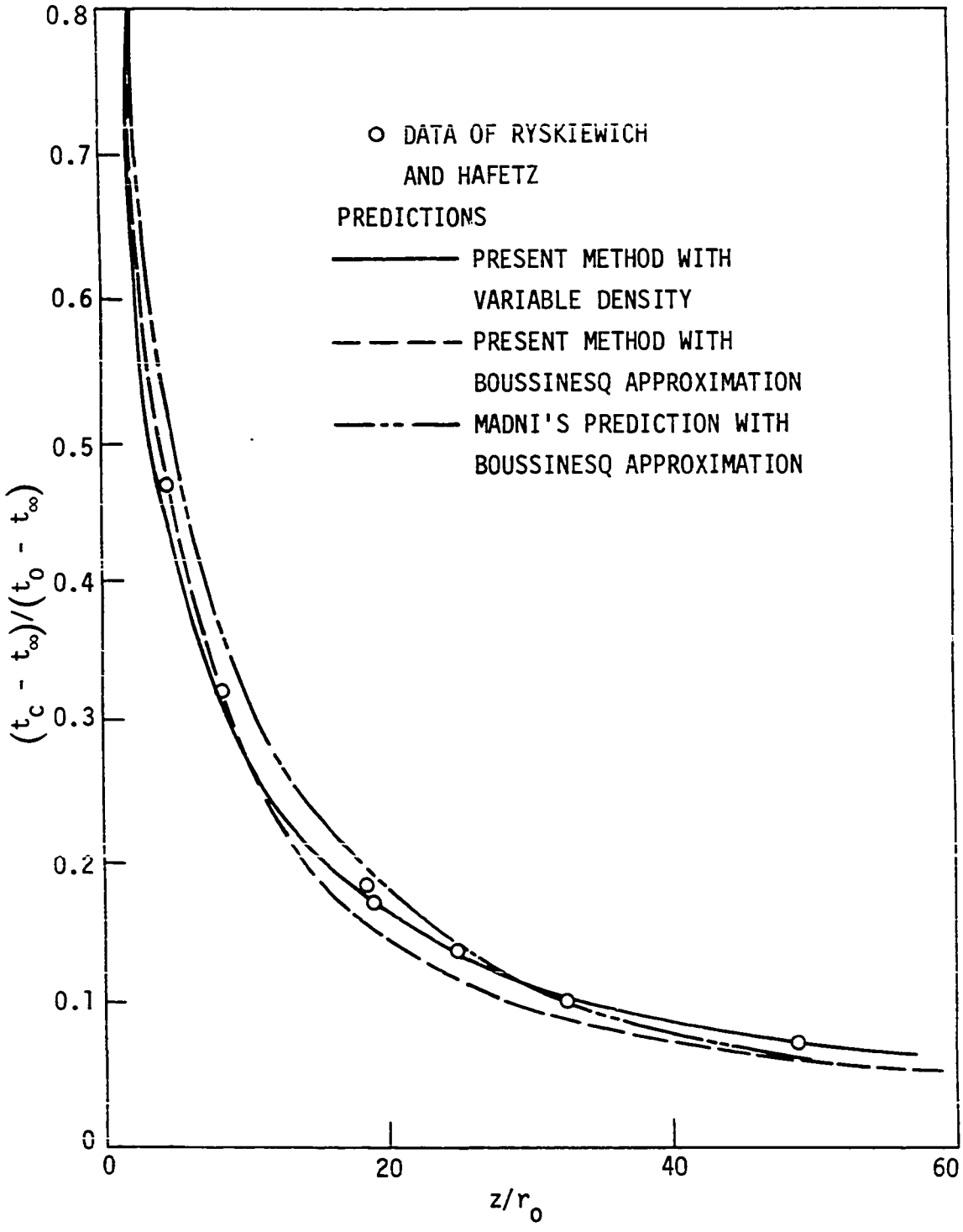

Fig. 4.12. Decay of centerline temperature for buoyant jet with Fr_o = 16 discharged horizontally to a uniform ambient.

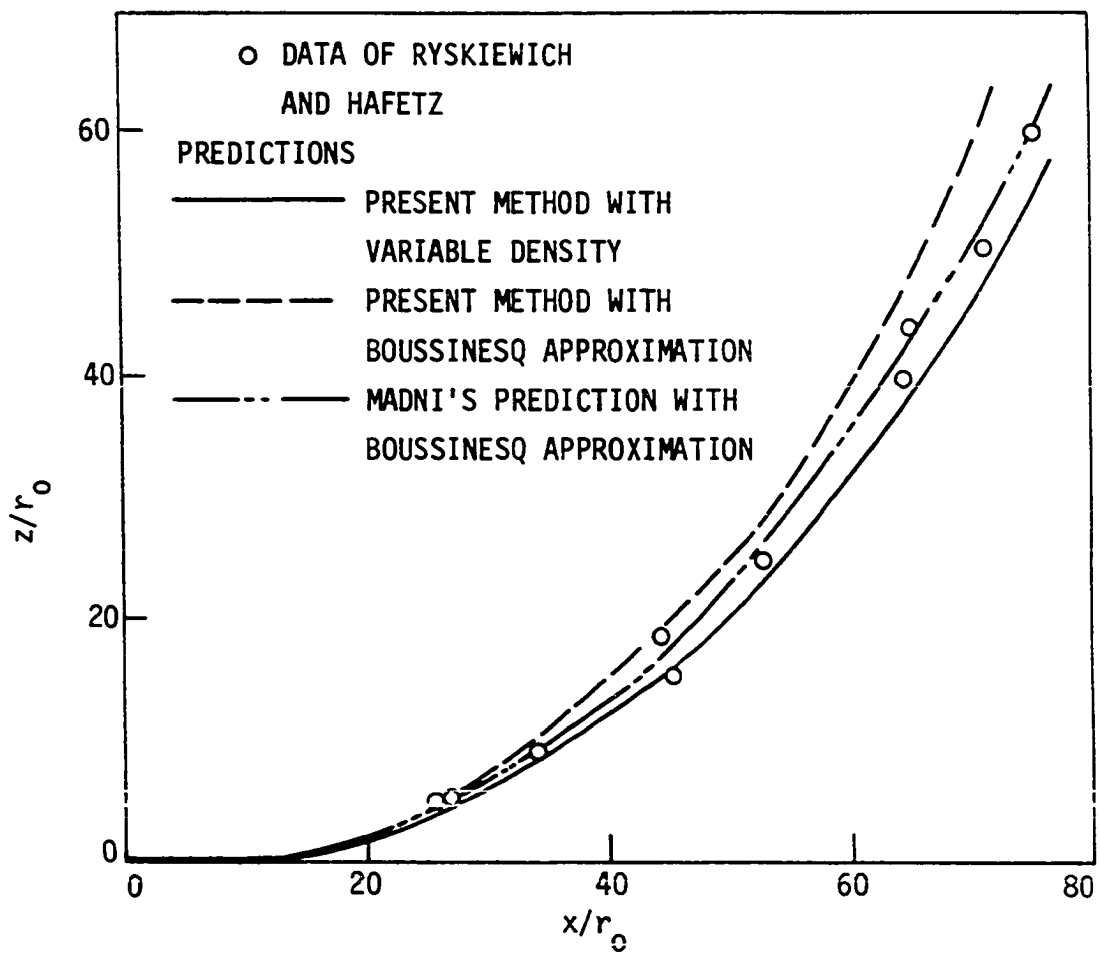

Fig. 4.13. Predicted trajectory for buoyant jet with $Fr_o = 64$ discharged horizontally to a uniform ambient.

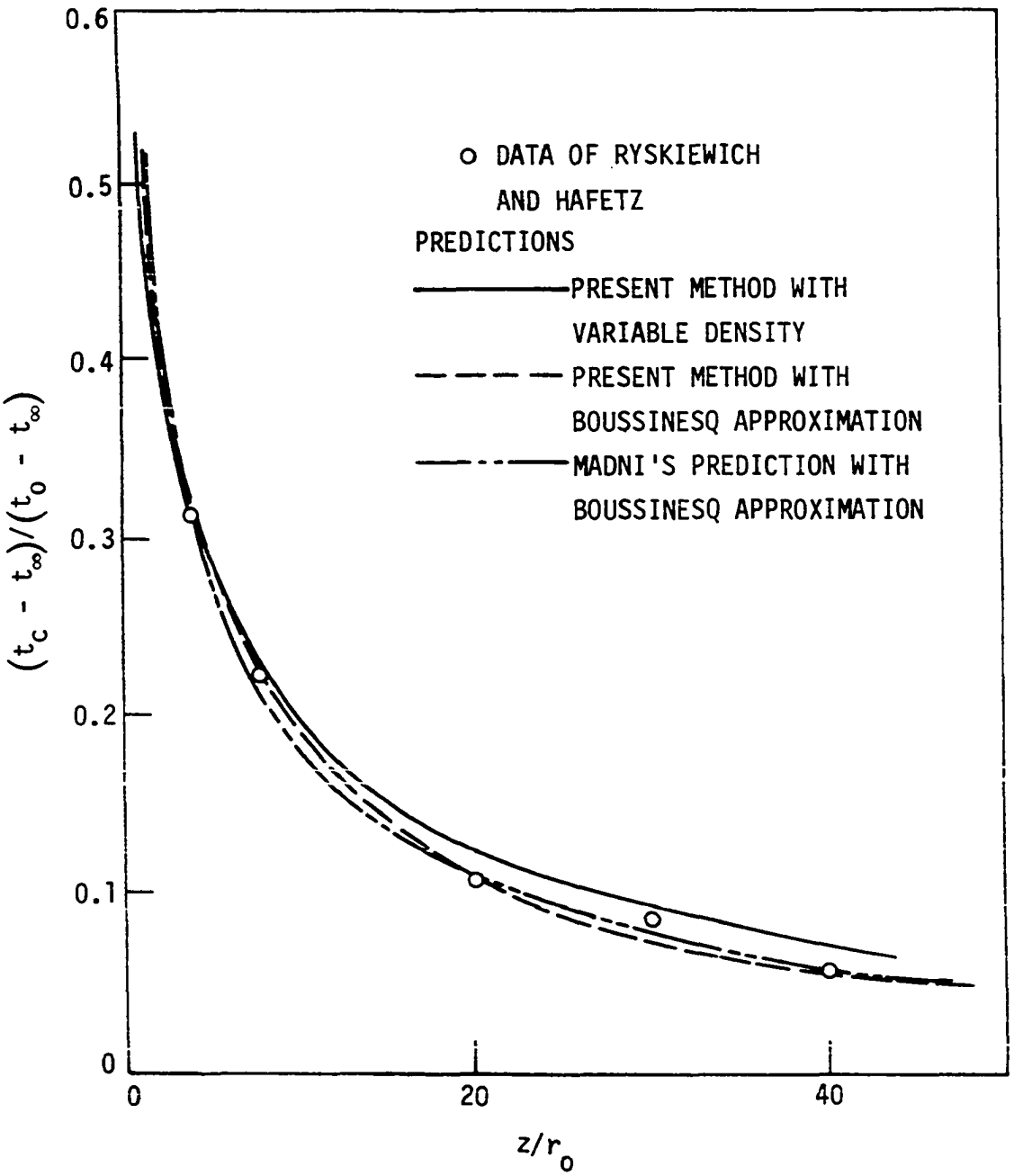

Fig. 4.14. Decay of centerline temperature for buoyant jet with Fr_o = 64 discharged horizontally to a uniform ambient.

the density variation (water) was very small, only 0.4%, viscosity (μ) varied by 50% and thermal expansion coefficient (β_{th}) by 54%. By comparing the predictions with variable properties analysis to the predictions with constant properties analysis and to Madni's predictions [3] which made use of the Bossinesq approximation, it is seen that the predictions with variable properties compare somewhat more favorably with the experimental data of Ryskiewich and Hafetz. However, the improvement is not considered significant. On the other hand, the variable properties analysis requires more computer time so it should only be used when the effects of property variations are expected to be significant. Since property variations for all the cases in this study were no greater than the above test cases, the Boussinesq approximation was employed.

V. THE AXISYMMETRIC JET IN A CROSSFLOW

All of the flow configurations studied in Chapter IV involved discharges into an ambient either at rest or flowing in the same direction as the discharging plume. However, in applications, plume trajectories are often influenced by atmospheric cross winds or crossflows in waterways. In this chapter, all the calculations are for jets in a crossflow. So, the drag force term in the r-momentum equation is significant.

A. Nonbuoyant Jet in a Uniform Ambient

For the nonbuoyant jet, the buoyancy term in the momentum equations, Equations (3.3) and (3.4), can be neglected. The experiments of Gordier [13] and Platten and Keffer [16] with nonbuoyant jets discharging to a crossflow provide a test for the proposed mathematical modeling of the drag force term in the transverse momentum equation, Equation (3.4). Figure 5.1 compares the centerline trajectory predicted by the present method for the jet discharging normal to a crossflow for various values of velocity ratio m, with the measurements of Gordier [13] and the analytical predictions of Hirst [4]. Figure 5.2 compares the maximum velocity decay predicted for the nonbuoyant jet with the experimental results of Gordier [13] for $m = 4, 6$ and 8. The predictions of the present method are seen to agree fairly well with the experimental results.

The other comparisons of the centerline trajectories with the data of Platten and Keffer [16] are shown for jets discharged at various

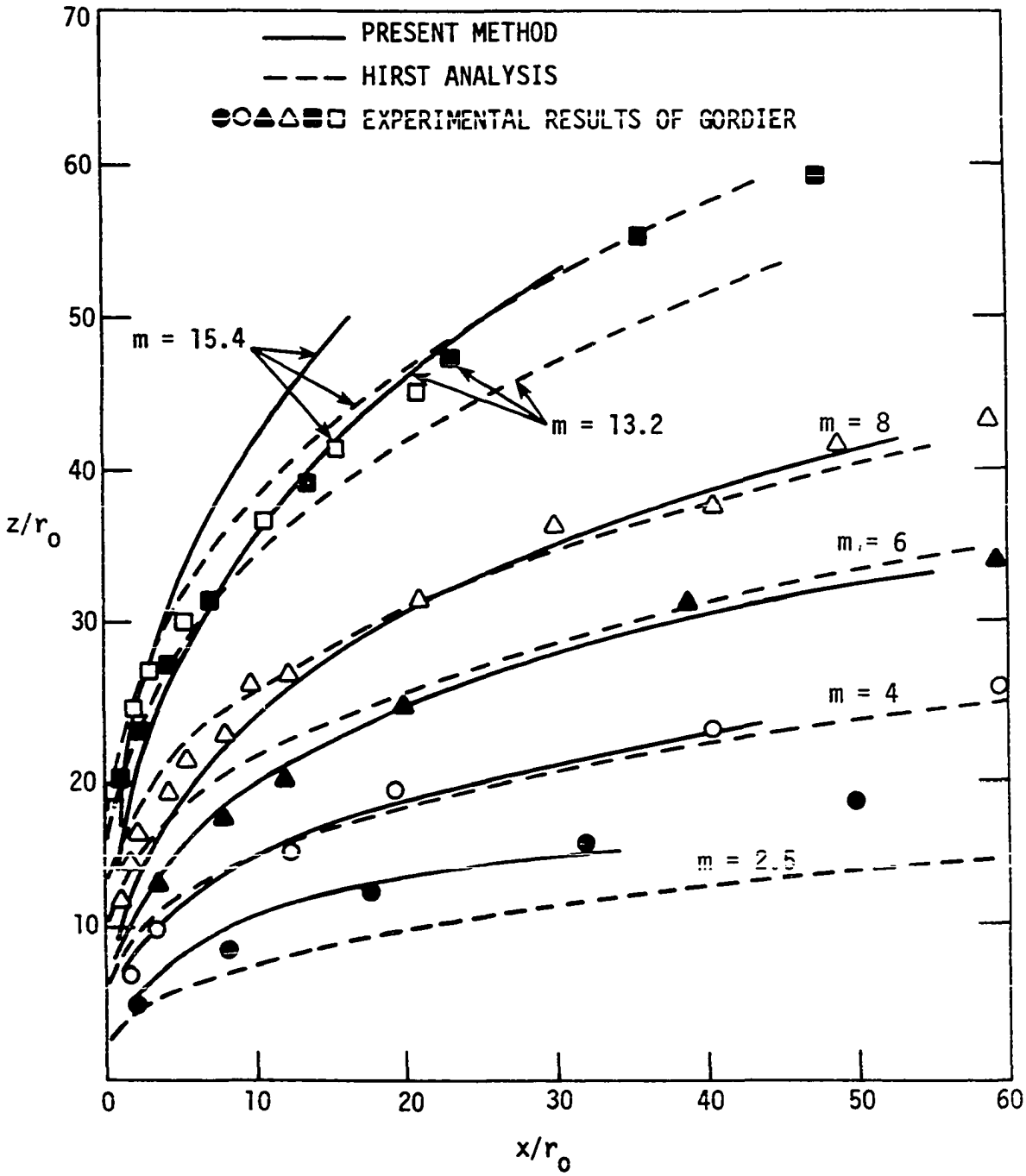

Fig. 5.1. Trajectories for nonbuoyant jets discharged normal to a crossflow.

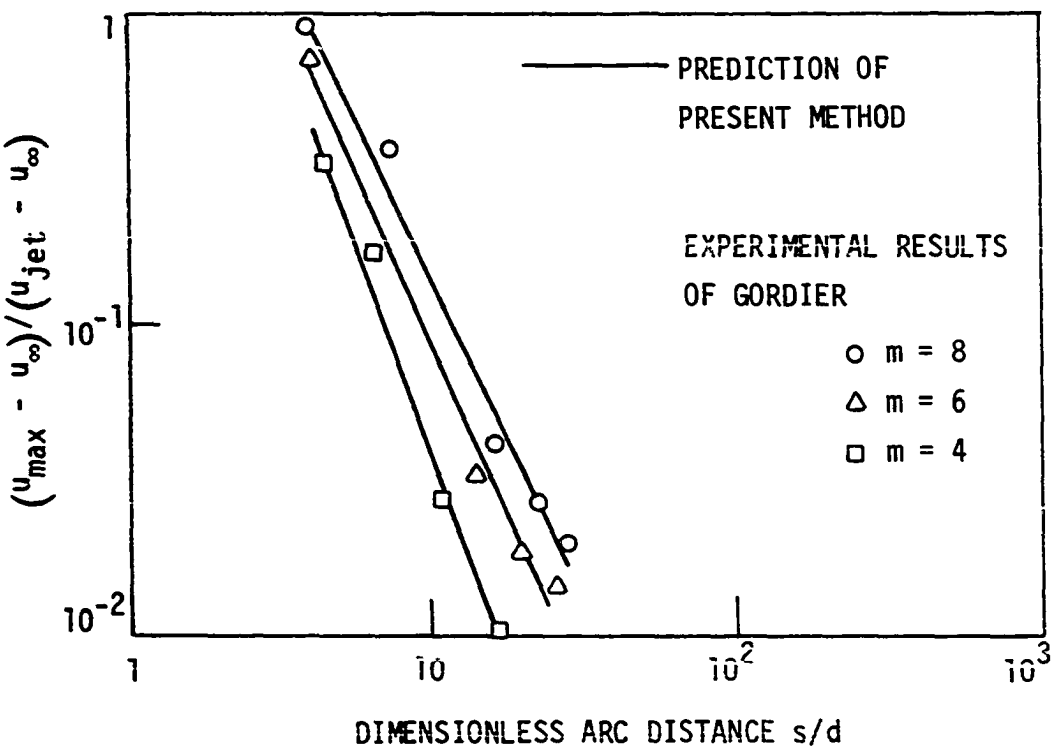

Fig. 5.2. Maximum velocity decay for nonbuoyant jets discharged to a crossflow.

angles to the free stream in Figure 5.3 for m = 8, in Figure 5.4 for m = 6, and in Figure 5.5 for m = 4. The predictions of Hirst [4] are also shown. The present analysis is seen to predict the trajectories quite well.

One additional comparison is shown in Figure 5.6 for the centerline velocity decay of the nonbuoyant jet discharged into a crossflow to illustrate the influence of the proposed curvature correction to the turbulence modeling. The correction is seen to provide noticeably better agreement with the measurements. On the other hand, the predicted trajectories were found not to be very sensitive to the curvature Richardson number.

B. Buoyant Jet in a Uniform Ambient

Some of the practical applications of this configuration are the submerged jet from the offshore outfalls of power plants into a flowing ambient, such as river or water pond, and the plume discharged from the cooling tower or stack into a cross wind in the atmosphere.

Theoretical analyses for the prediction of buoyant jet in a crossflow can be found in Hirst [4], and more recently in Fink [17] and Schatzmann [5]. These approaches are integral in nature.

The governing equations will be the same as those presented in Chapter III. The r-momentum equation, including both drag force and buoyancy force, is repeated here to facilitate the explanation.

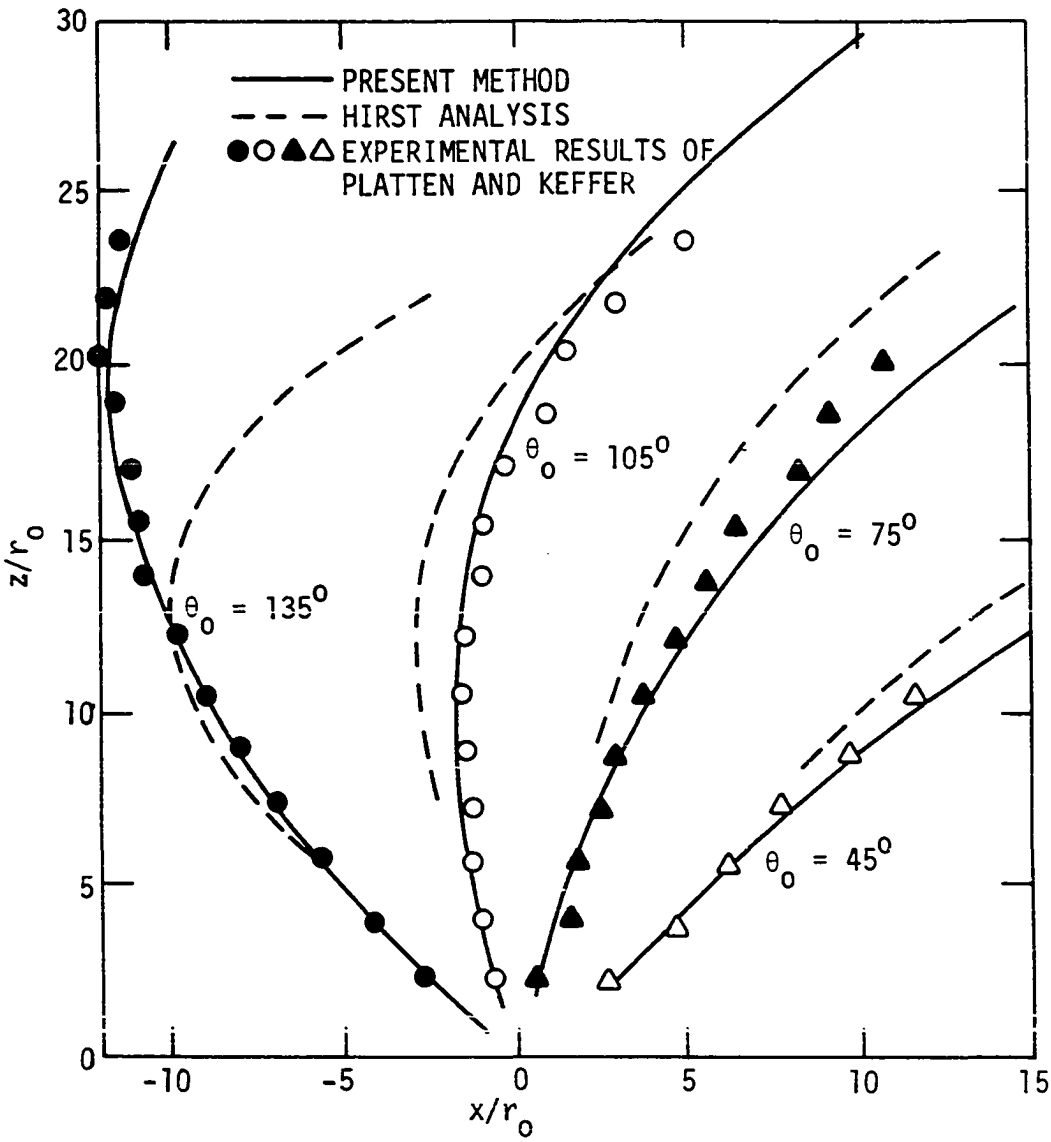

Fig. 5.3. Trajectories for nonbuoyant jets discharged at various angles to the free stream with m = 8.

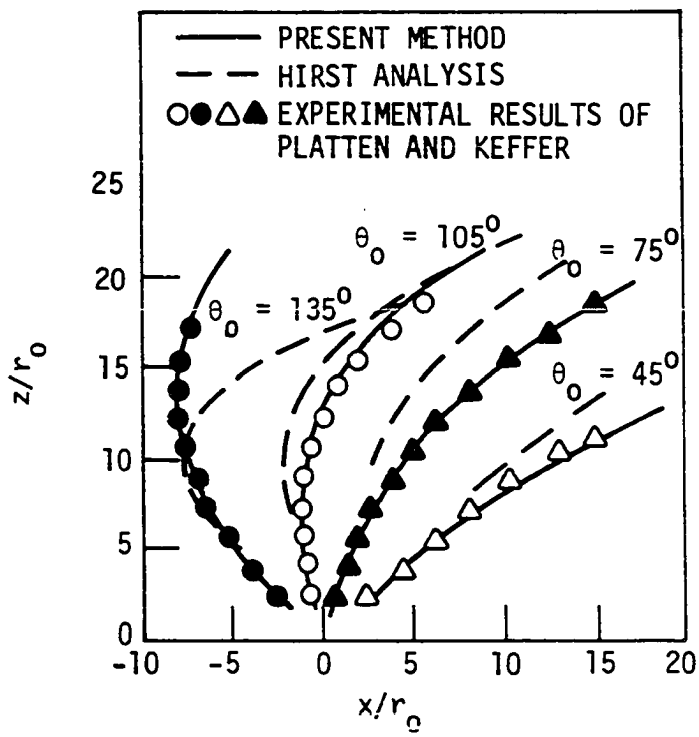

Fig. 5.4. Trajectories for nonbuoyant jets discharged at various angles to the free stream with m = 6.

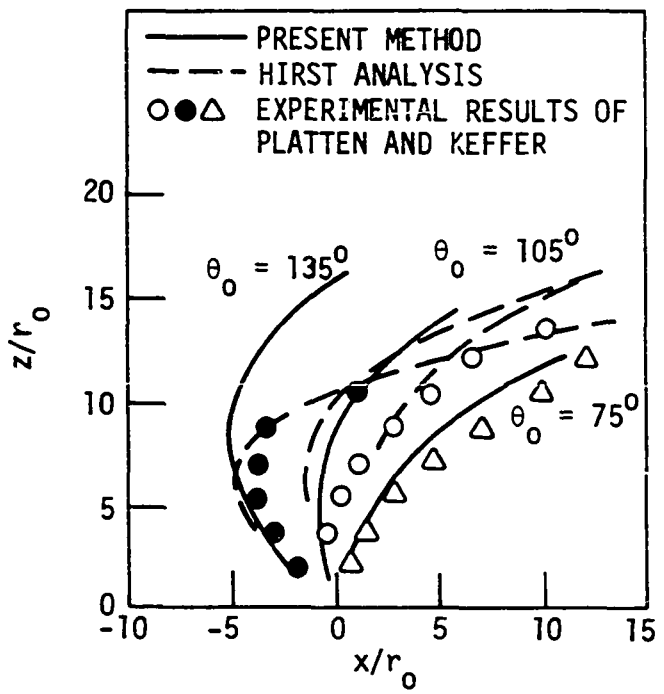

Fig. 5.5. Trajectories for nonbuoyant jets discharged at various angles to the free stream with m = 4.

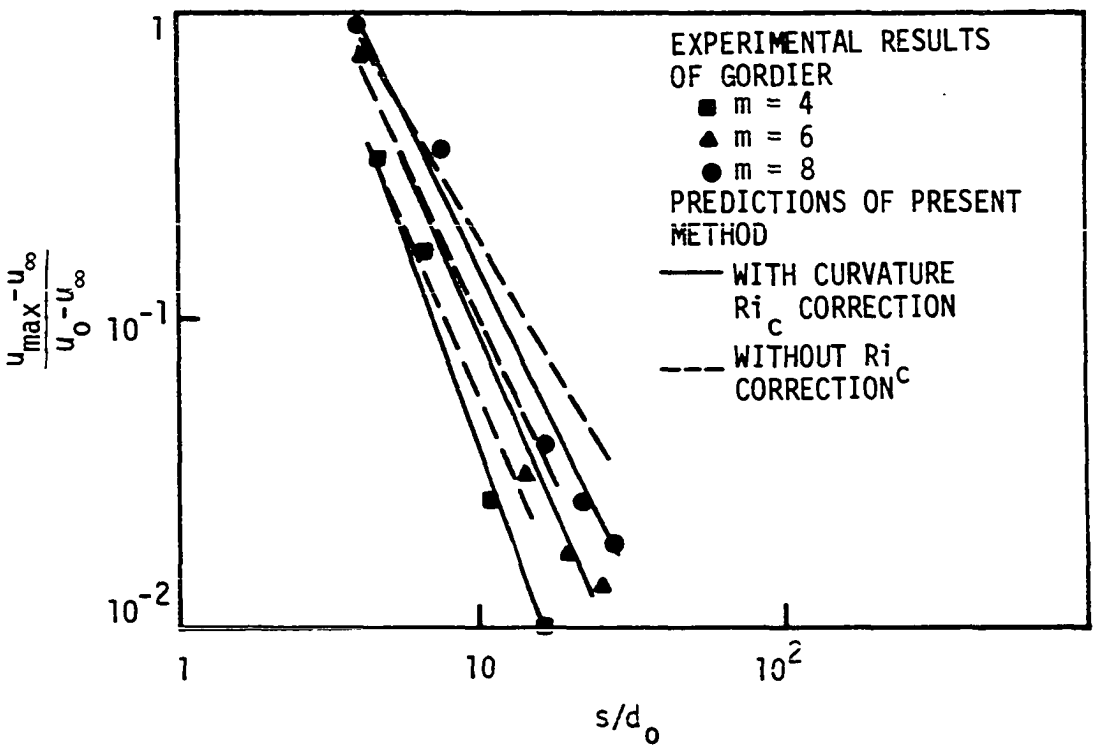

Fig. 5.6. Effect of curvature Richardson number on plume centerline velocity decay.

$$\widetilde{u^2}\,\frac{d\theta}{ds} = -C_D(u_\infty \sin\theta)^2\,\frac{2}{\pi\, D_{eff}}\,\frac{\rho_\infty}{\rho_o} + \frac{\widetilde{\rho_\infty - \rho}}{\rho_o}\, g_n \cos\theta \qquad (5.1)$$

The left hand side of the equation is the normal component of acceleration of the jet, which balances the buoyancy force and the drag force from the crossflow.

$$\text{Normal component of acceleration} = \frac{u^2}{\bar{R}} \qquad (5.2)$$

where $\bar{R}$, the radius of curvature of the centerline of the trajectory, is expressed as:

$$\frac{1}{\bar{R}} = \frac{d\theta}{ds} \qquad (5.3)$$

The sign of $\bar{R}$ is determined from Equation (5.3). D_{eff} is the effective diameter of the jet and equals twice the velocity half-width,

$$D_{eff} = 2\, r_{1/2} \qquad (5.4)$$

In order to calculate θ at station i+1, the r-momentum equation is integrated numerically over the cross section while assuming that θ is constant at each s-location.

$$\frac{\theta_{i+1}-\theta_i}{\Delta s_+}\int_0^{\delta_i} u_{i,j}^2 r_j\, dr$$

$$= -\int_0^{\delta_i} C_D(u_{\infty,i}\sin\theta_i)^2\,\frac{2}{\pi\, D_{eff,i}}[1-\beta_{i,j}(T_{\infty,i}-T_o)Tc_2]r_j\, dr$$

$$+\frac{\cos\theta_i}{Re_o}\int_0^{\delta_i}\frac{(T_{i,j}-T_{\infty,i})}{Fr_o}\, r_j\, dr \qquad (5.5)$$

The numerical integration was performed using the trapezoidal rule. No profile assumptions are needed for u and t. The values of $u_{i,j}$ and $t_{i,j}$ are obtained from the solutions of the s-momentum and energy equations at station i.

Referring to Figure 5.7, θ_{i+1} is calculated from the transverse momentum Equation (5.5), and then the coordinates of the trajectory are generated as follows:

$$\begin{aligned} \Delta x_+ &= \Delta s_+ \cos \theta_i \\ \Delta z_+ &= \Delta s_+ \sin \theta_i \\ s_{i+1} &= s_i + \Delta s_+ \\ x_{i+1} &= x_i + \Delta s_+ \cos \theta_i \\ z_{i+1} &= z_i + \Delta s_+ \sin \theta_i \end{aligned} \tag{5.6}$$

The same flow chart used by Madni [3] is shown in Figure 5.8 to illustrate briefly the solution procedure.

Figures 5.9 and 5.10 compare the predicted trajectories and centerline temperature decay with the experimental data of Fan [12] and the Hirst predictions [4] for buoyant jets discharging normal to a crossflow at two different velocity ratios, m = 4 and 8, for Fr_o = 85.

Similar comparisons are shown in Figures 5.11 and 5.12 for Fr_o = 400, m = 4 and 8, and in Figures 5.13 and 5.14 for Fr_o = 1600, m = 4 and 8.

In Figure 5.15, a comparison of some predicted and measured velocity half-widths for buoyant jets discharged normal to a crossflow with

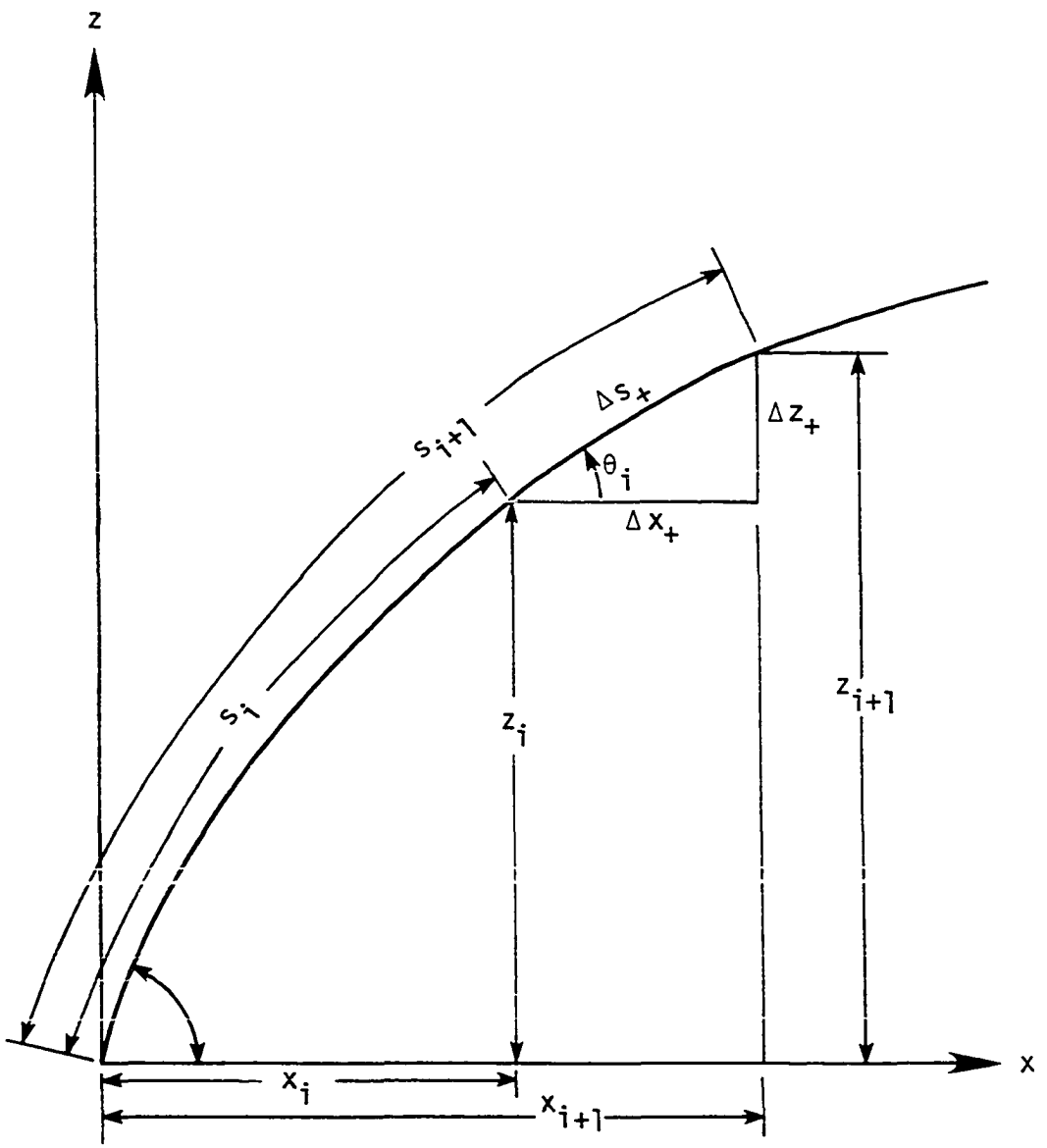

Fig. 5.7. Generation of jet trajectory.

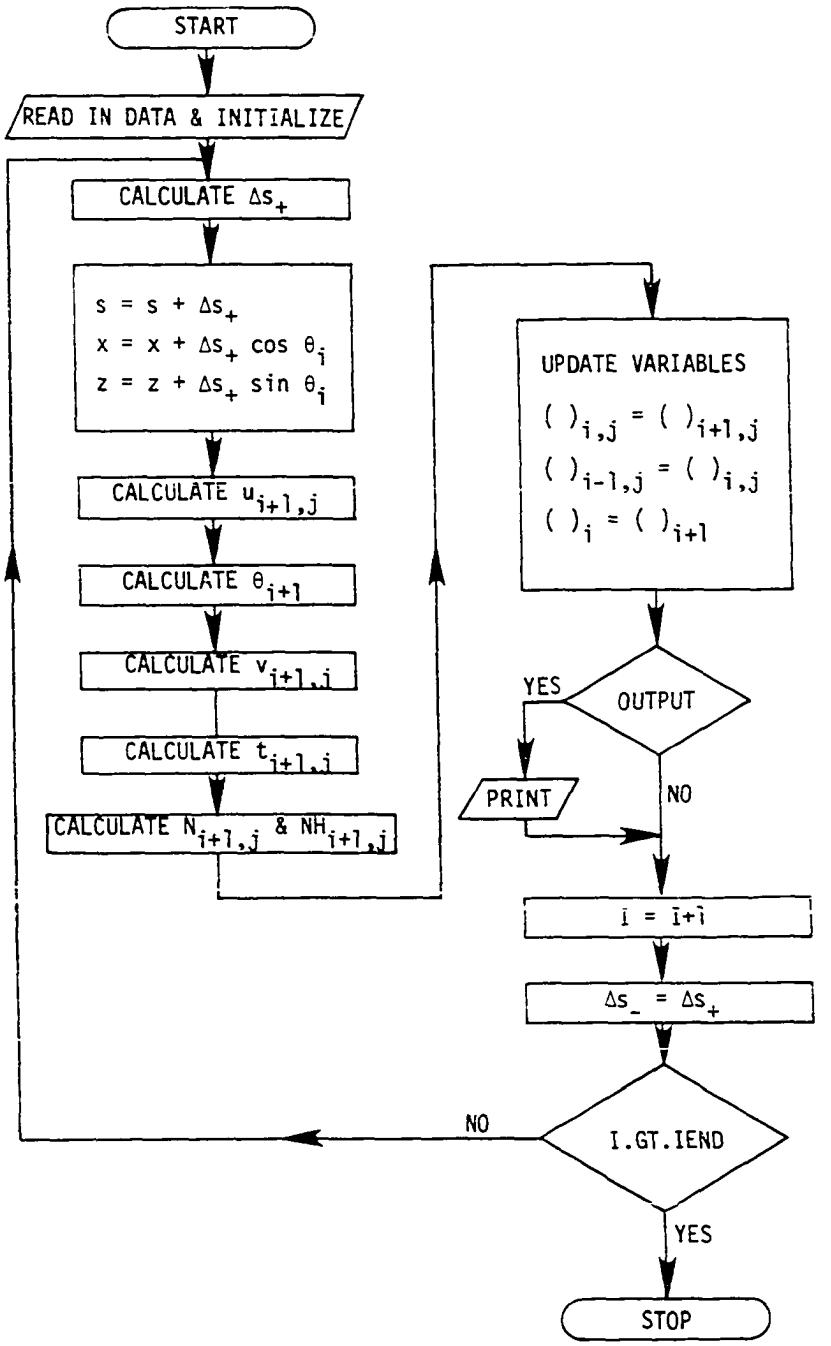

Fig. 5.8. Skeleton flow chart for the general calculation method.

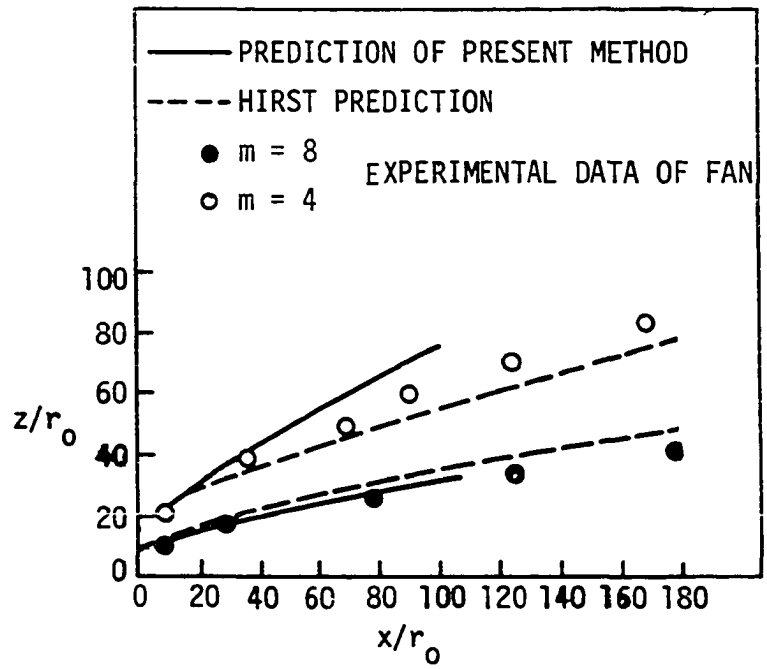

Fig. 5.9. Trajectories for buoyant jets discharged normal to a crossflow with Fr_o = 85.

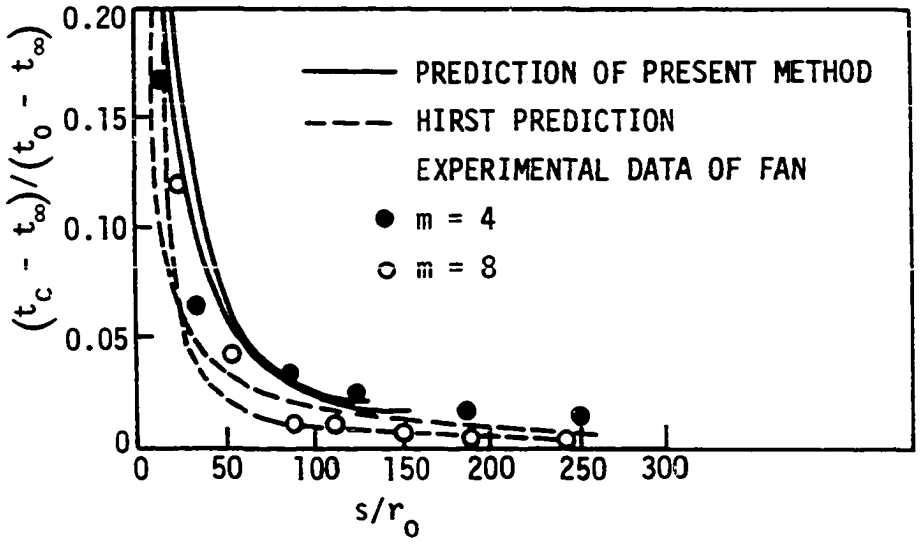

Fig. 5.10. Centerline temperature (or concentration) decay for buoyant jets discharged to a crossflow with $Fr_o = 85$

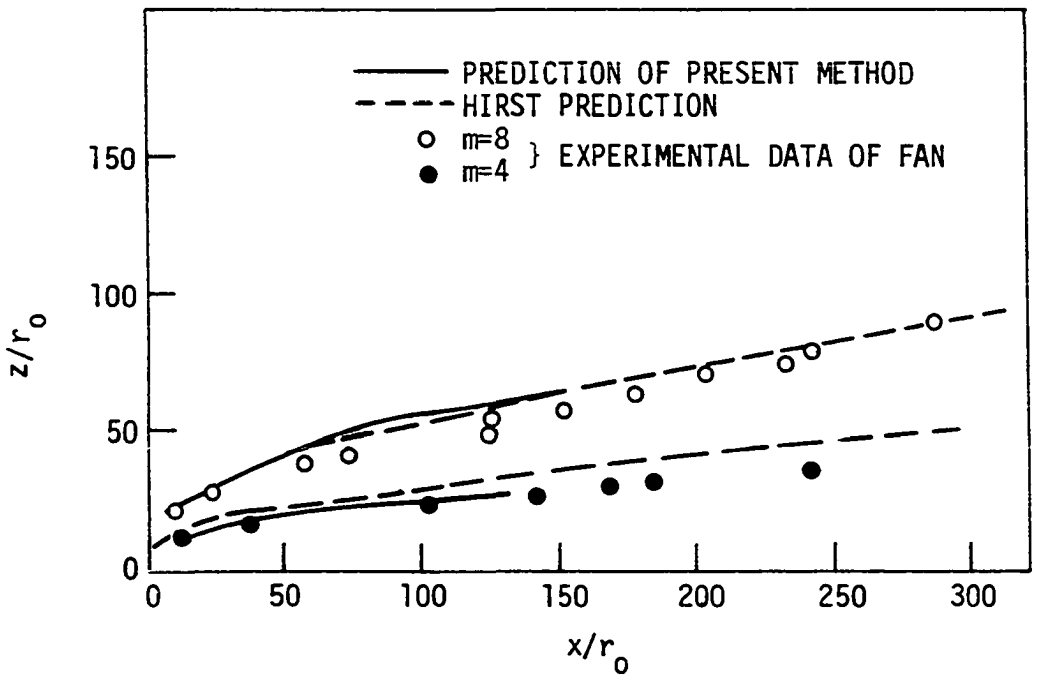

Fig. 5.11. Trajectories for buoyant jets discharged normal to a crossflow with $Fr_c = 400$.

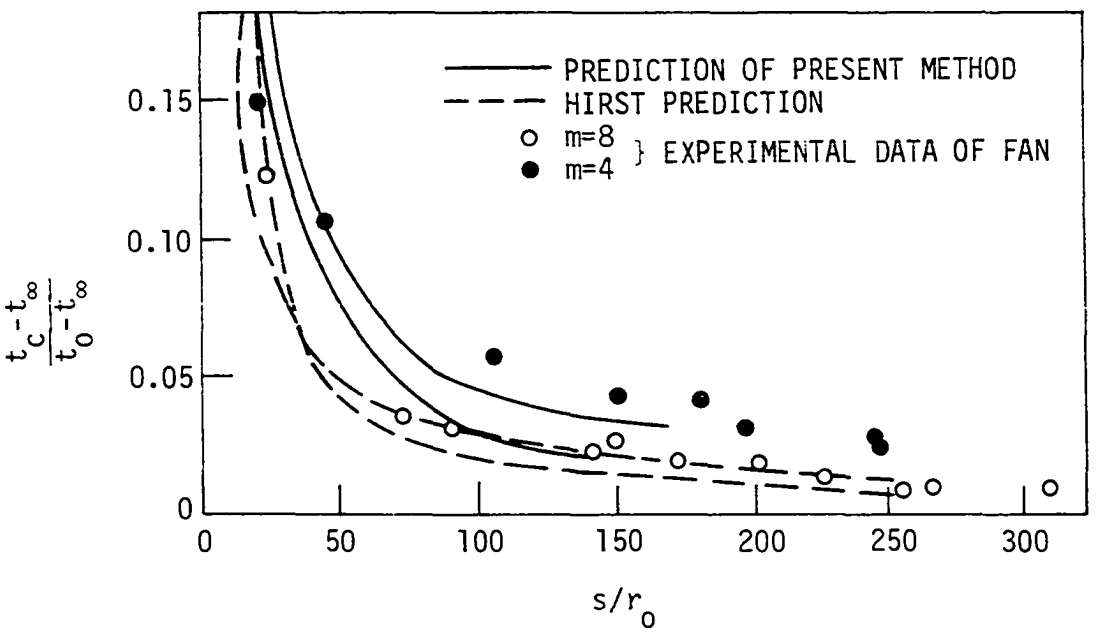

Fig. 5.12. Centerline temperature (or concentration) decay for buoyant jets discharged to a crossflow with $Fr_o = 400$.

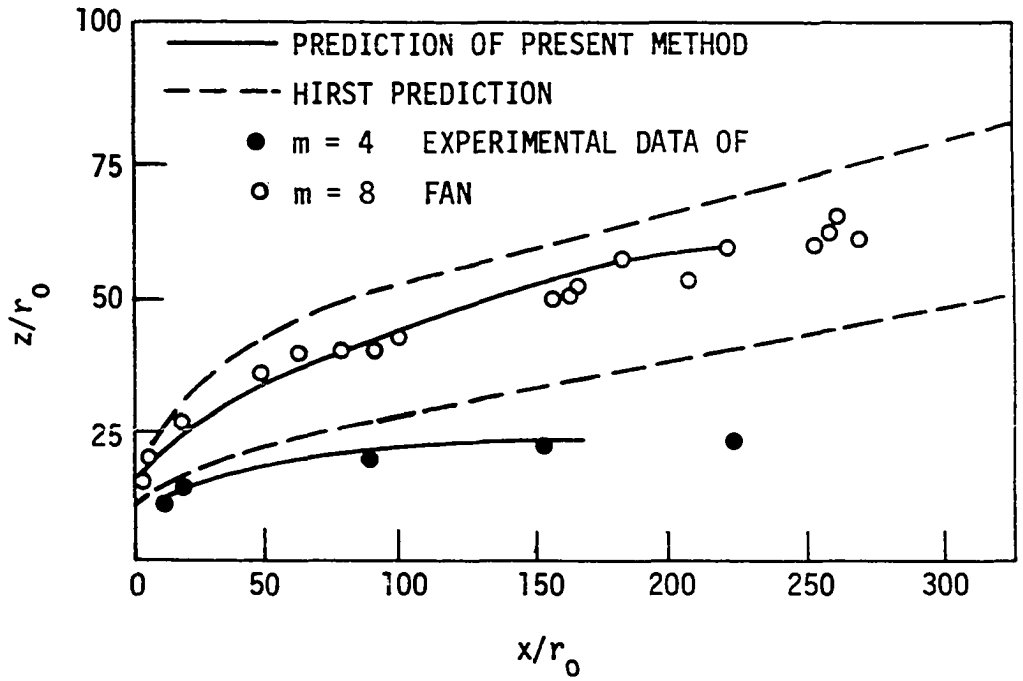

Fig. 5.13. Trajectories for buoyant jets discharged normal to a crossflow with Fr_o = 1600.

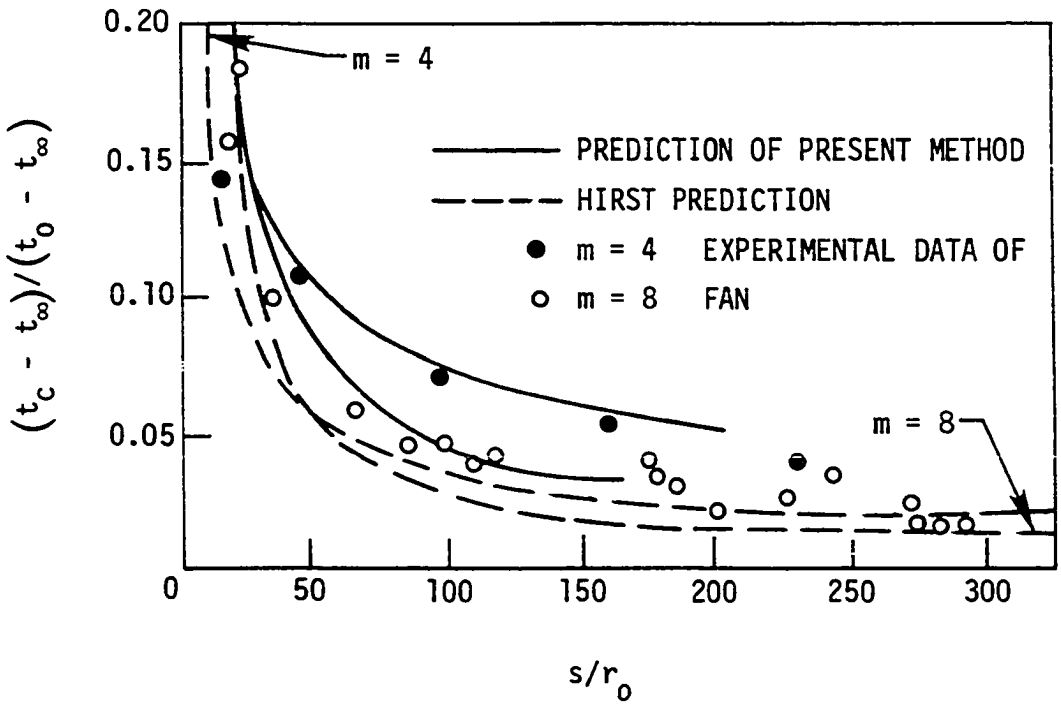

Fig. 5.14. Centerline temperature (or concentration) decay for buoyant jets discharged to a crossflow with Fr_o = 1600.

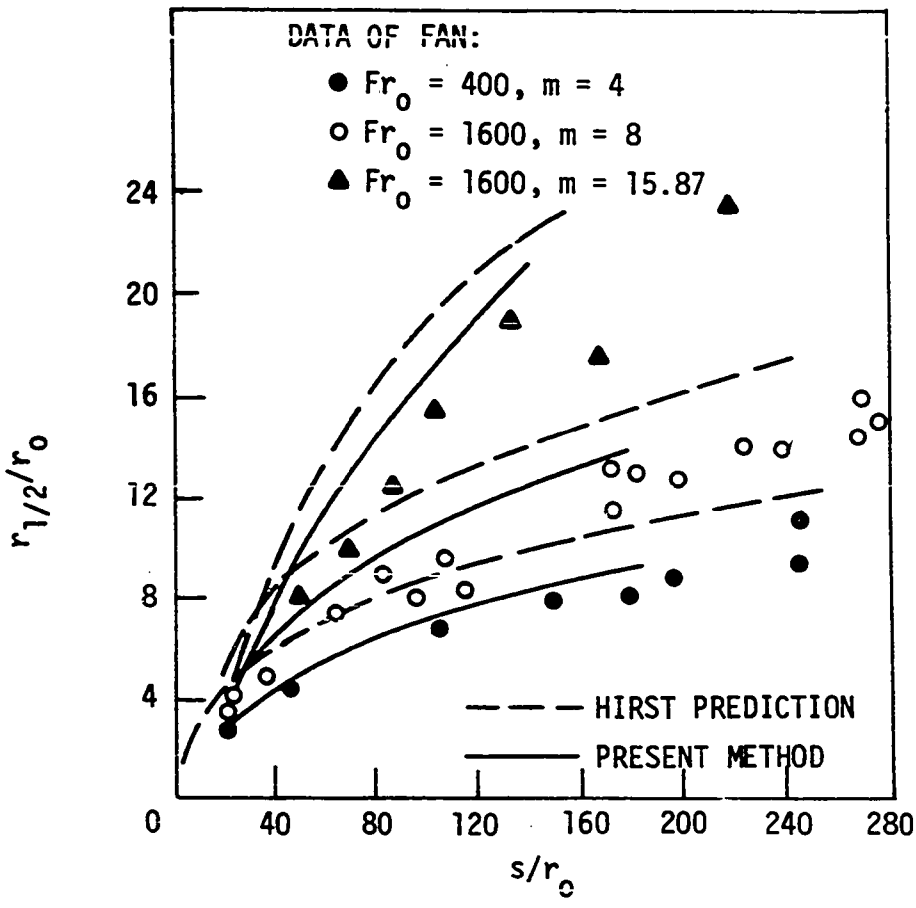

Fig. 5.15. Velocity halfwidth for some buoyant jets discharged to a crossflow.

Fr_o = 400 and m = 4, Fr_o = 1600 and m = 8, and Fr_o = 1600 and m = 15.87, are shown.

From Figures 5.9 through 5.15, the results for this configuration are encouraging. The general level of agreement between the predictions and the measurements is overall quite good, and the present prediction method appears to noticeably outperform the method of Hirst [4] which is based on an integral rather than a differential analysis.

C. Buoyant Vertical Jet in a Stratified Ambient

In the stratified ambient, the ambient temperature t_∞ varied as a function of the vertical height z.

$$T_{\infty,i} = \frac{-\lambda \ d_o}{Re_o(t_o - t_{\infty,o})} Z_i \tag{5.7}$$

where Z_i is the nondimensional vertical height at ith station, and $\lambda = -\frac{dt_\infty}{dz}$, is the ambient temperature stratification. This provides a variable boundary condition for the energy equation.

Before solving the s-momentum and r-momentum equations for the i+1 station, θ_i is known. So, Δz_+ is calculated from $\Delta z_+ = \Delta s_+ \sin \theta_i$, and the vertical height z can be found from $z_{i+1} = z_i + \Delta z_+$. The ambient temperature, $t_{\infty,i+1}$ is then computed for the next calculation.

The predicted trajectories for the buoyant jet discharged normal to a crossflow with a stratified ambient are compared with the experimental data of Hewett, Fay and Hoult [64] and the predictions of Hirst [4] in

(a) Figure 5.16 for $Fr_o = 12.3$, $\overline{T} = 35500$, $m = 1.869$,

(b) Figure 5.17 for $Fr_o = 11.35$, $\overline{T} = 2469$, $m = 2.016$,

(c) Figure 5.18 for $Fr_o = 11.30$, $\overline{T} = 3559$, $m = 2.058$, and

(d) Figure 5.19 for $Fr_o = 11.45$, $\overline{T} = 1127$, $m = 2.028$.

The present predictions agree with the experimental data as well as the predictions of Hirst [4] but neither prediction is generally in very good agreement with the experimental data of Hewett, Fay and Hoult [64].

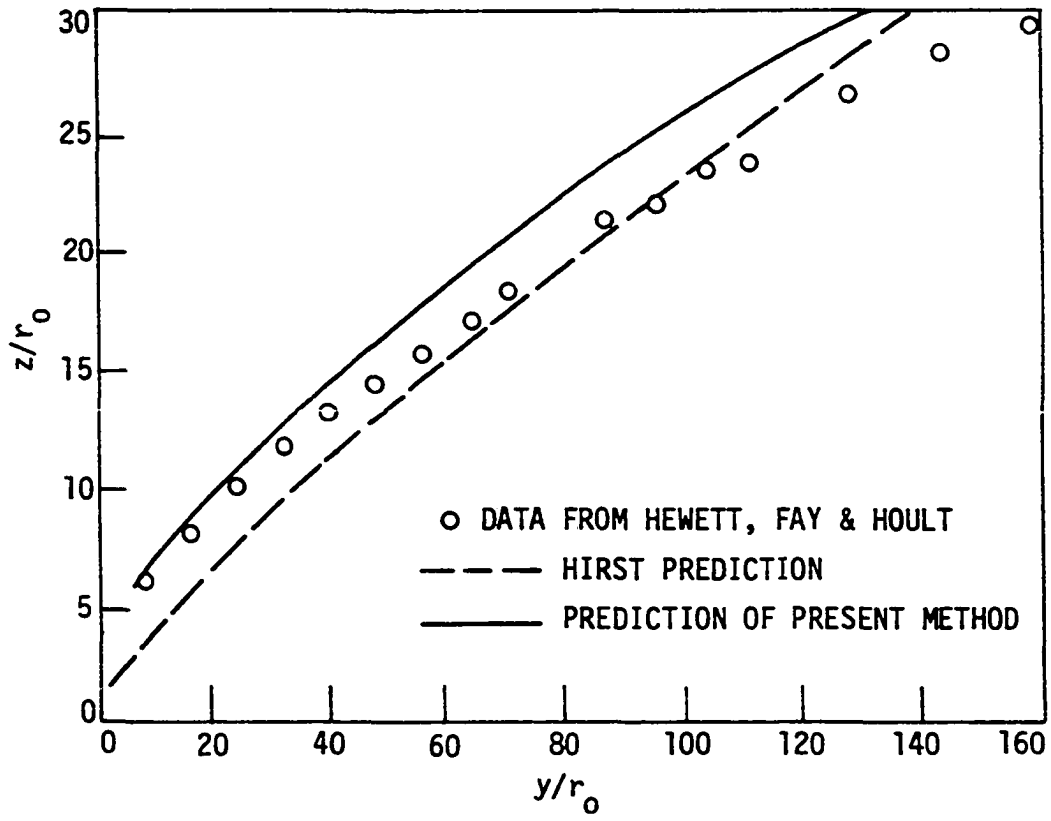

Fig. 5.16. Trajectory for buoyant jet discharged normal to a crossflow with stratified ambient, $Fr_o = 12.3$, $\bar{T} = 35500$, and $m = 1.869$.

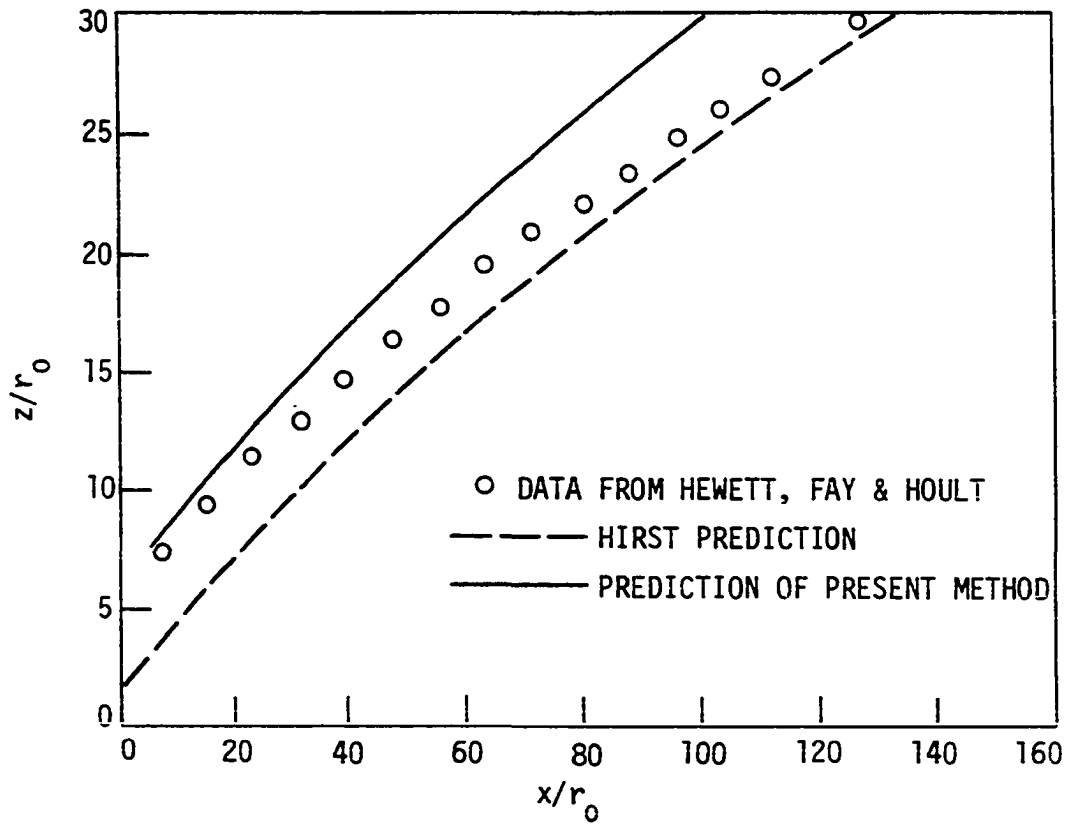

Fig. 5.17. Trajectory for buoyant jet discharged normal to a crossflow with stratified ambient, Fr_o = 11.35, $\overline{T}$ = 2469 and m = 2.016.

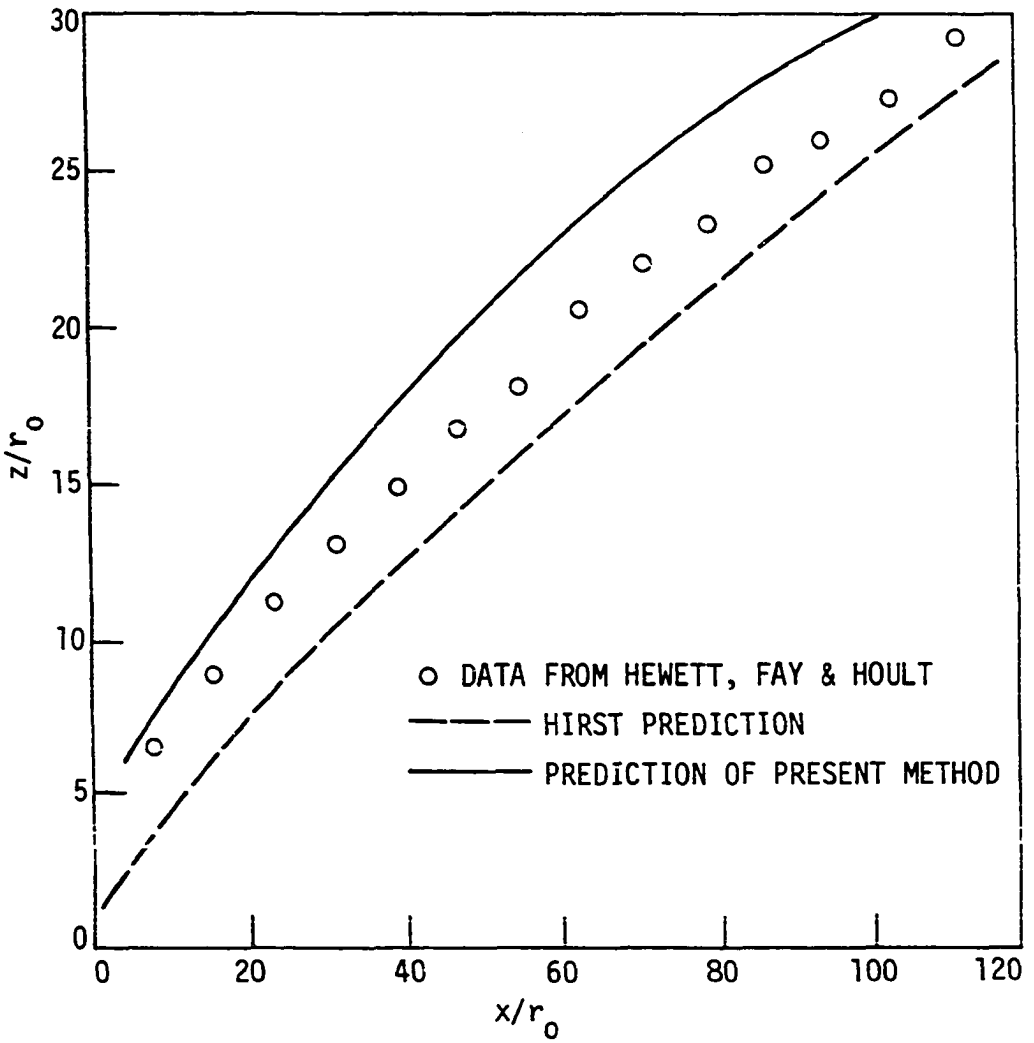

Fig. 5.18. Trajectory for buoyant jet discharged normal to a crossflow with stratified ambient, $Fr_o = 11.30$, $\bar{T} = 3559$, and $m = 2.058$.

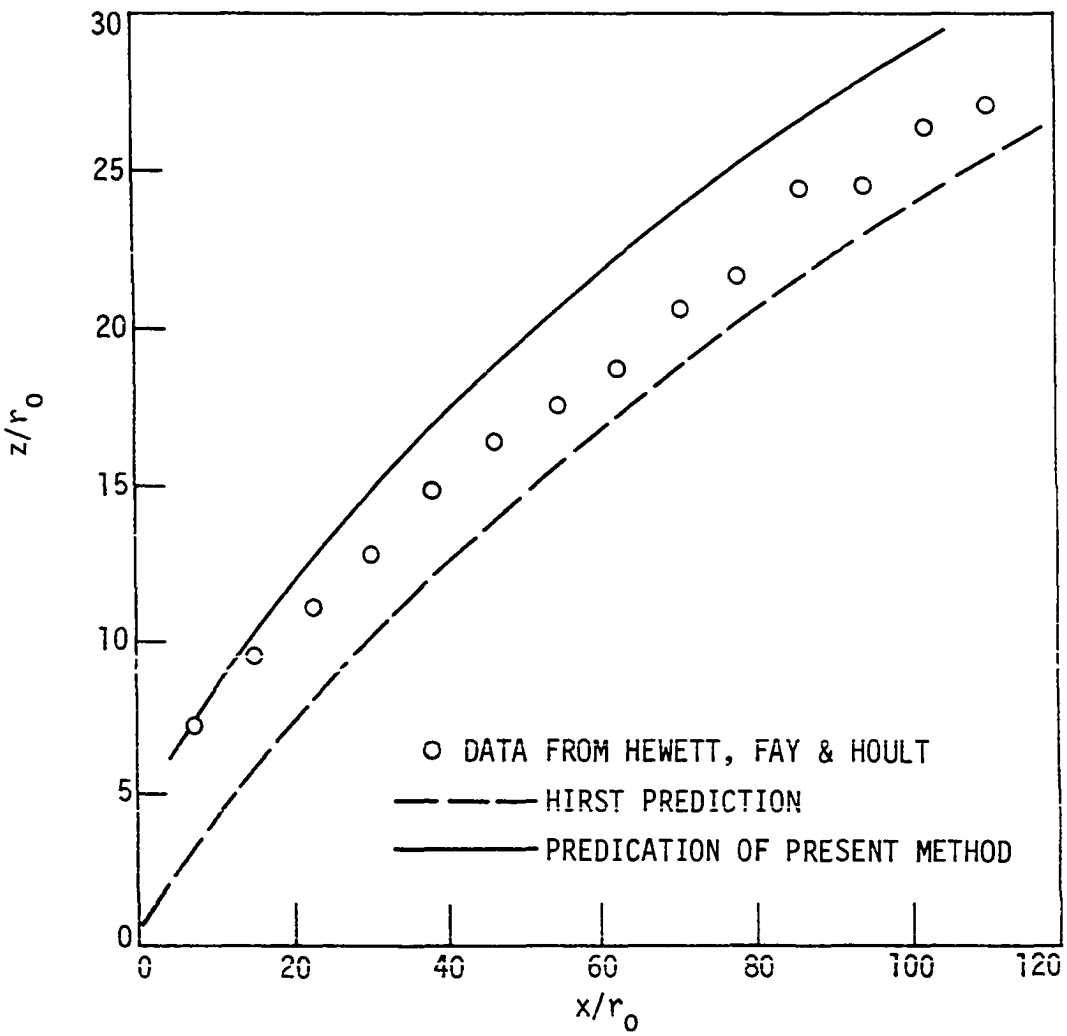

Fig. 5.19. Trajectory for buoyant jet discharged normal to a crossflow with stratified ambient, $Fr_o = 11.45$, $\overline{T} = 1127$ and m = 2.028.

VI. THREE-DIMENSIONAL FLOW

A. Introduction

Over the years, most analytical studies involving jets have dealt with two-dimensional or axisymmetric configurations. For those flows, the flow variables are functions of two spatial coordinates only [4, 65,66]. Chapters III through V described efforts mainly on the analysis and computation of the two-dimensional or axisymmetric jet. In true environmental applications, few flows will stay precisely axisymmetric especially for jets with curved trajectories. The flow of a jet from a rectangular orifice will be three dimensional even if the trajectory is straight. It is desirable to use the axisymmetric analysis for flows which deviate only slightly from two-dimensionality because of the significant savings in computer costs. However, it would appear that a fully three-dimensional analysis would be required for the more complex jet flows, such as jets involving interactions between adjacent cooling towers or from multiport diffusers, or jets involving surface or bottom effects.

Numerical approaches for solving three-dimensional flow problems have been studied extensively in the recent years by many researchers. Most of them worked on the flow in ducts or pipes [38,67,68], or boundary layer flows [69-71]. Little has been done for general three-dimensional jet flow problems. McGuirk and Rodi [72] calculated three-dimensional turbulent free jets issuing into coflowing surroundings by using a two-equation model, the k-ε model, which is relatively more complex.

Thompson [73], Aziz and Hellums [74] and Schetz et al. [23] solved three-dimensional jet problems by using vorticity as a dependent variable which makes the boundary conditions difficult to apply. Caretto et al. [75] predicted confined steady, laminar three-dimensional flows with recirculation by the SIVA (Simultaneous Variable Adjustment) and the SIMPLE (Semi-Implicit Method for Pressure-Linked Equations) methods. Generally speaking, three-dimensional calculations tend to employ primitive variables rather than vorticity and utilize a Poisson equation for pressure, or corrections to an assumed pressure. Patankar and Spalding [26] suggested a calculation procedure for three-dimensional internal flows whereby the longitudinal and lateral pressure gradients could be uncoupled permitting the use of a streamwise marching technique for the numerical solution. This concept can be adapted to free shear flows for conditions where the streamwise pressure gradient can be neglected or prescribed in advance. In this procedure, a pressure distribution is first assumed across the flow and the momentum equations solved for a streamwise marching step. These velocities will not generally satisfy the continuity equation giving rise to mass sources (or sinks) in the flow. The assumed pressure distribution is considered responsible for the mass sources and is corrected in a manner to result in the elimination of the sources. The various methods which have been used for this type of three-dimensional calculation [38,76] differ most noticeably in the approximations used in developing corrections for the pressure and velocities to satisfy the continuity equation.

In this chapter, initial work on a three-dimensional calculation procedure for jets is presented. A three-dimensional laminar jet flow is used as a test case to verify the method. Future work would likely involve the computation of turbulent flows. The experimental data of Sforza and Stasi [77] for the heated turbulent jet discharging from a rectangular orifice will provide a useful test case for future extensions of the present three-dimensional method to turbulent flows.

B. Formulation

Assuming that velocity derivatives in the main flow direction are much smaller than velocity derivatives across the jet permits the second streamwise derivative to be eliminated from the Navier-Stokes equations. Written in Cartesian coordinates, x, y, z, the governing equations for three-dimensional incompressible jet flows with constant properties are:

Continuity:

$$\frac{\partial u}{\partial x} + \frac{\partial v}{\partial y} + \frac{\partial w}{\partial z} = 0 \tag{6.1}$$

x-momentum:

$$u \frac{\partial u}{\partial x} + v \frac{\partial u}{\partial y} + w \frac{\partial u}{\partial z} = \nu\left(\frac{\partial^2 u}{\partial y^2} + \frac{\partial^2 u}{\partial z^2}\right) - \frac{1}{\rho} \frac{d\bar{p}}{dx} \tag{6.2}$$

y-momentum:

$$u \frac{\partial v}{\partial x} + v \frac{\partial v}{\partial y} + w \frac{\partial v}{\partial z} = \nu\left(\frac{\partial^2 v}{\partial y^2} + \frac{\partial^2 v}{\partial z^2}\right) - \frac{1}{\rho} \frac{\partial p}{\partial y} \tag{6.3}$$

z-momentum:

$$u \frac{\partial w}{\partial x} + v \frac{\partial w}{\partial y} + w \frac{\partial w}{\partial z} = \nu\left(\frac{\partial^2 w}{\partial y^2} + \frac{\partial^2 w}{\partial z^2}\right) - \frac{1}{\rho} \frac{\partial p}{\partial z} \tag{6.4}$$

Energy:

$$u \frac{\partial t}{\partial x} + v \frac{\partial t}{\partial y} + w \frac{\partial t}{\partial z} = \alpha\left(\frac{\partial^2 t}{\partial y^2} + \frac{\partial^2 t}{\partial z^2}\right) \tag{6.5}$$

The symbol $\bar{p}$ used for the pressure in the x-momentum equation, Equation (6.2), is different from p in the other two momentum equations. The pressure $\bar{p}$ can be thought as a space-averaged pressure over a cross section. This uncoupling of the pressure will permit the solution to be marched in the streamwise direction if some basis exists for the determination of $d\bar{p}/dx$ in advance of each streamwise step. For the present laminar jet test case, $d\bar{p}/dx$ was assumed to be zero since this pressure gradient must be very nearly zero outside the shear layer for this problem. The assumption in the pressure decoupling procedure is that small pressure variations across the flow play an important role in the distribution of the small v and w components of velocity but would have a negligible effect if included in the streamwise momentum equations.

The initial conditions for Equations (6.1) to (6.5) are, at $x = 0$:

$$u(y,z) = u_o \quad \text{for } y \leq y_o, \quad z \leq z_o,$$

$$u(y,z) = 0 \quad \text{for } y > y_o, \quad z > z_o,$$

$$v = w = 0,$$

$$t(y,z) = t_o \quad \text{for } y \leq y_o, \quad z \leq z_o,$$

$$t(y,z) = t_\infty \quad \text{for } y > y_o, \quad z > z_o,$$

$$p = p_o$$

where y_o and z_o are half-widths of orifice in y and z directions respectively. The boundary conditions are complicated:

(1) at $y = 0$

$$\frac{\partial u}{\partial y} = v = \frac{\partial w}{\partial y} = 0$$

$$\frac{\partial t}{\partial y} = 0, \quad \frac{\partial p}{\partial y} = \frac{\partial p'}{\partial y} = 0 \qquad (6.6)$$

(2) at $z = 0$

$$\frac{\partial u}{\partial z} = \frac{\partial v}{\partial z} = w = 0,$$

$$\frac{\partial t}{\partial z} = 0, \quad \frac{\partial p}{\partial z} = \frac{\partial p'}{\partial z} = 0 \qquad (6.7)$$

(3) at $y \to \infty$

$$u = u_\infty, \quad \frac{\partial v}{\partial y} = w = 0$$
$$t = t_\infty, \quad p = p_\infty, \quad p' = 0 \tag{6.8}$$

(4) at $z \to \infty$

$$u = u_\infty, \quad v = \frac{\partial w}{\partial z} = 0$$
$$t = t_\infty, \quad p = p_\infty, \quad p' = 0 \tag{6.9}$$

The flow configuration for three-dimensional jet discharging from a rectangular orifice is shown in Figure 6.1. The main flow direction is the x-direction. The rectangular orifice (or nozzle) has a dimension $2y_o$ by $2z_o$.

The pressure corrections and corresponding velocity corrections needed to satisfy the continuity equation must also satisfy the momentum equations, Equations (6.3) and (6.4). Utilizing all the terms in momentum equations for this purpose results in an unwieldy algebraic formulation and approximations are usually made which need not cause serious errors as long as the full momentum equations are used at some point in the iterative procedure.

As an example, the Patankar-Spalding method neglects all but the pressure term and the streamwise derivative:

$$u \frac{\partial v'}{\partial x} = - \frac{1}{\rho} \frac{\partial p'}{\partial y} \tag{6.10}$$

$$u \frac{\partial w'}{\partial x} = - \frac{1}{\rho} \frac{\partial p'}{\partial z} \tag{6.11}$$

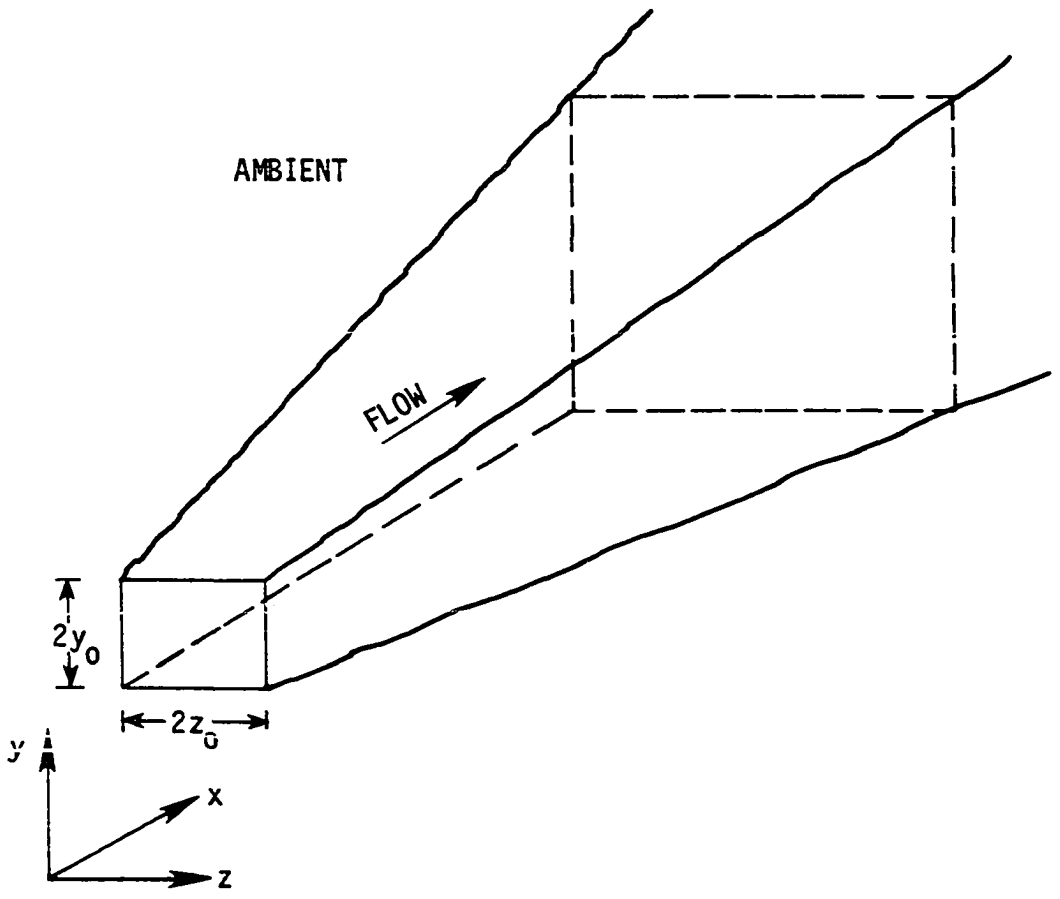

Fig. 6.1. Flow configuration for a three-dimensional jet discharged from a rectangular orifice.

For some flows this approximation causes difficulties. Briley [38], Raithby [36], and others have suggested alternative procedures. The present approach builds on a procedure suggested by Amsden and Harlow [78] for the driven cavity problem.

Near the edge of a jet developing in a quiescent ambient, there is no reason to expect $u\partial v'/\partial x$ to be more significant than the terms neglected in the momentum equation such as $v\partial v'/\partial y$. So in the present procedure, the correction step is thought of as an unsteady process whereby

$$\frac{\partial v}{\partial t} \simeq \frac{v-v^*}{\Delta t} = -\frac{1}{\rho}\frac{\partial p'}{\partial y} \tag{6.12}$$

$$\frac{\partial w}{\partial t} \simeq \frac{w-w^*}{\Delta t} = -\frac{1}{\rho}\frac{\partial p'}{\partial z} \tag{6.13}$$

Here, Δt can be thought as an imagined time step for maching, and for the iteration process to obtain v', w' and p' in steady state. From Equations (6.12) and (6.13), the corrected velocity components v and w can be evaluated from

$$v = v^* - \frac{1}{\rho}\frac{\Delta t}{\Delta y}(p'_{j,k} - p'_{j-1,k}) \tag{6.14}$$

$$w = w^* - \frac{1}{\rho}\frac{\Delta t}{\Delta z}(p'_{j,k} - p'_{j,k-1}) \tag{6.15}$$

This results in a Poisson equation for the pressure correction needed to annihilate the mass sources, taking Δt as unity,

$$\frac{1}{\rho}\left(\frac{\partial^2 p'}{\partial y^2} + \frac{\partial^2 p'}{\partial z^2}\right) = -S = -\left(\frac{\partial u}{\partial x} + \frac{\partial v^*}{\partial y} + \frac{\partial w^*}{\partial z}\right) \tag{6.16}$$

where S is a source term, v^* and w^* are velocity components calculated

from the momentum equations based on the estimated pressure p*, and p' is the pressure correction to correct p* by

$$p = p^* + p' \tag{6.17}$$

where p* is the uncorrected pressure, or initial estimate of pressure p.

The details of the derivation of the Poisson equation of p' and the corrections to velocity components v and w are shown in Appendix D.

C. Solution Method

The numerical scheme in the present study is similar to the three-dimensional parabolic procedure originated by Patankar and Spalding [26]. The velocity field is stored only two-dimensionally and the whole field is marched in the streamwise direction. This approach is much more economical of computer storage than would be a method requiring fully three-dimensional storage. The present solution method is based on the SMAC method [78] and the Patankar-Spalding method [26], and the modifications suggested by Briley [38] and Raithby [36].

Figure 6.2 shows the finite-difference grid points at two levels. It is supposed that all the variables are known at the ith level. They are marched to the i+1 level in the calculation procedure shown in summary as follows:

(1) A pressure field, p*, is assumed.

(2) The three momentum equations are solved using the guessed pressure p* to get u, v* and w* at i+1 level.

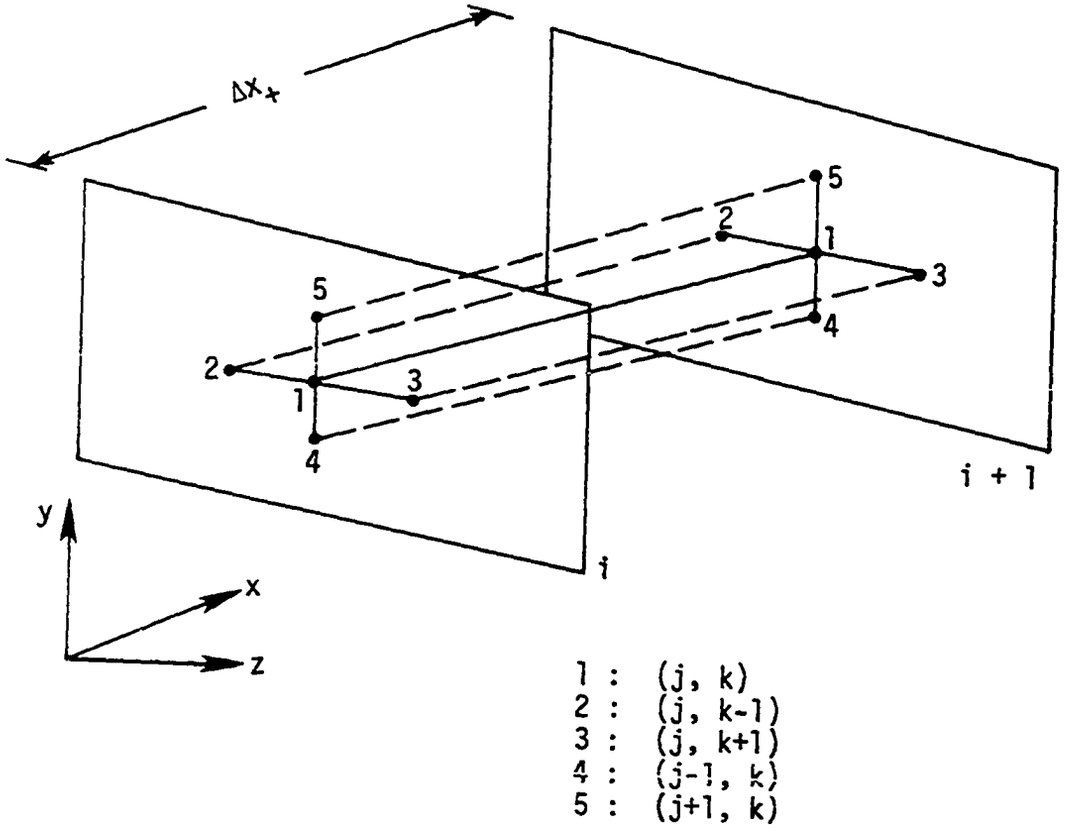

Fig. 6.2. Finite-difference grid points for three-dimensional calculations.

(3) This is known to be incorrect, since in general u, v* and w* will not satisfy the continuity equation. So the pressure correction equation is solved for p'. Several iterations using the Gauss-Seidel procedure are needed to obtain convergence.

(4) Corrected v's and w's are computed by solving the y and z momentum equations again using the corrected pressure. This procedure was used in the present test case. A faster but more approximate corrected velocity can be obtained from Equations (6.14) and (6.15). The u's do not need correction because the guessed pressure was not used in the x-momentum equation.

(5) The predicted u and the corrected v and w are checked to see if they satisfy the continuity equation. If not, iteration is needed through steps (3) to (5) until div $\vec{V}$ approaches an acceptable number ε.

(6) The energy equation is solved to obtain the temperature.

The finite-difference form of governing equations [Equations (6.2) to (6.5) and Equation (6.16)] will all contain five unknowns at i+1 level. Generally, the ADI method can be used for all of them. The grid is swept line by line using a tri-diagonal matrix algorithm (see [76]). The first sweep is in y-direction assuming that terms at (j,k+1) and (j,k-1) in the finite difference equation are temporarily fixed using values at ith level. The second sweep is in z-direction using values from the first sweep for terms at (j+1,k) and (j-1,k).

For each sweep, only three unknowns are to be determined, so TDMA can be applied.

For the jets discharged from a rectangular orifice, in general, the above mentioned ADI technique can be employed for any aspect ratios y_o/z_o. Only one quadrant (one-fourth of the cross section) of the jet is needed for the computation domain. Two of the boundaries consist of the symmetry planes at the centerlines. All variables have a zero normal gradient boundary conditions along these symmetry planes except the lateral velocity perpendicular to the plane. The test case used in the present study consists of a square orifice (aspect ratio equals 1). From the boundary conditions, it can be shown that a jet of this type has additional symmetry. In a quadrant, u, t, p and p' in the upper triangle are symmetrical about the diagonal line connected from the jet center point to an outer corner to those values in the lower triangle. The solution for u, t, p and p' can be obtained from calculations within just one-eighth of the jet cross section. Variables in the whole cross section can be determined from this triangle through symmetry. A full quadrant is needed for the calculation of v and w which are not symmetrical to the diagonal line. However, a solution is only needed for one of these variables, say v, because the other variable, w, can be set equal to v according to w(k,j) = v(j,k) which is required by symmetry. For calculations in the triangular domain, Gauss-Seidel iteration scheme was used for the x-momentum, energy and pressure correction equations instead of the ADI method because of the additional

difficulties the triangular geometry imposed on treatment of boundary conditions in the tri-diagonal matrix procedure. The reason for using a triangular domain for a square orifice was to assure a symmetry about diagonal line. A full quadrant can be used also, but the symmetry relations will not be exactly achieved. The use of the smaller triangular domain also reduced the computer costs for the calculation.

D. Results and Discussion

For three-dimensional laminar jet flows, no experimental data are available for comparison. Pai and Hsieh [79] predicted numerically the three-dimensional laminar jet without free stream for velocity and half-widths in an approximate analysis which neglected the crossflow velocity components in the x-momentum equation and which neglected the y and z momentum equations entirely. Figure 6.3 shows a secondary flow pattern for a three-dimensional laminar jet discharged from a square orifice at a cross section $x/y_o = 77$. The secondary flows formed a pair of "vortices" symmetrical to the diagonal line. Figure 6.4 shows the growth of the half-width of the same three-dimensional laminar jet. It can be seen that the jet cross section tends to approach a round contour downstream. Eventually, the jet cross section will adjust to an axisymmetrical form no matter whether the initial shape is square or rectangular. A comparison of the velocity profiles at center planes computed by the present method with the prediction of Pai and Hsieh [79] was shown in Figure 6.5. The comparison shows an acceptable agreement between these two predictions.

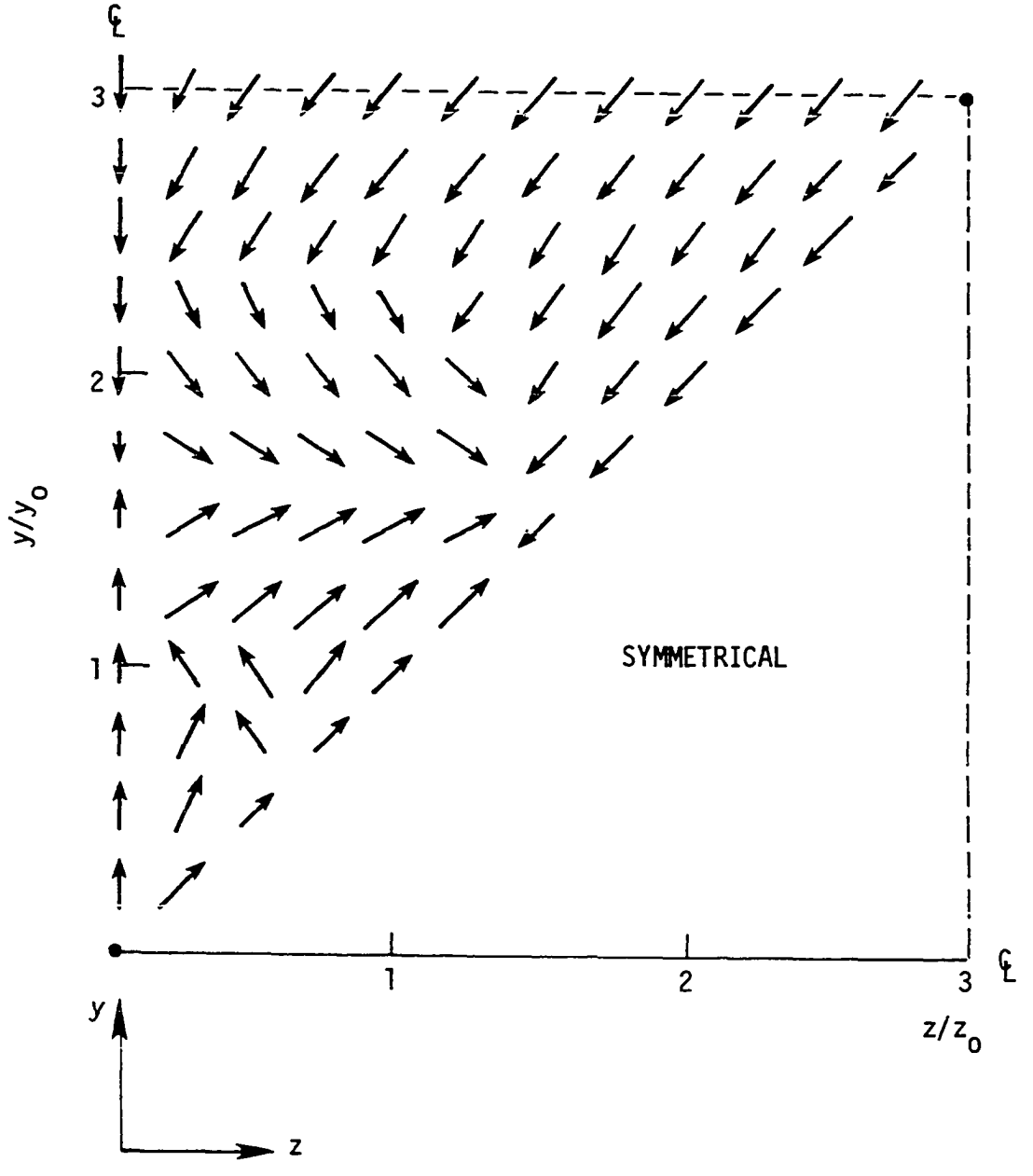

Fig. 6.3. Secondary flow pattern for a three-dimensional jet discharged from a square orifice at a cross section $x/y_o = 77$ ($x^* = 0.042$).

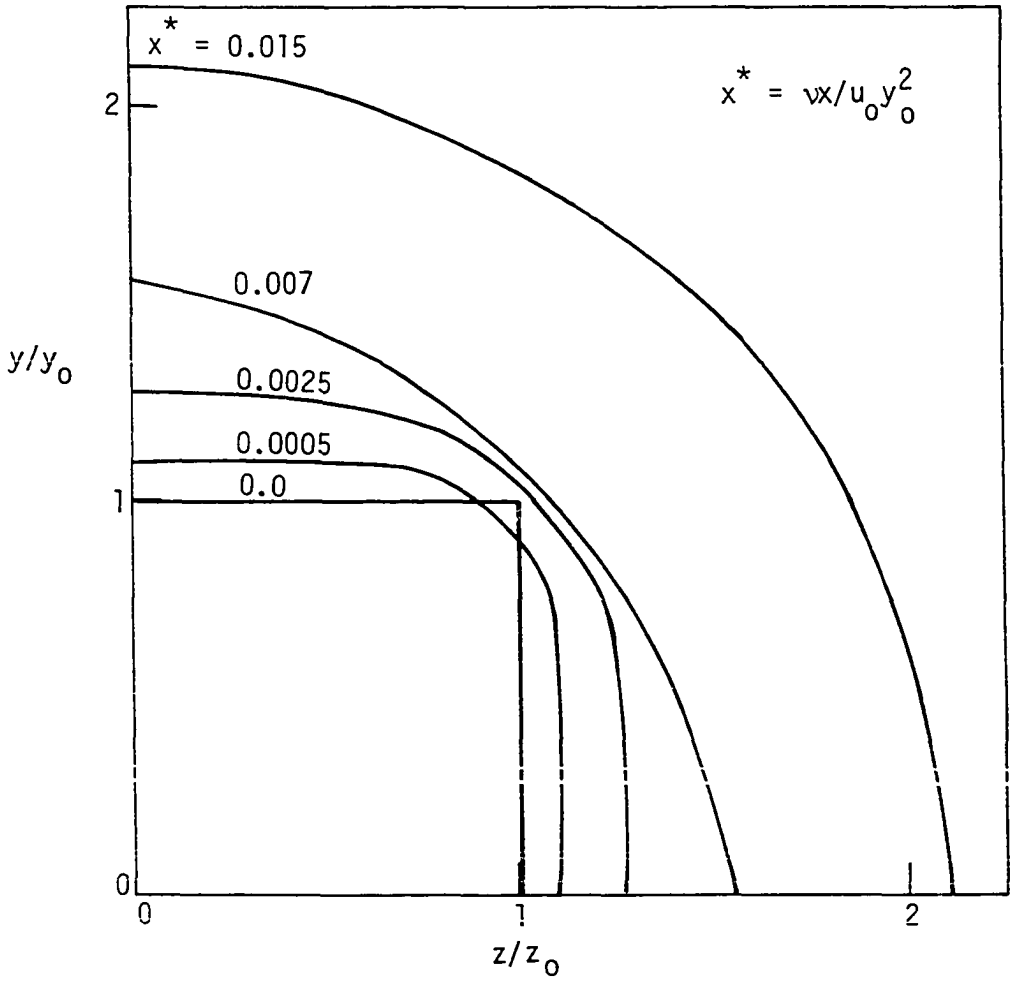

Fig. 6.4. Growth of half-width of a three-dimensional laminar jet.

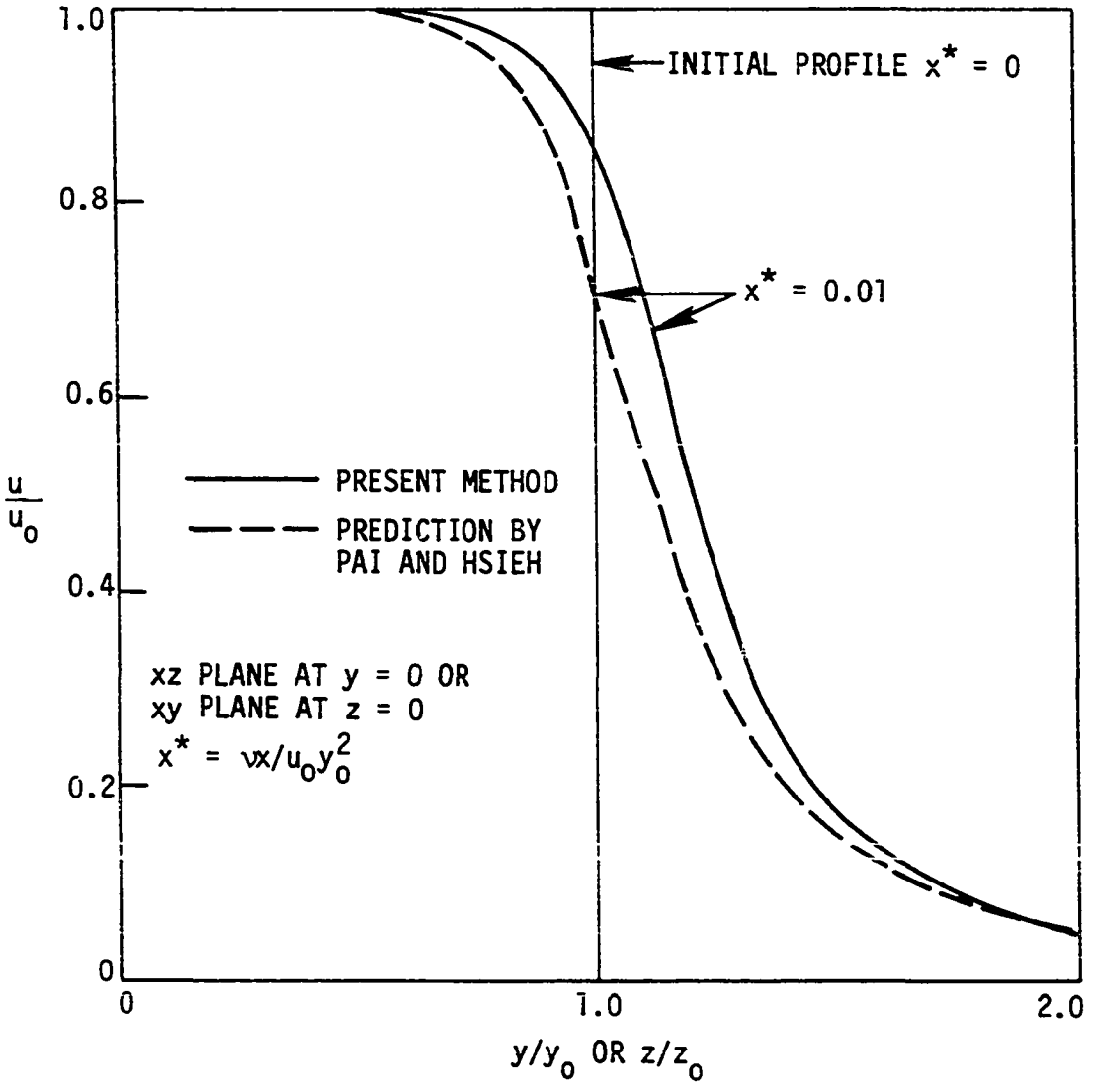

Fig. 6.5. Velocity profile for a three-dimensional laminar jet.

Some comments related to the development of the three-dimensional calculation scheme are as follows:

(1) Often the pressure correction p' changed sign after each iteration through the momentum equations. An under-relaxation parameter was needed to maintain convergence.

(2) The calculation procedure is very sensitive to the boundary location. Care has been taken on the determination of the boundary location and the way to apply boundary conditions.

(3) The source term S can not be exactly zero even after pressure correction. It is acceptable when S is less than a very small number, ε.

(4) The boundary layer model, i.e., neglecting $\partial^2/\partial x^2$ terms, is a good approximation for the three-dimensional free jet problem provided that the Reynolds number at the discharge (nozzle exit) is not too low.

(5) Although no experimental data are available for the three-dimensional jet, based on the results of axisymmetric jets and the comparison with the predictions of Pai and Hsieh, it is felt that the numerical solutions of the three-dimensional jet presented here are reasonably accurate.

VII. CONCLUSIONS AND RECOMMENDATIONS

The principal conclusions of the present investigation are:

(1) The finite-difference prediction method which is based on an axisymmetric flow model is seen to work quite well for the analysis of turbulent jets following curved trajectories in flowing ambients and offers the potential of a significant savings in computation time over fully three-dimensional predictions methods for flows of the type considered in the present study. Special emphasis has been placed on the thermal discharge from power plants and other sources into adjacent water bodies or the atmosphere. It is hoped that some of the prediction procedures will be of assistance in the discharge design process.

(2) The lumped parameter treatment of the transverse momentum equation appears to be adequate for the cases considered and was seen to yield good predictions of jet trajectories over a wide range of discharge angles into a crossflow.

(3) The proposed curvature correction factor for mixing length appears to improve predictions for the decay of centerline temperatures and velocity. It is interesting to note that the prediction of trajectories themselves seemed relatively insensitive to the effects of curvature and buoyancy on the turbulent viscosity.

(4) The present axisymmetric model worked well for a wide range of applications, including buoyant and nonbuoyant jets discharged at various angles to quiescent, coflowing or crossflowing ambients.

(5) For the jets in stratified ambients, the predictions were not as good as those in uniform ambients when compared to the experimental data.

(6) The three-dimensional calculation procedure developed here for three-dimensional laminar flows appears to give reasonable predictions and shows promise for extension to three-dimensional turbulent flows.

(7) Much larger computer time was required for the evaluation of the three-dimensional flows than for the axisymmetric flows.

The following areas of study are recommended as extensions of the present work:

(1) Further development of the numerical scheme to include turbulent jets and a turbulence model for the three-dimensional flows.

(2) Prediction of three-dimensional turbulent jet flows with a curved trajectory such as jets in crossflowing ambients.

(3) Prediction of flows having three-dimensional trajectories and involving complex interactions such as those between adjacent cooling towers or from multiport diffusers.

VIII. REFERENCES

1. Ades, M. "Analysis of Round Turbulent Buoyant Jets Discharged to a Cross Flow." M.S. Thesis, Israel Institute of Technology, 1975.

2. El-Wakil, M. M. Nuclear Energy Conversion. New York: Intext Educational Publishers, 1971.

3. Madni, I. K. "A Finite-Difference Analysis of Turbulent, Axisymmetric, Buoyant Jets and Plumes." Ph.D. Thesis, Library, Iowa State University, 1975.

4. Hirst, E. A. "Analysis of Round Turbulent, Buoyant Jets Discharged to Flowing Stratified Ambients." Report No. ORNL-4585, Oak Ridge National Laboratory, 1971.

5. Schatzmann, M. "Auftriebsstrahlen in Natürlichen Strömungen Entwicklung eines Mathematischen Modells." Doktor-Ingenieurs Dissertation, Univ. Karlsruhe, West Germany, 1976.

6. Madni, I. K., and Pletcher, R. H. "Buoyant Jets Discharging Nonvertically into a Uniform, Quescent Ambient — A Finite-Difference Analysis and Turbulence Modeling." ASME Journal of Heat Transfer 99, No. 4 (November 1977):641-647.

7. Hirst, E. A. "Buoyant Jets Discharged to Quiescent Stratified Ambients." Journal of Geophysical Research 76, No. 30 (1971): 7375-7384.

8. Campbell, J. F., and Schetz, J. A. "Analysis of the Injection of a Heated, Turbulent Jet into a Moving Mainstream, with Emphasis on a Thermal Discharge in a Waterway." Report No. VIP-E-72-24, 1972. College of Engineering, Virginia Polytechnic Institute and State University.

9. Abraham, G. "Jet Diffusion in Stagnant Ambient Fluid." Delft Hydraulics Lab. No. 29, 1963.

10. Frankel, R. J., and Cumming, J. D. "Turbulent Mixing Phenomena of Ocean Outfalls," ASCE Journal of Sanitary Engineering Division 91, SA2 (1965):33-59.

11. Anwar, H. O. "Behavior of Buoyant Jet in Calm Fluid." ASCE Journal of the Hydraulics Division 91, HY4 (1969):139-153.

12. Fan, L. N. "Turbulent Buoyant Jets into Stratified or Flowing Ambient Fluids." Keck Lab. of Hydraulics and Water Resources, California Institute of Technology, Report No. KH-R-15, 1967.

13. Gordier, R. L. "Studies on Fluid Jets Discharging Normally into Moving Liquid." University of Minnesota, St. Anthony Falls Hydraulic Lab., Tech. Paper No. 28, Series B, 1959.

14. Keffer, J. F., and Baines, W. D. "The Round Turbulent Jet in a Cross-Wind." Journal of Fluid Mechanics 15, No. 4 (1963):481-497.

15. Pratte, B. D., and Baines, W. D. "Profiles of the Round Turbulent Jet in a Cross Flow." ASCE Journal of the Hydraulics Division 93, HY 6 (1967):53-64.

16. Platten, J. L., and Keffer, J. F. "Entrainment in Deflected Axisymmetric Jets at Various Angles to the Stream." University of Toronto, Mechanical Engineering Department, UTME-TP-6808, 1968.

17. Fink, L. "Strahl in Turbulenzarmer und Turbulenter Grundströmung." Doktor-Ingenieurs Dissertation, University Karlsruhe, West Germany, 1975.

18. Briggs, G. A. Plume Rise. USAEC Division of Technical Information, 1969.

19. Hoult, D. P., Fay, J. A., and Forney, L. J. "A Theory of Plume Rise Compared with Field Observations." Journal Air Pollution Control Association 19(9) (1969):585-590.

20. Fay, J. A., Escudier, M., and Hoult, D. P. "A Correlation of Field Observations of Plume Rise." Journal Air Pollution Control Association 20(6) (1970):391-397.

21. Fan, L. N., and Brooks, N. H. "Numerical Solutions of Turbulent Buoyant Jet Problems." Keck Lab. of Hydraulics and Water Resources, California Institute of Technology, Report No. KH-R-18, 1969.

22. Shirazi, M. A., and Davis, L. R. "Workbook of Thermal Plume Prediction, Volume 1, Submerged Discharge." Environmental Protection Technology Series, EPA-R2-72-005a, August 1972.

23. Schetz, J. A., Chien, C. J., and Sill, B. L. "Heat Transfer and Fluid Mechanics of the Thermal Pollution Problem." Proceedings of the 5th International Heat Transfer Conference 5 (1974): 129-133.

24. Zelazny, S. W., and Baker, A. J. "Predictions in Environmental Hydrodynamics Using the Finite Element Method: II. Application." AIAA Journal 13, No. 1 (January 1975):43-46.

25. McGuirk, J. J., and Spalding, D. B. "Mathematical Modeling of Thermal Pollution in Rivers." Proceedings of International Conference on Mathematical Models for Environmental Problems, University of Southampton, England, September 1975.

26. Patankar, S. V., and Spalding, D. B. "A Calculation Procedure for Heat, Mass and Momentum Transfer in Three-Dimensional Parabolic Flows." International Journal of Heat and Mass Transfer 15, (1972):1787-1806.

27. Madni, I. K., and Pletcher, R. H. "Prediction of Turbulent Jets in Coflowing and Quiescent Ambients." Trans. ASME, Journal of Fluids Engineering 97 (1975):558-567.

28. Hwang, S. S., and Pletcher, R. H. "Prediction of Thermal Plumes From Power Plants." Affiliate Research Program in Electrical Power, Iowa State University, Annual Report ISU-ERI-Ames-77338, 1977.

29. Hwang, S. S., and Pletcher, R. H. "Prediction of Buoyant Turbulent Jets and Plumes in a Cross Flow." Proceedings of the Sixth International Heat Transfer Conference, August 1978.

30. Ryskiewich, B. S., and Hafetz, L. "An Experimental Study of the Free Surface Effect on a Buoyant Jet." General Dynamics Report No. U440-74-103, 1975.

31. Pryputniewicz, R. J., and Bowley, W. W. "An Experimental Study of Vertical Buoyant Jets Discharged into Water of Finite Depth." ASME Journal of Heat Transfer 97 (May 1975):274-281.

32. Fox, D. G. "Forced Plume in a Stratified Fluid." Journal of Geophysical Research 75, No. 33 (1970):6818-6835.

33. Sneck, H. J., and Brown, D. H. "Plume Rise from Large Thermal Sources Such as Cooling Towers." General Electric Report No. 72GEN025, Nov. 1972.

34. Madni, I. K., and Pletcher, R. H. "Prediction of Turbulent Forced Plumes Issuing Vertically into Stratified or Uniform Ambients." Trans. ASME, Journal of Heat Transfer 99 (1977):99-104.

35. Trent, D. S., and Welty, J. R. "Numerical Thermal Plume Model for Vertical Outfalls in Shallow Water." Environmental Protection Agency Report No. EPA-R2-73-162, 1973.

36. Raithby, G. D. "Prediction of Dispersion by Surface Discharge." Basin Investigation and Modeling Section, Applied Research Division, Canada Centre for Inland Waters, Burlington, Ontario, Canada, August 1976.

37. Zoby, E. V. "Finite-Difference Solution for the Incompressible Driven Cavity Flow Problem." Numerical Study of Incompressible Viscous Flow in a Driven Cavity, NASA SP-378, 1975.

38. Briley, W. R. "Numerical Method for Predicting Three-Dimensional Steady Viscous Flow in Ducts." Journal of Computational Physics 14.(1974):8-28.

39. Laasonen, P. "Über eine Methode zur Lösung der Wärmeleitungleichung." Acta Math. 81 (1949):309.

40. Crank, J., and Nicolson, P. "A Practical Method for Numerical Evaluation of Partial Differential Equations of the Heat Conduction Type." Proceedings of the Cambridge Philosophical Society 43 (1947):50-67.

41. DuFort, E. C., and Frankel, S. P. "Stability Conditions in the Numerical Treatment of Parabolic Differential Equations." Mathematical Tables Aid Computation 7 (1953):135-152.

42. Saul'yev, V. K. Integration of Equations of Parabolic Type by the Method of Nets. New York: Macmillan, 1964.

43. Barakat, H. Z., and Clark, J. A. "On the Solution of the Diffusion Equation by Numerical Methods." Journal of Heat Transfer, Trans. ASME, Series C, 88 (1966):421-427.

44. Larkin, B. K. "Some Stable Explicit Difference Approximations to the Diffusion Equation." Math. Computation 18 (1964):196-202.

45. White, F. M. Viscous Fluid Flow. New York: McGraw-Hill, Inc., 1974.

46. Schlichting, H. Boundary-Layer Theory. 6th edition. New York: McGraw-Hill, Inc., 1968.

47. Launder, B. E., and Spalding, D. B. Mathematical Models of Turbulence. New York: Academic Press, 1972.

48. Bradshaw, P. "The Analogy Between Streamline Curvature and Buoyancy in Turbulent Shear Slow." Journal of Fluid Mechanics 36, part 1 (1969):177-191.

49. Bradshaw, P. "Effects of Streamline Curvature on Turbulent Flow." North Atlantic Treaty Organization, AGARDograph 169, 1973.

50. Johnston, J. P., and Eide, S. A. "Turbulent Boundary Layers on Centrifugal Compressor Blades: Prediction of the Effects of Surface Curvature and Rotatior." ASME Paper No. 76-FE-10, 1976.

51. Irwin, H. P. A. H., and Smith, P. A. "Prediction of the Effect of Streamline Curvature cn Turbulence." Physics of Fluids 18, (1975):624-630.

52. Ames, W. F. Numerical Methods for Partial Differential Equations. New York: Barnes and Noble, Inc., 1969.

53. Thomas, L. H. "Elliptic Problems in Linear Difference Equations Over a Network." Watson Sci. Comp. Lab. Report, Columbia University, New York, 1949.

54. Bruce, G. H., Peaceman, D. W., Rachford, H. H., and Rice, J. D. Trans. Am. Inst. Min. Engineers (Petrol. Division) 198 (1953):79.

55. Carnahan, B., Luther, H. A., and Wilkes. J. O. Applied Numerical Methods. New York: John Wiley and Sons, Inc., 1971.

56. Hirsch, R. S., and Rudy, D. H. "The Role of Diagonal Dominance and Cell Reynolds Number in Implicit Methods for Fluid Mechanics Problems." Journal Computational Physics 16 (1974):304-310.

57. Varga, R. S. Matrix Iterative Numerical Analysis. New York: Wiley, 1962.

58. Boussinesq, J. "Sur la Maniere Dent les Vitesse, Dans Tube Cylindrique de Section Circulaire, Evase a son Entree, se Distribuent Depuis Cette Entree Jusq' aux Endroit ou se Trouve Establi un Regime Uniforme." Comptes Rendus 113 (1891):49-59.

59. Abraham, G. "Horizontal Jets in Stagnant Fluid of Other Density." ASCE Journal of Hydraulics Division 91, HY4 (1965):139-153.

60. Launder, B. E., and Spalding, D. B. "The Numerical Computation of Turbulent Flows." Computer Methods in Applied Mechanics and Engineering 3 (1974):269-289.

61. Ayoub, G. M. "Dispersion of Buoyant Jets in a Coflowing Ambient Flow." Ph.D. Thesis, University of London, March 1971.

62. McGuirk, J. J. "Prediction of Turbulent Buoyant Jets in a Coflowing Stream." Ph.D. Thesis, University of London, July 1975.

63. Hong, S. W. "Laminar Flow Heat Transfer in Ordinary and Augmented Tubes." Doctoral Dissertation, Library, Iowa State University, Ames, Iowa, 1974.

64. Hewett, T. A., Fay, J. A., and Hoult, D. P. "Laboratory Experiments of Smokestack Plumes in a Stable Atmosphere." MIT Fluid Mechanics Lab., Publication No. 70-9, 1970.

65. Pai, S. I. Fluid Dynamics of Jets. Princeton, New Jersey: D. Van Nostrand Co., Inc., 1954.

66. Abramovich, G. N. The Theory of Turbulent Jets. Cambridge, Mass.: M.I.T. Press, 1963.

67. Majumdar, A. K., and Spalding, D. B. "A Numerical Investigation of Three-Dimensional Flows in a Rotating Duct by a Partially-Parabolic Procedure." ASME Paper No. 77-WA/FE-7, 1977.

68. Skiadaressis, D., and Spalding, D. B. "Heat Transfer in a Pipe Rotating Around a Perpendicular Axis." ASME Paper No. 77-WA/HT-39, 1977.

69. Cebeci, T. "Calculation of Three Dimensional Boundary Layers: II. Three-Dimensional Flows in Cartesian Coordinates." AIAA Journal 13, No. 8 (August 1975):1056-1064.

70. Cebeci, T., Kaups, K., and Moser, A. "Calculation of Three-Dimensional Boundary Layers: III. Three-Dimensional Flows in Orthogonal Curvilinear Coordinates." AIAA Journal 14, No. 8 (August 1976):1090-1094.

71. Bradshaw, P. "Calculation of Three-Dimensional Turbulent Boundary Layers." Journal Fluid Mechanics 46, Part 3 (1971):417-445.

72. McGuirk, J. J., and Rodi, W. "The Calculation of Three-Dimensional Turbulent Free Jets." Symposium on Turbulent Shear Flows, Vol. 1, April 18-20, 1977. Pennsylvania State University, Univ. Park, Pennsylvania.

73. Thompson, J., Jr. "Two Approaches to the Three-Dimensional Jet-in-Cross-Wind Problem: A Vortex Lattice Model and a Numerical Solution of the Navier-Stokes Equations." Ph.D. Thesis, Georgia Institute of Technology, 1971.

74. Aziz, K., and Hellums, J. D. "Numerical Solution of the Three-Dimensional Equations of Motion for Laminar Natural Convection." The Physics of Fluids 10, No. 2 (February 1967):314-324.

75. Caretto, L. S., Gosman, A. D., Patankar, S. V., and Spalding, D. B. "Two Calculation Procedures for Steady, Three-Dimensional Flows with Recirculation." Proceedings of Third International Conference on Numerical Methods in Fluid Dynamics, Paris, July 1972.

76. Roache, P. J. Computational Fluid Dynamics. Albuquerque, N.M.: Hormosa Publishers, 1972.

77. Sforza, P. M., and Stasi, W. "Heated Three-Dimensional Turbulent Jets." ASME Paper No. 77-WA/HT-27.

78. Amsden, A. A., and Harlow, F. H. "The SMAC Method: A Numerical Techniques for Calculating Incompressible Fluid Flows." LA-4370, Los Alamos Sci. Lab., Univ. of California, February 17, 1970.

79. Pai, S. I., and Hsieh, T. "Numerical Solution of Laminar Jet Mixing with and without Free Stream." Applied Scientific Research 27 (October 1972):39-62.

IX. ACKNOWLEDGMENTS

This work was partially supported by the Iowa State University Power Affiliate Research Program and by the Engineering Research Institute through funds provided by the National Science Foundation under Grant ENG 74-22193.

The author wishes to express his sincere appreciation to:

- Dr. Richard H. Pletcher for his supervision, encouragement and assistance throughout the course of this work, and his editorial comments and recommendations for the reporting of this work.

- Dr. Arthur E. Bergles, Dr. William J. Cook, Dr. John C. Tannehill and Dr. Donald F. Young for their helpful suggestions and comments during the Ph.D. program.

- Mr. Henry McDonald of Scientific Research Associates, Incorporation for his helpful suggestions regarding the pressure correction procedure.

- His wife, Mei-Ping, for her continuous encouragement.

X. APPENDIX A: FINITE DIFFERENCE FORMULATION FOR THE PRELIMINARY STUDIES

In the preliminary studies, several finite-difference methods, including two implicit methods and five explicit methods, were tested to solve a simpler boundary layer flow problem in order to choose an appropriate method for the present calculations.

The governing partial differential equation for the boundary layer flow problem is of the form

$$u \frac{\partial u}{\partial x} + v \frac{\partial u}{\partial y} = \nu \frac{\partial^2 u}{\partial y^2} \tag{10.1}$$

where ν, the viscosity, is assumed constant in this evaluation for simplicity. Naturally the continuity equation is needed to complete the problem formulation but is being omitted here since the same standard difference form [Equation (3.43)] was used in all cases shown below. The finite-difference formulation for Equation (10.1) by these seven schemes are presented as follows:

1. Fully implicit method:

$$u_j^i \frac{(u_j^{i+1} - u_j^i)}{\Delta x_+} + v_j^i \frac{(u_{j+1}^{i+1} - u_{j-1}^{i+1})}{2\Delta y} = \nu \frac{(u_{j+1}^{i+1} - 2u_j^{i+1} + u_{j-1}^{i+1})}{(\Delta y)^2} \tag{10.2}$$

Here, the coefficients of convective terms, u_j^i and v_j^i, took the values from previous step, i.e., ith station. This procedure linearized the equation and reduced the time required for the computation.

2. Crank-Nicolson method:

The implicit Crank-Nicolson method used the average values at ith and i+1st stations for the y-derivative terms. Linearization was again employed for the coefficients.

$$u_j^i \frac{(u_j^{i+1} - u_j^i)}{\Delta x_+} + \frac{v_j^i}{2}\left[\frac{(u_{j+1}^{i+1} - u_{j-1}^{i+1})}{2\Delta y} + \frac{(u_{j+1}^i - u_{j-1}^i)}{2\Delta y}\right]$$

$$= \nu \frac{(\delta^2 u)_j^i + (\delta^2 u)_j^{i+1}}{2(\Delta y)^2} \tag{10.3}$$

where

$$(\delta^2 u)_j^i = u_{j+1}^i - 2u_j^i + u_{j-1}^i$$

$$(\delta^2 u)_j^{i+1} = u_{j+1}^{i+1} - 2u_j^{i+1} + u_{j-1}^{i+1} \tag{10.4}$$

3. DuFort-Frankel method:

This is an explicit procedure proposed by DuFort and Frankel [41]. In the second derivative term, $(2u_j^i)$ was replaced by $(u_j^{i+1} + u_j^{i-1})$.

$$u_j^i \frac{(u_j^{i+1} - u_j^{i-1})}{(\Delta x_+ + \Delta x_-)} + v_j^i \frac{(u_{j+1}^i - u_{j-1}^i)}{2\Delta y}$$

$$= \nu \frac{(u_{j+1}^i - u_j^{i+1} - u_j^{i-1} + u_{j-1}^i)}{(\Delta y)^2} \tag{10.5}$$

4. ADE method by Saul'yev:

This is the original ADE scheme suggested by Saul'yev [42]. The calculation procedure of the alternating-direction-explicit method marches in the opposite directions, positive y and negative y,

alternatively from step to step.

1st step in positive y-direction:

$$u_j^i \frac{(u_j^{i+1} - u_j^i)}{\Delta x_+} + v_j^i \frac{(u_{j+1}^i - u_{j-1}^i)}{2\Delta y} = \nu \frac{(u_{j-1}^{i+1} - u_j^{i+1} - u_j^i + u_{j+1}^i)}{(\Delta y)^2} \tag{10.6}$$

2nd step in negative y-direction:

$$u_j^{i+1} \frac{(u_j^{i+2} - u_j^{i+1})}{\Delta x_{++}} + v_j^{i+1} \frac{(u_{j+1}^{i+1} - u_{j-1}^{i+1})}{2\Delta y} = \nu \frac{(u_{j-1}^{i+1} - u_j^{i+1} - u_j^{i+2} + u_{j+1}^{i+2})}{(\Delta y)^2} \tag{10.7}$$

5. ADE method by Larkin:

Larkin [44], based on the work of Saul'yev, suggested that both sweeps in the different direction can be done at the same marching step and then averaged to obtain the new values.

1st sweep:

$$u_j^i \frac{(p_j^{i+1} - u_j^i)}{\Delta x_+} + v_j^i \frac{(u_{j+1}^i - u_{j-1}^i)}{2\Delta y} = \nu \frac{(p_{j-1}^{i+1} - p_j^{i+1} - u_j^i + u_{j+1}^i)}{(\Delta y)^2} \tag{10.8}$$

2nd sweep:

$$u_j^i \frac{(q_j^{i+1} - u_j^i)}{\Delta x_+} + v_j^i \frac{(u_{j+1}^i - u_{j-1}^i)}{2\Delta y}$$

$$= \nu \frac{(u_{j-1}^i - u_j^i - q_j^{i+1} + q_{j+1}^{i+1})}{(\Delta y)^2} \tag{10.9}$$

and finally, taking the average

$$u_j^{i+1} = \frac{1}{2}(p_j^{i+1} + q_j^{i+1}) \tag{10.10}$$

6. ADE method by Barakat and Clark:

The Barakat and Clark method differs from the averaged Larkin method only through the use of the provisional functions p and q everywhere in the difference equations.

1st sweep:

$$u_j^i \frac{(p_j^{i+1} - p_j^i)}{\Delta x_+} + v_j^i \frac{(p_{j+1}^i - p_{j-1}^i)}{2\Delta y}$$

$$= \nu \frac{(p_{j-1}^{i+1} - p_j^{i+1} - p_j^i + p_{j+1}^i)}{(\Delta y)^2} \tag{10.11}$$

2nd sweep:

$$u_j^i \frac{(q_j^{i+1} - q_j^i)}{\Delta x_+} + v_j^i \frac{(q_{j+1}^i - q_{j-1}^i)}{2\Delta y}$$

$$= \nu \frac{(q_{j-1}^i - q_j^i - q_j^{i+1} - q_{j+1}^{i+1})}{(\Delta y)^2} \tag{10.12}$$

then averaging

$$u_j^{i+1} = \frac{1}{2}(p_j^{i+1} + q_j^{i+1}) \tag{10.13}$$

7. ADE method modified by Pletcher:

Pletcher (in an unpublished report) observed that the accuracy of the Barakat and Clark procedure could generally be improved by using u_j^i instead of p_j^i and q_j^i for the $u \frac{\partial u}{\partial x}$ term in Equations (10.11) and (10.12).

1st sweep:

$$u_j^i \frac{(p_j^{i+1} - u_j^i)}{\Delta x_+} + v_j^i \frac{(p_{j+1}^i - p_{j-1}^i)}{2\Delta y} = \nu \frac{(p_{j-1}^{i+1} - p_j^{i+1} - p_j^i + p_{j+1}^i)}{(\Delta y)^2} \tag{10.14}$$

2nd sweep:

$$u_j^i \frac{(q_j^{i+1} - u_j^i)}{\Delta x_+} + v_j^i \frac{(q_{j+1}^i - q_{j-1}^i)}{2\Delta y} = \nu \frac{(q_{j-1}^i - q_j^i - q_j^{i+1} + q_{j+1}^{i+1})}{(\Delta y)^2} \tag{10.15}$$

then

$$u_j^{i+1} = \frac{1}{2}(p_j^{i+1} + q_j^{i+1}) \tag{10.16}$$

XI. APPENDIX B: DERIVATION OF NONDIMENSIONAL FORMS

The governing equations, Equations (3.2) to (3.5), are nondimensionalized by introducing the nondimensional parameters as follows:

$$U = \frac{u}{u_o}, \quad V = \frac{v}{u_o}, \quad R = \frac{ru_o}{\nu}$$

$$T = \frac{t-t_{\infty,o}}{t_o-t_{\infty,o}}, \quad S = \frac{su_o}{\nu} \tag{11.1}$$

$$N = \frac{n}{\nu}, \quad N_H = \frac{n_H}{\nu}$$

Combining the s-momentum equation [Equation (3.3)] and shear stress equation [Equation (3.12)], and using the Boussinesq assumption, the s-momentum equation takes the following form:

$$u \frac{\partial u}{\partial s} + v \frac{\partial u}{\partial r} = \frac{1}{r} \frac{\partial}{\partial r}(rn \frac{\partial u}{\partial r}) + \frac{(\rho_\infty-\rho)}{\rho_o} g_n \sin\theta \tag{11.2}$$

Substituting the nondimensional parameters of Equation (11.1) into Equation (11.2) yields

$$\frac{u_o^3}{\nu}(U \frac{\partial U}{\partial S} + V \frac{\partial U}{\partial R}) = \frac{u_o^3}{\nu} \frac{1}{R} \frac{\partial}{\partial R}(RN \frac{\partial U}{\partial R}) + \frac{(\rho_\infty-\rho)}{\rho_o} g_n \sin\theta \tag{11.3}$$

which can be simplified to

$$U \frac{\partial U}{\partial S} + V \frac{\partial U}{\partial R} = \frac{1}{R} \frac{\partial}{\partial R}(RN \frac{\partial U}{\partial R}) + \frac{\nu}{u_o^3} \frac{(\rho_\infty-\rho)}{\rho_o} g_n \sin\theta \tag{11.4}$$

By expanding $\rho(t)$ in a Taylor series about the reference density

ρ_{ref}, one can obtain:

$$\rho(t) = \rho_{ref} + (\frac{\partial \rho}{\partial t})_{p,ref}(t-t_{ref}) + \ldots \tag{11.5}$$

Neglecting the higher order terms:

$$\rho = \rho_{ref} + (\frac{\partial \rho}{\partial t})_{p,ref}(t-t_{ref}) \tag{11.6}$$

From the definition of the isobaric volume expansivity:

$$\beta_{th} = -\frac{1}{\rho_{ref}}(\frac{\partial \rho}{\partial t})_p \tag{11.7}$$

Inserting Equation (11.7) into Equation (11.6), a linear equation of state for ρ can be derived:

$$\rho = \rho_{ref}[1-\beta_{th}(t-t_{ref})] \tag{11.8}$$

or

$$\frac{\rho}{\rho_{ref}} = 1-\beta_{th}(t-t_{ref}) \tag{11.9}$$

ρ is density at any point, and ρ_{ref} refers to the value of density at a reference point which has a temperature t_{ref}.

By choosing a reference point at t_o and ρ_o, Equation (11.9) becomes

$$\frac{\rho}{\rho_o} = 1-\beta_{th}(t-t_o) \tag{11.10}$$

and

$$\frac{\rho_\infty}{\rho_o} = 1-\beta_{th}(t_\infty-t_o) \tag{11.11}$$

Subtracting Equation (11.10) from Equation (11.11) yields

$$\frac{(\rho_\infty - \rho)}{\rho_o} = \beta_{th}(t - t_\infty) \tag{11.12}$$

In the same way,

$$\frac{(\rho_{\infty,o} - \rho_o)}{\rho_o} = \beta_{th}(t_o - t_{\infty,o}) \tag{11.13}$$

The discharge Froude number is defined as

$$Fr_o = \frac{u_o^2}{d_o g_n \frac{(\rho_{\infty,o} - \rho_o)}{\rho_o}} \tag{11.14}$$

Introducing Equation (11.13) into (11.14),

$$Fr_o = \frac{u_o^2}{d_o g_n \beta_{th}(t_o - t_{\infty,o})} \tag{11.15}$$

Now, considering the buoyancy term in Equation (11.4), which can be expressed as

$$\frac{\nu}{u_o^3} \frac{(\rho_\infty - \rho)}{\rho_o} g_n \sin\theta = \frac{\nu}{u_o^3} \beta_{th}(t - t_\infty) g_n \sin\theta$$

$$= \frac{\nu}{u_o d_o} \frac{d_o}{u_o^2} \beta_{th} \{[T(t_o - t_{\infty,o}) + t_{\infty,o}]$$

$$- [T_\infty(t_o - t_{\infty,o}) + t_{\infty,o}]\} \times g_n \sin\theta \tag{11.16}$$

i.e.,

$$\frac{1}{Re_o}\frac{d_o}{u_o^2}\beta_{th}(T-T_\infty)(t_o-t_{\infty,o})g_n \sin\theta$$

or

$$\frac{1}{Re_o}\frac{(T-T_\infty)\sin\theta}{u_o^2/[d_o g_n \beta_{th}(t_o-t_{\infty,o})]}$$

which finally gives

$$\frac{\nu}{u_o^3}\frac{(\rho_\infty-\rho)}{\rho_o} g_n \sin\theta = \frac{(T-T_\infty)}{Re_o Fr_o}\sin\theta \qquad (11.17)$$

The s-momentum equation, Equation (11.4), finally can be written in nondimensional form as

$$U\frac{\partial U}{\partial S} + V\frac{\partial U}{\partial R} = \frac{1}{R}\frac{\partial}{\partial R}(RN\frac{\partial U}{\partial R}) + \frac{(T-T_\infty)\sin\theta}{Re_o Fr_o} \qquad (11.18)$$

Equation (3.37), r-momentum equation, Equation (3.35), continuity equation, and Equation (3.38), energy equation are derived in a similar procedure.

XII. APPENDIX C: A COMPUTER PROGRAM FOR AXISYMMETRIC JET CASES

In this appendix, a listing of the computer program used to solve the governing equations for the buoyant jet discharged into a crossflow is presented for the readers' convenience. This general program, with different input data, can also be used for a nonbuoyant jet in a crossflowing or quiescent ambient, a buoyant jet in a quiescent ambient, a jet at arbitrary angles to the horizontal. The ambient can be uniform or stratified.

The computer code includes a main program and eight subroutines. The main program coordinates the overall computational procedure. It reads in the input data, initializes all necessary parameters, calls the subroutines as needed and calculates new values for the parameters. It also resets the grid points in transverse direction when the number of grid points in that direction exceeds the assigned storage location.

The subroutines called in main program are described in order as follows:

- SDELX
- THETA
- UVEL
- TRIDIA
- VVEL
- TEMP
- EFVISC
- OUTPUT

The subroutine SDELX calculates the streamwise step size for each station. The step size is varied with the growth of the jet radius.

The subroutine UVEL calculates the axial velocity components $u_{i+1,j}$ for each station by solving the finite-difference form of the s-momentum equation and determines the jet growth in terms of half-width and plume boundary. The subroutine VVEL solves the continuity equation for velocity components $v_{i+1,j+1}$.

Subroutine THETA determines the new angle (θ_{i+1}) between the jet centerline and the horizontal by solving the r-momentum equation. This determines the jet trajectory. Subroutine TRIDIA is used to solve the system of algebraic equations having the tri-diagonal matrix form.

Subroutine TEMP calculates the temperature distribution ($t_{i+1,j}$) in the plume by solving the energy equation. The temperature half-width and thermal boundary are determined here.

Subroutine EFVISC computes the effective viscosities and thermal diffusivities needed in the s-momentum and energy equations through the turbulence model proposed in the present analysis.

Finally, the subroutine OUTPUT prints out all the important numerical results.

The main program and eight subroutines are listed as they appeared in the present version of the program.

XII. APPENDIX C: A COMPUTER PROGRAM FOR AXISYMMETRIC JET CASES

```
C ***************************************************************
C *                                                             *
C *                        PROGRAM I                            *
C *                                                             *
C *    TWO-DIMENSIONAL OR AXISYMMETRIC JETS AND PLUMES          *
C *     PROBLEMS SOLVED IN A GENERAL COMPUTER PROGRAM           *
C *                                                             *
C ***************************************************************
C
C
C     THE  PARAMETERS USED IN THIS PROGRAM ARE EXPLAINED
C      BELOW:
C
C
C     ICASE   : NUMBER OF CASES TO BE RUN AT THE SAME TIME
C     LURT    : .GT. 0 FOR TURBULENT JET FLOW CASES
C             : .LE. 0 FOR LAMINAR JET FLOW CASES
C     LAMDA   : DEGREE OF AMBIENT STRATIFICATION
C     BETA    : ISOBARIC VOLUME EXPANSIVITY OF FLUID
C     I       : THE ITH STATION ALONG STREAMWISE DIRECTION
C     IEND    : MAXIMUM NUMBER OF I STEPS TO BE COMPUTED IN A
C               RUN. THE CALCULATION WILL STOP AFTER I = IEND
C     IOUT    : NUMBER OF I STEPS BETWEEN OUTPUTS
C     NYI     : NUMBER OF GRID SPACES OVER NOZZLE RADIUS
C     CONST1  : CONSTANT IN TURBULENCE MODEL FOR INITIAL REGION
C     CONST2  : CONSTANT IN TURBULENCE MODEL FOR MAIN REGION
C
C     DENS    : DENSITY OF FLUID AT DISCHARGE
C     ANU     : KINEMATIC VISCOSITY OF FLUID
C     USTART  : JET VELOCITY AT DISCHARGE
C     TSTART  : JET TEMPERATURE AT DISCHARGE
C     RAD     : RADIUS OF DISCHARGED PIPE
C     VAXIS   : TRANSVERSE VELOCITY AT JET CENTERLINE
C     PRT     : TURBULENT PRANDTL NUMBER
C     UF      : FREE STREAM (AMBIENT) VELOCITY
C     UE      : VELOCITY AT ADGE OF JET
C     TF      : AMBIENT TEMPERATURE
C     TE      : TEMPERATURE AT EDGE OF JET
C     TFO     : AMBIENT TEMPERATURE AT DISCHARGE FOR STRATIFIED
C               AMBIENT
C     TFR     : DIMENSIONAL AMBIENT TEMPERATURE
C     YUHA_F  : VELOCITY HALF-WIDTH
C     YTHALF  : TEMPERATURE HALF-WIDTH
C     CP      : SPECIFIC HEAT AT CONSTANT PRESSURE
C     HTK     : THERMAL CONDUCTIVITY
C     THE     : ANGLE BETWEEN JET CENTERLINE AND HORIZONTAL,
C               AT ITH STATION
C     THEP    : ANGLE BETWEEN JET CENTERLINE AND HORIZONTAL,
C               AT I+1ST STATION
C
```

```
C      DXF     : A PARAMETER TO RESET THE Y-GRID POINT
C      M       : A PARAMETER TO CONTROL THE OUTPUT
C      FRO     : FROUDE NUMBER OF BUOYANT JETS
C      RCOE    : IN CASE OF QUIESCENT AMBIENT, THE MINIMUM
C                PERCENTAGE OF JET VELOCITY USED AS EDGE VELOCITY
C      BUC     : .EQ. 1.0 FOR BUOYANT JET FLOW CASES
C                .EQ. 0.0 FOR NON-BUOYANT JET FLOW CASES
C      SCOE    : COEFFICIENT TO GET STREAMWISE STEP SIZE
C                DELXP = RCOE * DELTA
C      DELTA   : JET RADIUS COMPUTED FROM VELOCITY BOUNDARY
C      TDELTA  : JET RADIUS COMPUTED FRCM TEMPERATURE BOUNDARY
C
C      CD      : DRAG COEFFICIENT, FOR QUIESCENT AMBIENT CD = 0.0
C      UP,U,UM : STREAMWISE VELOCITIES AT I+1,I,I-1 STATIONS
C      VP,V,VM : TRANSVERSE VELOCITIES AT I+1,I,I-1 STATIONS
C      TP,T,TM : TEMPERATURE AT I+1,I,I-1 STATIONS
C      UTEST   : A PARAMETER TO CALCULATE THE BOUNDARY LOCATION
C                FROM VELOCITY PROFILE,
C      TTEST   : A PARAMETER TO COMPUTE THE BOUNDARY LOCATION
C                FROM TEMPERATURE PROFILE
C      EV(J)   : VISCOSITY AT (I,J)
C      EK(J)   : THERMAL DIFFUSIVITY AT (I,J)
C
C      AL1     : EQUALS TO EV(J)+EV(J+1)
C      AL2     : EQUALS TO EV(J)+EV(J-1)
C      BL1     : EQUALS TO EK(J)+EK(J+1)
C      BL2     : EQUALS TO EK(J)+EK(J-1)
C      EVP,EVM : VISCOSITY AT I+1 AND I-1 STATIONS
C      EKP,EKM : THERMAL DIFFUSIVITY AT I+1 AND I-1 STATIONS
C      UVIN    : A COEFFICIENT TO COMPUTE MIXING LENGTH FOR
C                TURBULENCE MODEL
C      UFIN    : A COEFFICIENT TO COMPUTE JET RADIUS BY VELOCITY
C                PROFILE, A STANDARD VALUE FOR UFIN IS 0.9995
C      TFIN    : A COEFFICIENT TO COMPUTE JET RADIUS BY
C                TEMPERATURE PROFILE, A STANDARD VALUE FOR TFIN IS 0.999
C      STRAT   : STRATIFICATION PARAMETER
C
C
C
C
```

```
C
C   *****MAIN PROGRAM*****
C
C
C      USING FULLY IMPLICIT FINITE-DIFFERENCE METHOD,
C       WITH LAGGING FOR COEFFICIENTS.
C
C
      REAL LAMDA
      COMMON/AREA1/U(200),UP(200),UM(200),V(200),VP(200),VM(20
     10),T(200),TP(200),TM(200),UTEST,UE,UF,TTEST,TE,TF,VAXIS,
     2LORT,USTART,AL1,AL2,BL1,BL2
      COMMON/AREA2/DELXP,DELXM,DELXT,DELY,DELTA,TDELTA,Y(200),
     1I,NS,NY,NYT,EV(200),EK(200),ECONV,UCONV,XCONV,TCONV,N,
     2DELMIX
      COMMON/AREA3/SMUP(200),SMUM(200),SKCP(200),SKCM(200)
      COMMON/AREA4/XL,ANU,PRT,HTK,DENS,CP,ALPHA
      COMMON/AREA5/X,XO,RAD,LT
      COMMON/AREA6/CONST1,CONST2
      COMMON/AREA7/YUHALF,YTHALF,YMAX
      COMMON/AREA8/TC1,TC2
      COMMON/AREA9/JCORE,JJ
      COMMON/AREA10/THE,THEP,THEM,HX,VZ
      COMMON/AREA11/FRO,REO
      COMMON/AREA12/EVP(200),EKP(200),EVM(200),EKM(200),SMUMP(
     1200),SMUPP(200),SKCMP(200),SKCPP(200)
      COMMON/AREA14/UFIN,UVIN,CK4,CKI,BK4,BKI
      COMMON/AREA15/STRAT,LAMDA
      COMMON/AREA16/BETA
      COMMON/AREA17/UFIN,UVIN,TFIN
      COMMON/AREA18/CK4,CKI,BK4,BKI
      COMMON/AREA19/CD,BUC
      COMMON/AREA20/SCOE
C   *   *   *   *   *   *   *   *
C
C     READING IN THE INPUT
C
C    *    *   *   *   *   *   *
C
      READ(5,8) ICASE
    8 FORMAT(I6)
      DO 600 IIND=1,ICASE
      READ(5,2) LAMDA,BETA
    2 FORMAT(2F12.5)
      WRITE(6,3) LAMDA,BETA
    3 FORMAT(2X,'LAMDA =',F12.5,5X,'BETA =',F12.5)
      READ(5,8) LORT
      READ(5,10) IEND,IOUT,NYI,IPUNCH
   10 FORMAT(4I6)
      WRITE(6,11) IEND,IOUT,NYI,IPUNCH
```

```
 11   FORMAT(2X,'IEND =',I4,10X,'ICUT =',I3,10X,'NYI =',I3,
     110X,'IPUNCH =',I4)
      READ(5,12) CONST1,CONST2
 12   FORMAT(2F12.5)
      WRITE(6,13) CONST1,CONST2
 13   FORMAT(2X,'CONST1 =',F12.5,5X,'CONST2 =',F12.5)
      READ(5,15) DENS,ANU,USTART,RAD,TSTART,VAXIS,PRT,UE,UF,
     1TE,TF,CP,HTK
 15   FORMAT(6G12.5)
      WRITE(6,16) DENS,ANU,USTART,RAD,TSTART,VAXIS,PRT,UE,UF,
     1TE,TF,CP,HTK
 16   FORMAT (2X,'DENS =',F12.5,5X,'ANU =',G12.5,5X,'USTART ='
     1,F12.5,5X,'RAD =',F12.5,5X,'TSTART =',F12.5,'VAXIS =',
     2F12.5/3X,'PRT =',F12.5,5X,'UE =',F12.5,5X,'UF =',F12.5,
     35X,'TE =',F12.5,5X,'TF =',F12.5,5X,'CP =',F12.5/3X,'HTK
     4 =',G12.5)
      READ (5,19) DXF,M
 19   FORMAT(F6.2,I5)
      WRITE (6,20) DXF,M
 20   FORMAT(2X,'DXF =',F6.2,3X,'M =',I5)
225   READ (5,226) THE,CD
226   FORMAT (2F12.6)
      WRITE(6,227) THE,CD
227   FORMAT(3X,'INITIAL ANGLE=',F12.6,5X,'DRAG COEFF.=',F12.6)
      READ(5,121) FRO
121   FORMAT(F12.6)
      WRITE (6,122) FRO
122   FORMAT(2X,'FROUDE NO. =',F12.6)
      READ (5,5) RCOE
 5    FORMAT(F10.5)
      READ(5,31) SCOE,BUC
 31   FORMAT(2F10.5)
      WRITE(6,32) SCOE,BUC,RCOE
 32   FORMAT(3X,'SCOE=',F10.5,5X,'BUC=',F10.5,5X,'RCOE=',F10.5)
      READ(5,7) UFIN,UVIN,TFIN
 7    FORMAT(3F10.5)
      WRITE(6,8) UFIN,UVIN,TFIN
 8    FORMAT(3X,'UFIN=',F10.5,'UVIN=',F10.5,'TFIN=',F10.5)
      READ(5,88) CK4,CKI,BK4,BKI
 88   FORMAT(4F10.4)
      WRITE (6,90) CK4,CKI,BK4,BKI
 90   FORMAT(2X,'CK4 =',F10.4,3X,'INITIAL CK4 =',F10.4,5X,'BK4
     1 =',F10.4,5X,'BKI =',F10.4)
C
C
C     COMPUTE THE EDGE VELOCITY OF JET
C
      UE1=UF*COS(THE)
      UE2=USTART*RCOE
      UE=AMAX1(UE1,UE2)
```

```
      REO=USTART*2.0*RAD/ANU
C
  28  R=UE/USTART
C
C   NON-DIMENSIONALIZING
C
C
C    CONVERSION FACTORS
C
  29  XCONV=ANU/USTART
      ECONV=ANU
      UCONV=USTART
      TC1=TE
      TC2=TSTART-TE
      STRAT=(-LAMDA*2.0*RAD)/(REO*TC2)
C
C    VARIABLES
C
      TE1=(TE-TE)/TC2
      TF1=(TF-TE)/TC2
      TSTAR1=(TSTART-TE)/(TSTART-TE)
      TE=TE1
      TF=TF1
      TSTART=TSTAR1
      RAD=RAD/XCONV
C
C   Y-GRID SPACING
C
      DELY=RAD/NYI
      UE=UE/UCONV
      UF=UF/UCONV
      USTART=USTART/UCONV
      ALPHA=(HTK/(DENS*CP))*1.0/ECONV
C
C   STARTING PROFILES
C
C   ASSUMED UNIFORM PROFILE
C
      I=0
      X=0.0
      HX=0.0
      VZ=0.0
      NNYI=NYI+1
      DO 25 J=1,NNYI
      Y(J)=(J-1)*DELY
      U(J)=1.0
      V(J)=0.0
      T(J)=1.0
      EV(J)=1.0
      EK(J)=ALPHA
```

```
  25  CONTINUE
      NNNYI=NNYI+1
      DO 40 J=NNNYI,200
      Y(J)=(J-1)*DELY
      U(J)=UE
      UP(J)=UE
      V(J)=0.0
      T(J)=TE
      TP(J)=TE
      EV(J)=1.0
      EK(J)=ALPHA
  40  CONTINUE
      DELTA=RAD
      DELMIX=0.0
      IF(LORT .GT. 0.0) GO TO 54
C     LAMINAR JET FLOW CASE
C
C
      WRITE (6,58)
  58  FORMAT (10X,'LAMINAR JET CASE')
      AL1=2.0
      AL2=2.0
      BL1=2.0*ALPHA
      BL2=2.0*ALPHA
C     TURBULENT JET FLOW CASE
C
C
  54  WRITE (6,56)
  56  FORMAT (6X,'TURBULENT JET CASE')
C
C   BEGINNING OF COMPUTATION LOOP
C
      NY=NNYI
      NYT=NNYI
      LT=0.0
      N=1
      K=1
  67  IF(U(1) .LT. USTART) GO TO 63
      GO TO 61
  63  IF(K .EQ. 1) GO TO 77
      GO TO 61
  77  DIST=X*XCONV
      WRITE (6,62) DIST
  62  FORMAT(3X,'PREDICTED STARTING LENGTH =',G14.8)
      K=K+1
  61  CALL SDELX
      X=X+DELXP
      CALL THETA
C
C     UPDATING THE HORIZONTAL AND VERTICAL DISTANCE
```

```
C
      HX=HX+DELXP*COS(THEP)
      VZ=VZ+DELXP*SIN(THEP)
      TF=STRAT*VZ
      TE=TF
      TFR=TF*TC2+TC1
      WRITE(6,4) TFR
    4 FORMAT(2X,'TF =',F12.5)
      UE1=UF*COS(THEP)
      UE2=UF*RCOE
      UE=AMAX1(UE1,UE2)
      R=UE/USTART
      I=I+1
      IF(I .GT. 1) GO TO 141
      DELXM=DELXP
  141 DELXT=DELXM+DELXP
      CALL UVEL
  112 CALL VVEL
      CALL TEMP
C
C     UPDATING VALUES
C
      DO 60 J=1,200
      UM(J)=U(J)
      U(J)=UP(J)
      VM(J)=V(J)
      V(J)=VP(J)
      TM(J)=T(J)
   60 T(J)=TP(J)
      REDELX=DELXP*XCONV
      WRITE (6,111) REDELX
  111 FORMAT (/,5X,'DELXP =',G14.7)
      IF(LORT .GT. 0.0) CALL EFVISC
      THEM=THE
      THE=THEP
      DELXM=DELXP
      IF(I .GT. 10) GO TO 55
      CALL OUTPUT
      GO TO 65
   55 II=IOUT*M
      IF(I .EQ. II) GO TO 22
      GO TO 65
   22 CALL OUTPUT
      M=M+1
      LT=1.0
C
C     WHEN NUMBER OF Y-GRID POINTS GREATER THAN 200, RESET THE
C      SYSTEMS BY USING BIGGER STEP SIZE IN Y-DIRECTION,
C      NEW DELY = 2.0*DELY
C
```

```
 65   IF((NY .LE. 180) .AND. (NYT .LE. 180)) GO TO 501
      IF(DXF .NE. 1.0) GO TO 500
      IM=0
      DO 505 J=1,200,2
      IM=IM+1
      U(IM)=U(J)
      UP(IM)=UP(J)
      UM(IM)=UM(J)
      T(IM)=T(J)
      TP(IM)=TP(J)
      TM(IM)=TM(J)
      V(IM)=V(J)
      Y(IM)=Y(J)
      EV(IM)=EV(J)
505   EK(IM)=EK(J)
      DELY=DELY*2.0
      NY=NY/2.+1
      NYT=NYT/2.+1
      NY3=NY+5
      DO 506 J=NY3,200
      Y(J)=(J-1)*DELY
      U(J)=UE
      UP(J)=UE
      UM(J)=UE
      TP(J)=TE
      TM(J)=TE
      V(J)=0.0
      EV(J)=1.0
      VP(J)=0.0
      EK(J)=ALPHA
506   T(J)=TE
      DXF=DXF+1.0
500   IF((NY .GT. 195) .OR. (NYT .GT. 195)) GO TO 600
501   IF(I .LT. IEND) GO TO 67
600   CONTINUE
      STOP
      END
```

```
      SUBROUTINE UVEL
      COMMON/AREA1/U(200),UP(200),UM(200),V(200),VP(200),VM(20
     10),T(200),TP(200),TM(200),UTEST,UE,UF,TTEST,TE,TF,VAXIS,
     2LORT,USTART,AL1,AL2,BL1,BL2
      COMMON/AREA2/DELXP,DELXM,DELXT,DELY,DELTA,TDELTA,Y(200),
     1I,NS,NY,NYT,EV(200),EK(200),ECONV,UCONV,XCONV,TCONV,N,
     2DELMIX
      COMMON/AREA3/SMUP(200),SMUM(200),SKCP(200),SKCM(200)
      COMMON/AREA4/XL,ANU,PRT,HTK,DENS,CP,ALPHA
      COMMON/AREA5/X,XO,RAD,LT
      COMMON/AREA7/YUHALF,YTHALF,YMAX
      COMMON/AREA9/JCORE,JJ
      COMMON/AREA10/THE,THEP,THEM,HX,VZ
      COMMON/AREA11/FRO,REO
      COMMON/AREA12/EVP(200),EKP(200),EVM(200),EKM(200),SMUMP(
     1200),SMUPP(200),SKCMP(200),SKCPP(200)
      COMMON/AREA17/UFIN,UVIN,TFIN
C
C     THETA : PARAMETER IN U & T SUBROUTINES TO DECIDE THE
C      FINITE DIFFERENCE METHOD TO BE USED
C      THETA = 0.0  FULLY EXPLICIT METHOD
C      THETA = 1.0  FULLY IMPLICIT METHOD
C
C
C   FULLY IMPLICIT METHOD
C
      DIMENSION A(200),B(200),C(200),D(200)
      IF(I .NE. 1) GO TO 5
      READ(5,6) THETA
    6 FORMAT(F10.5)
    5 L=1
      K=1
      M=1
      JT=NY+5
      SMUP(1)=EV(1)+EV(2)
      SMUPP(1)=SMUP(1)
      H1=U(1)/DELXP
      H2=2.0*THETA*SMUPP(1)/(DELY*DELY)
      H3=2.0*(1.0-THETA)*SMUP(1)/(DELY*DELY)
      D(1)=H1+H2
      A(1)=-H2
      C(1)=H3*(U(2)-U(1))+H1*U(1)+SIN(THEP)*(T(1)-TE)/(REO*FRO)
      DO 26 J=2,JT
      YJ=Y(J)
      UJ=U(J)
      UJP=U(J+1)
      UJM=U(J-1)
      UMJ=UM(J)
      IF(LORT .LE. 0.0) GO TO 25
      SMUP(J)=EV(J)+EV(J+1)
```

```
      SMUM(J)=EV(J)+EV(J-1)
      AL1=SMUP(J)
      AL2=SMUM(J)
      ALP1=AL1
      ALP2=AL2
      UB1=4.0*Y(J)*DELY*DELY
      UB=THETA*(Y(J+1)+Y(J))*ALP1/UB1
      UC=THETA*(Y(J)+Y(J-1))*ALP2/UB1
      UD=V(J)/(2.0*DELY)
      UH=V(J)*(1.0-THETA)/(2.0*DELY)
      B(J)=-UD-UC
      D(J)=UA+UB+UC
      A(J)=UD-UB
C
C     CHECK STABILITY BY USING GRID REYNALD NUMBER
C     GRID REYNALD MUST .LT. 2.0
C
      STAB=ABS(V(J)*DELY/EV(J))
      IF(STAB .LT. 2.0) GO TO 86
      IF(V(J) .GT. 0.0) GO TO 84
      B(J)=-UC
      D(J)=UA+UB+UC-2.0*UD
      A(J)=2.0*UD-UB
      GO TO 86
   84 B(J)=-2.0*UD-UC
      D(J)=UA+UB+UC+2.0*UD
      A(J)=-UB
   86 C(J)=UA*U(J)-UH*(U(J+1)-U(J))+(1.0-THETA)*((Y(J+1)+Y(J))
     1*AL1*(U(J+1)-U(J))-(Y(J)+Y(J-1))*AL2*(U(J)-U(J-1)))/UB1
     2+SIN(THEP)*(T(J)-TE)/(REO*FRO)
   26 CONTINUE
      C(JT)=C(JT)-A(JT)*UE
      A(JT)=0.0
      CALL TRIDIA (A,B,C,D,JT)
      DO 52 J=1,JT
   52 UP(J)=C(J)
C
C    CALCULATING YUHALF ***
C
      DO 54 J=2,199
      UPJ=UP(J)
      IF(K .EQ. 1) GO TO 33
      IF(M .GT. 1) GO TO 33
      UPMEAN=(UP(1)+UE)/2.0
      IF(UPJ .LE. UPMEAN) GO TO 42
      GO TO 33
   42 JJ=J
      JM=J-1
      YUHALF=Y(JM)+DELY*(UPMEAN-UP(JM))/(UP(JJ)-UP(JM))
      M=M+1
```

```
   33  K=K+1
       IF(K .LT. 3) GO TO 21
       IF(UP(1) .LT. USTART) GO TO 23
C
C***   CALCULATING YCORE ***
C
   21  IF(L .GT. 1) GO TO 22
       IF(UPJ .LT. USTART) GO TO 24
       GO TO 22
   24  YCORE=(J-1)*DELY
       JCORE=J
       L=L+1
       GO TO 22
   23  YCORE=0.0
       JCORE=1
   22  IF(K .LT. 3) GO TO 54
       UTEST=(UP(1)-UPJ)/(UP(1)-UE)
       IF(UTEST .GE. UFIN)    GO TO 27
   54  CONTINUE
   27  DELTA=(J-1)*DELY
       NY=J
       NNY=J+1
       DO 11 J=2,199
       UTEST=(UP(1)-UP(J))/(UP(1)-UE)
       IF (UTEST .GE. UVIN ) GO TO 12
   11  CONTINUE
   12  VDELTA=(J-1)*DELY
       DELMIX=VDELTA-YCORE
       DO 28 J=NY,200
   28  UP(J)=UE
C
C
C  ***BOUNDARY CONDITIONS ***
C
       VP(1)=VAXIS
       RETURN
       END
```

```
      SUBROUTINE TEMP
      COMMON/AREA1/U(200),UP(200),UM(200),V(200),VP(200),VM(20
     10),T(200),TP(200),TM(200),UTEST,UE,UF,TTEST,TE,TF,VAXIS,
     2LORT,USTART,AL1,AL2,BL1,BL2
      COMMON/AREA2/DELXP,DELXM,DELXT,DELY,DELTA,TDELTA,Y(200),
     1I,NS,NY,NYT,EV(200),EK(200),ECONV,UCONV,XCONV,TCONV,N,
     2DELMIX
      COMMON/AREA3/SMUP(200),SMUM(200),SKCP(200),SKCM(200)
      COMMON/AREA4/XL,ANU,PRT,HTK,DENS,CP,ALPHA
      COMMON/AREA5/X,XO,RAD,LT
      COMMON/AREA7/YUHALF,YTHALF,YMAX
      COMMON/AREA8/TC1,TC2
      COMMON/AREA9/JCORE,JJ
      COMMON/AREA10/THE,THEP,THEM,HX,VZ
      COMMON/AREA11/FRO,REO
      COMMON/AREA12/EVP(200),EKP(200),EVM(200),EKM(200),SMUMP(
     1200),SMUPP(200),SKCMP(200),SKCPP(200)
      COMMON/AREA17/UFIN,UVIN,TFIN
C
      DIMENSION A(200),B(200),C(200),D(200)
      IF(I .NE. 1) GO TO 5
      READ(5,6) THETA
      READ(5,6) TFIN
    6 FORMAT(F10.5)
    5 K=1
      M=1
      SKCP(1)=EK(1)+EK(2)
      SKCPP(1)=SKCP(1)
      H1=U(1)/DELXP
      H2=2.0*THETA*SKCPP(1)/(DELY*DELY)
      H3=2.0*(1.0-THETA)*SKCP(1)/(DELY*DELY)
      D(1)=H1+H2
      A(1)=-H2
      C(1)=H3*(T(2)-T(1))+H1*T(1)
      JT=NYT+4
      DO 26 J=2,JT
      YJ=Y(J)
      TJ=T(J)
      TJP=T(J+1)
      TJM=T(J-1)
      TMJ=TM(J)
      IF(LORT .LE. 0.0) GO TO 25
      SKCP(J)=EK(J)+EK(J+1)
      SKCM(J)=EK(J)+EK(J-1)
      BL1=SKCP(J)
      BL2=SKCM(J)
      BLP1=BL1
      BLP2=BL2
   25 TA=U(J)/DELXP
      TB1=4.0*Y(J)*DELY*DELY
```

```
      TB=THETA*(Y(J+1)+Y(J))*BLP1/TB1
      TC=THETA*(Y(J)+Y(J-1))*BLP2/TB1
      TD=V(J)*THETA/(2.0*DELY)
      TH=V(J)*(1.0-THETA)/(2.0*DELY)
      B(J)=-TD-TC
      D(J)=TA+TB+TC
      A(J)=TD-TB
   26 C(J)=TA*T(J)-TH*(T(J+1)-T(J-1))+(1.0-THETA)*((Y(J+1)+Y(J)
     1)*BL1*(T(J+1)-T(J))-(Y(J)+Y(J-1))*BL2*(T(J)-T(J-1)))/TB1
      C(JT)=C(JT)-A(JT)*TE
      A(JT)=0.
      CALL TRIDIA (A,B,C,D,JT)
      DO 52 J=1,JT
   52 TP(J)=C(J)
C
C    CALCULATING YTHALF
C
      DO 54 J=2,199
      TPJ=TP(J)
      IF(K .EQ. 1) GO TO 33
      IF(M .GT. 1) GO TO 33
      TPMEAN=(TP(1)+TE)/2.0
      IF(TPJ .LE. TPMEAN) GO TO 42
      GO TO 33
   42 JJ=J
      JM=J-1
      YTHALF=Y(JM)+DELY*(TPMEAN-TP(JM))/(TP(JJ)-TP(JM))
      M=M+1
   33 K=K+1
      IF(K .LT. 3) GO TO 54
      TTEST=(TP(1)-TPJ)/(TP(1)-TE)
      IF(TTEST .GE. TFIN)   GO TO 27
   54 CONTINUE
   27 TDELTA=(J-1)*DELY
      NYT=J
      NNYT=NYT+1
      DO 28 J=NYT,200
   28 TP(J)=TE
   29 RETURN
      END
```

```
      SUBROUTINE THETA
      COMMON/AREA1/U(200),UP(200),UM(200),V(200),VP(200),VM(20
     10),T(200),TP(200),TM(200),UTEST,UE,UF,TTEST,TE,TF,VAXIS,
     2LORT,USTART,AL1,AL2,BL1,BL2
      COMMON/AREA2/DELXP,DELXM,DELXT,DELY,DELTA,TDELTA,Y(200),
     1I,NS,NY,NYT,EV(200),EK(200),ECONV,UCONV,XCONV,TCONV,N,
     2DELMIX
      COMMON/AREA5/X,XO,RAD,LT
      COMMON/AREA6/CONST1,CONST2
      COMMON/AREA7/YUHALF,YTHALF,YMAX
      COMMON/AREA10/THE,THEP,THEM,HX,VZ
      COMMON/AREA11/FRO,REO
      COMMON/AREA19/CD,BUC
C
C   CALCULATING THE ANGLE BETWEEN THE CENTERLINE AND THE
C    HORIZONTAL DIRECTION
C
      IF (I .EQ. 0) YUHALF=RAD+0.5*DELY
      NY1=NY-1
      BUOY=0.0
      DRAG=0.0
      IF(CD .EQ. 0.0) GO TO 30
      SUM1=U(1)*U(1)*Y(1)+U(NY)*U(NY)*Y(NY)
      DO 10 J=2,NY1
      SUM1=SUM1+2.0*U(J)*U(J)*Y(J)
   10 CONTINUE
      ARE=DELTA*DELTA/2.0
      UINT=DELY*SUM1/2.0
      A=UF*SIN(THE)
      DRAG=CD*A*A*ARE/(3.1415926*YUHALF)
   30 IF(BUC .EQ. 0.0) GO TO 40
      SUM2=(T(1)-TE)*Y(1)+(T(NY)-TE)*Y(NY)
      DO 50 J=2,NY1
      SUM2=SUM2+2.0*(T(J)-TE)*Y(J)
   50 CONTINUE
      TINT=DELY*SUM2/2.0
   20 BUOY=COS(THE)*TINT/(REO*FRO)
   40 SLOP=(BUOY-DRAG)/UINT
      THEP=THE+DELXP*SLOP
      RETURN
      END
```

```
      SUBROUTINE SDELX
C
C     CALCULATE THE STREAMWISE STEP SIZE DELXP
C
      COMMON/AREA1/U(200),UP(200),UM(200),V(200),VP(200),VM(20
     10),T(200),TP(200),TM(200),UTEST,UE,UF,TTEST,TE,TF,VAXIS,
     2LORT,USTART,AL1,AL2,BL1,BL2
      COMMON/AREA2/DELXP,DELXM,DELXT,DELY,DELTA,TDELTA,Y(200),
     1I,NS,NY,NYT,EV(200),EK(200),ECONV,UCONV,XCONV,TCONV,N,
     2DELMIX
      COMMON/AREA5/X,XO,RAD,LT
      COMMON/AREA20/SCOE
C
      DELXP=SCOE*DELTA
      RETURN
      END
```

```
      SUBROUTINE EFVISC
C
C   CALCULATE THE EFFECTIVE VISCOSITY AND THERMAL DIFFUSIVITY
C
      COMMON/AREA1/U(200),UP(200),UM(200),V(200),VP(200),VM(20
     10),T(200),TP(200),TM(200),UTEST,UE,UF,TTEST,TE,TF,VAXIS,
     2LORT,USTART,AL1,AL2,BL1,BL2
      COMMON/AREA2/DELXP,DELXM,DELXT,DELY,DELTA,TDELTA,Y(200),
     1I,NS,NY,NYT,EV(200),EK(200),ECONV,UCONV,XCONV,TCONV,N,
     2DELMIX
      COMMON/AREA4/XL,ANU,PRT,HTK,DENS,CP,ALPHA
      COMMON/AREA5/X,XO,RAD,LT
      COMMON/AREA6/CONST1,CONST2
      COMMON/AREA7/YUHALF,YTHALF,YMAX
      COMMON/AREA8/TC1,TC2
      COMMON/AREA9/JCORE,JJ
      COMMON/AREA10/THE,THEP,THEM,HX,VZ
      COMMON/AREA11/FRO,REO
      COMMON/AREA16/BETA
      COMMON/AREA18/CK4,CKI,BK4,BKI
C
      JC=JCORE
      G=32.2
      FRI=G*ANU*TC2*BETA/(UCONV*UCONV*UCONV)
      RIB=FRI*DELTA*(TE-T(1))/((UE-U(1))*(UE-U(1)))
      IF(NY.GT. NYT) GO TO 5
      NYJ=NYT
      GO TO 6
    5 NYJ=NY
    6 R=UF/USTART
      RCREP=(THEP-THE)/DELXP
      RIC=2.0*U(1)*DELTA*RCREP/(U(1)-UE)
      WRITE(6,56) RIC,RIB
   56 FORMAT(5X,'CURVATURE RICH NO =',F12.6,6X,'BUOY RICH NO
     1 =',F12.5)
   89 PRC=RCREP/XCONV
      FBUOI=(1.0-BKI*RIB*COS(THEP))**0.5
      FBUOY=(1.0-BK4*RIB*COS(THEP))**0.5
      IF(U(1) .LT. USTART) GO TO 100
      XL=CONST1*DELMIX
   40 DO 45 J=2,NYJ
      EV(J)=1.0+(XL*XL)*ABS((U(J+1)-U(J-1))/(2.0*DELY))
     1*(1.0+CKI*ABS(RIC))*FBUOI
      EVJ=EV(J)
      EK(J)=ALPHA+(EVJ-1.0)/PRT
   45 CONTINUE
      GO TO 200
  100 DO 10 J=1,NYJ
      YY=Y(J)/YUHALF
      IF(YY.GT. 0.8) GO TO 15
```

```
      GM=1.0
      GO TO 20
   15 ZZ=(YY-0.8)**2.5
      GM=(0.5)**ZZ
   20 CONSK=0.0246*(1.0+2.13*R*R)*GM
      EV(J)=CONSK*YUHALF*(U(1)-UE)*(1.0+CK4*ABS(RIC))*FBUOY
   10 EK(J)=EV(J)/PRT
  200 RETURN
      END
```

```
      SUBROUTINE TRIDIA (A,B,C,D,N)
C
C    THIS SUBROUTINE COMPUTES THE VALUES OF TEMPERATURE IN THE
C    EQUATIONS
C
C   THE RESULTS ARE STORED IN THE C VECTOR.
C   IN THE MAIN PROGRAM NEED TO REASSIGN C AS THE NEW VALUE
C     OF TEMPERATURE.
C
      DIMENSION A(1),B(1),C(1),D(1)
      DO 10 I=2,N
      P=B(I)/D(I-1)
      D(I)= D(I)-P*A(I-1)
   10 C(I)=C(I)-P*C(I-1)
C  BACK SUBSTITUTION
      C(N)=C(N)/D(N)
      DO 20 I=2,N
      J=N-I+1
   20 C(J)=(C(J)-A(J)*C(J+1))/D(J)
      RETURN
      END
```

```
      SUBROUTINE VVEL
      COMMON/AREA1/U(200),UP(200),UM(200),V(200),VP(200),VM(20
     10),T(200),TP(200),TM(200),UTEST,UE,UF,TTEST,TE,TF,VAXIS,
     2LORT,USTART,AL1,AL2,BL1,BL2
      COMMON/AREA2/DELXP,DELXM,DELXT,DELY,DELTA,TDELTA,Y(200),
     1I,NS,NY,NYT,EV(200),EK(200),ECONV,UCONV,XCONV,TCONV,N,
     2DELMIX
C
C     TRANSVERSE VELOCITY COMPONENT
C
      VP(1)=0.
      DO 60 J=2,NY
      VA1=DELY*(Y(J)+Y(J-1))/(4.0*DELXP)
      VA2=Y(J-1)*VP(J-1)
      VA3=VA1*(UP(J)-U(J)+UP(J-1)-U(J-1))
   60 VP(J)=(VA2-VA3)/Y(J)
      RETURN
      END
```

```
      SUBROUTINE OUTPUT
C
      COMMON/AREA1/U(200),UP(200),UM(200),V(200),VP(200),VM(20
     10),T(200),TP(200),TM(200),UTEST,UE,UF,TTEST,TE,TF,VAXIS,
     2LORT,USTART,AL1,AL2,BL1,BL2
      COMMON/AREA2/DELXP,DELXM,DELXT,DELY,DELTA,TDELTA,Y(200),
     1I,NS,NY,NYT,EV(200),EK(200),ECONV,UCONV,XCONV,TCONV,N,
     2DELMIX
      COMMON/AREA5/X,XO,RAD,LT
      COMMON/AREA7/YUHALF,YTHALF,YMAX
      COMMON/AREA8/TC1,TC2
      COMMON/AREA10/THE,THEP,THEM,HX,VZ
C
      N=N+1
      NNY=NY+1
      NNYT=NYT+1
      IF(NNY .GE.NNYT) GO TO 22
      GO TO 23
   22 NNJ=NNY
      GO TO 24
   23 NNJ=NNYT
   24 WRITE(6,10)
   10 FORMAT('0')
      RHX=HX/2.0/RAD
      RVZ=VZ/2.0/RAD
      RTHE=THE*180.0/3.14159
      DIST=X*XCONV
      DDEL=DELTA*XCONV
      DTDEL=TDELTA*XCONV
      XBAR=X/RAD
      PRT1=(YUHALF*YUHALF)/(YTHALF*YTHALF)
      RUHALF=YUHALF/RAD
      RTHALF=YTHALF/RAD
      UCL=(U(1)-UE)/(USTART-UE)
      TCL=T(1)
      WRITE(6,15) I,DIST,DDEL,DTDEL,PRT1,RHX,RVZ,RTHE
   15 FORMAT(' ',5X,'I=',I4,5X,'X DISTANCE=',G12.5,'HALF-WIDTH
     1=',G12.5,5X,'THERMAL HALF-WIDTH=',G12.5,5X,'PRT1=',G12.5
     2,/,2X,'HORI. X =',G12.5,5X,'VERT. Z =',G12.5,'THETA ='
     3,G10.5)
      UCL2=(U(1)-UF)/(USTART-UF)
      WRITE (6,80) UCL2
   80 FORMAT(2X,'UCL2 =',F12.5)
      WRITE(6,16) XBAR,RUHALF,RTHALF,UCL,TCL
   16 FORMAT('0',16X,'X BAR=',G12.5,3X,'RUHALF=',G12.5,3X,
     1'RTHALF =',G12.5,3X,'UCL=',G12.5,3X,'TCL=',G12.5)
      WRITE (6,10)
      IF(I .GT. 5) GO TO 41
      WRITE(6,21)
   21 FORMAT(' ',7X,'J',5X,'Y DISTANCE',7X,'U VELO',8X,'V VELO'
```

```
     1,9X,'VISCOSITY',6X,'JET TEMP',7X,'CONDUCTIVITY')
      DO 40 J=1,NNJ
      DUJ=U(J)*UCONV
      DVJ=V(J)*UCONV
      DTJ=T(J)*TC2+TC1
      DEVJ=EV(J)*ECONV
      DEKJ=EK(J)*ECONV
      YDIST=Y(J)*XCONV
      WRITE (6,26) J,YDIST,DUJ,DVJ,DEVJ,DTJ,DEKJ
26    FORMAT(' ',5X,I3,5X,G12.5,3X,G12.5,3X,G12.5,3X,G12.5,3X,
     1G12.5,3X,G12.5)
40    CONTINUE
41    RETURN
      END
```

XIII. APPENDIX D: DERIVATION OF THE POISSON EQUATION FOR PRESSURE CORRECTION

In order to obtain values of u, v and w which satisfy the continuity equation, a correction to these estimated values is necessary, assuming

$$\begin{aligned} p &= p^* + p' \\ v &= v^* + v' \\ w &= w^* + w' \end{aligned} \tag{13.1}$$

The superscript (*) stands for the estimated values or computed values based on p*; superscript (') indicates the corrections.

Using approximate forms of the momentum equations for the imaginary time over which the correction occurs:

$$\frac{\partial v}{\partial t} \simeq \frac{v-v^*}{\Delta t} = -\frac{1}{\rho}\frac{\partial p'}{\partial y} \tag{13.2}$$

$$\frac{\partial w}{\partial t} \simeq \frac{w-w^*}{\Delta t} = -\frac{1}{\rho}\frac{\partial p'}{\partial z} \tag{13.3}$$

Using the relations in Equation (13.1), Equations (13.2) and (13.3) become:

$$\frac{v'}{\Delta t} = -\frac{1}{\rho}\frac{\partial p'}{\partial y} \tag{13.4}$$

$$\frac{w'}{\Delta t} = -\frac{1}{\rho}\frac{\partial p'}{\partial z} \tag{13.5}$$

Since v' and w' are zero before the velocity correction, $v'/\Delta t$ and $w'/\Delta t$

are approximations to $\partial v'/\partial t$ and $\partial w'/\partial t$. Equations (13.4) and (13.5) then yield:

$$\frac{\partial v'}{\partial t} = -\frac{1}{\rho}\frac{\partial p'}{\partial y} \tag{13.6}$$

$$\frac{\partial w'}{\partial t} = -\frac{1}{\rho}\frac{\partial p'}{\partial z} \tag{13.7}$$

Now, from the continuity equation,

$$\frac{\partial u}{\partial x} + \frac{\partial v}{\partial y} + \frac{\partial w}{\partial z} = 0 \tag{13.8}$$

Substituting Equation (13.1) into Equation (13.8),

$$\frac{\partial u}{\partial x} + \frac{\partial}{\partial y}(v^*+v') + \frac{\partial}{\partial z}(w^*+w') = 0$$

or

$$\frac{\partial v'}{\partial y} + \frac{\partial w'}{\partial z} = -S = -(\frac{\partial u}{\partial x} + \frac{\partial v^*}{\partial y} + \frac{\partial w^*}{\partial z}) \tag{13.9}$$

Differentiating Equation (13.9) with respect to t yields

$$\frac{\partial}{\partial t}\frac{\partial v'}{\partial y} + \frac{\partial}{\partial t}\frac{\partial w'}{\partial z} = \frac{\partial}{\partial t}(-S)$$

or

$$\frac{\partial}{\partial y}(\frac{\partial v'}{\partial t}) + \frac{\partial}{\partial z}(\frac{\partial w'}{\partial t}) = \frac{\partial}{\partial t}(-S) \tag{13.10}$$

Substituting Equation (13.6) and (13.7) into Equation (13.10),

$$-\frac{1}{\rho}(\frac{\partial^2 p'}{\partial y^2} + \frac{\partial^2 p'}{\partial z^2}) = -\frac{S_o - S}{\Delta t} \tag{13.11}$$

Where S_o is the source term after the mass sources have been eliminated. Theoretically, S_o should be zero after the pressure correction, so Equation (13.11) becomes:

$$\frac{1}{\rho}\left(\frac{\partial^2 p'}{\partial y^2} + \frac{\partial^2 p'}{\partial z^2}\right) = - \frac{\text{Div } \vec{V}^*}{\Delta t} \tag{13.12}$$

Where $\vec{V}^*$ is the vector form of velocity. Equation (13.12) is the Poisson equation for pressure correction used in the present study.

The velocity corrections themselves can be seen to be independent of the choice of Δt (taken as unity in the present calculation). Further analysis reveals that the present scheme for velocity and pressure corrections is equivalent to assuming that the correction flow is irrotational being driven by a potential function equal to $-p'/\rho$ in such a manner as to remove the mass sources.

XIV. APPENDIX E: A COMPUTER PROGRAM FOR THREE-DIMENSIONAL JET CASES

In this appendix, a computer program used to solve the three-dimensional laminar jet discharged from a rectangular or square orifice into a quiescent ambient is listed. The computer code in this case includes a main program and eleven subroutines. The subroutines called in main program are listed in order as it appeared in the main program:

- o SDELX
- o UVEL
- o VVELY
- o VVELZ
- o WVEL
- o PRESS
- o TEMP
- o TRIDIA
- o TRID2
- o OUTPUT
- o PROFIL

The calculation procedure and functions of the subprograms are mostly similar to those in axisymmetric jet cases as described in Appendix C. Some additional subroutines and different procedures which were used for three-dimensional characteristics are described below.

Subroutine UVEL calculates the axial velocity component $u_{i+1,j,k}$ for each station by solving the x-momentum equation in a triangular

domain (this is one-eighth of the jet cross section). For a square orifice, because of symmetry, the variables interested such as u, v, w, t and p, can be determined for the whole cross section from this one-eighth triangle. For a rectangular orifice, one quadrant of the jet (one-fourth of the cross section) is needed for calculation.

Subroutines VVELY and VVELZ compute the y-component of velocities $v_{i+1,j,k}$ for a quadrant section. The alternating-direction-implicit method was used in this subroutine. Subroutine WVEL gives numerical values to w's according to the symmetrical location of v's through $w_{i+1,j,k} = v_{i+1,k,j}$.

Subroutine PRESS calculates the pressure correction $p'_{i+1,j,k}$ for each station such that after correction, the velocity components u, v and w satisfy the continuity equation.

TRIDIA and TRID2 are used to solve the system of algebraic equations having tri-diagonal matrix form, TRIDIA for j = 1 to n, and TRID2 for j = 2 to n.

After the pressure correction, the y and z momentum equations are calculated again using the corrected pressure. Then new pressure correction p' is calculated from new v's and w's. This is done for five iterations by using a under-relaxation parameter $\omega < 1$.

Finally, OUTPUT prints out the parameters, or calls PROFIL for printing u, v, w, t and p profiles.

```
C
C ***************************************************************
C *                                                             *
C *                        PROGRAM II                           *
C *                                                             *
C *     ********************************************           *
C *                                                             *
C *                                                             *
C *   THREE-DIMENSIONAL PROGRAM TO SOLVE THE 3-D JETS           *
C *                AND PLUME PROBLEMS                           *
C *                                                             *
C ***************************************************************
C
C     ADISC    :  .EQ. 1.0 READ INPUT FROM DISC
C                 .EQ. 0.0 READ INPUT FROM CARD
C     RY       :  HALF-WIDTH IN Y-DIRECTION
C     RZ       :  HALF-WIDTH IN Z-DIRECTION
C     VO       :  Y-COMPONENT VELOCITY
C     VE       :  V-VELOCITY AT EDGE
C     WE       :  W-VELOCITY AT EDGE
C     LORT     :  .GT. 0.0 FOR TURBULENT JET FLOW CASES
                  .LE. 0.0 FOR LAMINAR JET FLOW CASES
C     IEND     :  MAXIMUM NUMBER OF I STEPS TO BE COMPUTED IN
                   A RUN. THE CALCULATION WILL STOP AFTER I=IEND
C     IOUT     :  NUMBER OF I STEPS BETWEEN OUTPUTS
C     NYI      :  NUMBER OF GRID SPACES IN Y-DIRECTION INITIALLY
C     NZI      :  NUMBER OF GRID SPACES IN Z-DIRECTION INITIALLY
C     DENO     :  DENSITY OF FLUID AT DISCHARGE
C     DELTAY   :  JET HALF-WIDTH IN Y-DIRECTION AT I STATION
C     DELTAZ   :  JET HALF-WIDTH IN Z-DIRECTION AT I STATION
C     ANU      :  KINEMATIC VISCOSITY OF FLUID
C     M        :  A PARAMETER TO CONTROL THE OUTPUT
C     RCOE     :  THE MINIMUM PERCENTAGE OF JET VELOCITY USED
C                   AS EDGE VELOCITY IN QUIESCENT AMBIENT.
C     SCOE     :  COEFFICIENT TO GET STREAMWISE STEP SIZE
```

```
C
C       MAIN PROGRAM
C
        COMMON/A1/U(20,20),UP(20,20),V(20,20),VP(20,20),W(20,20)
       1,WP(20,20),T(20,20),TP(20,20),PPL(20,20),P(20,20),UE,UF,
       2TE,TF,VE,WE,LORT,USTART,AL1,AL2,BL1,BL2
        COMMON/A2/DELXP,DELY,DELZ,RY,RZ,DELTAY,DELTAZ,NJY,NKZ,
       1NYI,NZI,NJY1,NKZ1,INDP,TC1,TC2,JCORE,RCOE,XCONV,UCONV,
       2ECONV,PCONV
        COMMON/A3/ANU,PRT,HTK,DENO,CP,ALPHA,X,XO,YUHALF
        COMMON/A4/A(25),B(25),C(25),D(25),UVIN,I
        COMMON/A5/NY,NZ
        COMMON/A6/NZK,NYJ
        COMMON/A7/SCOE
C
C    .    .    .    .    .    .    .    .    .
C    READING IN THE INPUT DATA
C    .    .    .    .    .    .    .    .    .
C
        READ(5,1000) ADISC
 1000 FORMAT(F10.4)
        READ (5,1) LORT,IEND,IOUT,NYI,NZI,NJY,NKZ
    1   FORMAT(7I6)
        WRITE (6,2) IEND,IOUT,NYI,NZI,NJY,NKZ
    2   FORMAT (2X,'IEND =',I4,5X,'IOUT =',I3,5X,'NYI =',I3,5X,
       1'NZI =',I3,5X,'NJY =',I3,5X,'NKZ =',I3)
        READ(5,151) UVIN,OMEGA,ITEND
  151   FORMAT(2F10.5,I5)
        WRITE(6,21) UVIN,ITEND,OMEGA
   21   FORMAT(3X,'UVIN =',F10.5,5X,'ITEND =',I5,5X,'OMEGA =',
       1F10.5)
        READ (5,1051) SCOE
 1051 FORMAT(F10.5)
        WRITE(6,1052) SCOE
 1052 FORMAT(4X,'COEFFICIENT FOR STEP SIZE DELXP =',F10.5)
        READ (5,15) M
   15   FORMAT(I5)
        WRITE (6,16) M
   16   FORMAT(2X,'M =',I5)
        IF(ADISC .GE. 1.0) GO TO 2000
        READ(5,11) DENO,ANU,USTART,RY,RZ,TSTART,VO,PRT,UE,UF,TE,
       1TF,CP,HTK,VE,WE
   11   FORMAT(6G12.5)
        WRITE(6,12) DENO,ANU,USTART,RY,RZ,TSTART,VO,PRT,UE,UF,
       1TE,TF,CP,HTK,VE,WE
   12   FORMAT(2X,'DENO =',F12.5,5X,'ANU =',G12.5,5X,'USTART =',
       1F12.5,5X,'RY =',F12.5,5X,'RZ =',F12.5/3X,'TSTART =',
       2F12.5,5X,'VO =',F12.5,5X,'PRT =',F12.5,5X,'UE =',F12.5,
       35X,'UF =',F12.5/3X,'TE =',F12.5,5X,'TF =',F12.5,5X,'CP ='
       4,F12.5,5X,'HTK =',F12.5,5X,'VE =',F12.5,'WE =',F12.5)
```

```
      READ(5,17) RCOE
   17 FORMAT(F12.6)
      WRITE(6,18) RCOE
   18 FORMAT(2X,'RCOE =',F12.6)
      UE=USTART*RCOE
C
  128 R=UE/USTART
C
C   NON-DIMENSIONALIZING
C
C   CONVERSION FACTORS
C
   29 XCONV=ANU/USTART
      ECONV=ANU
      UCONV=USTART
      TC1=TE
      TC2=TSTART-TE
      GCI=32.174*144.0
      PCONV=USTART*USTART*DENO
C
C   VARIABLES
C
      TE1=(TE-TE)/TC2
      TF1=(TF-TE)/TC2
      TSTART=(TSTART-TE)/TC2
      TE=TE1
      TF=TF1
      RY=RY/XCONV
      RZ=RZ/XCONV
      NY=NYI+1
      NZ=NZI+1
C
C   Y-GRID AND Z-GRID SPACING
C
      DELY=RY/NYI
      DELZ=RZ/NZI
      UE=UE/UCONV
      UF=UF/UCONV
      USTART=USTART/UCONV
      ANU=ANU/ECONV
      ALPHA=(HTK/DENO/CP)/ECONV
C
C   STARTING PROFILES
C
C   ASSUMED UNIFORM PROFILE
C
      I=0.0
      X=0.0
C
      DO 25 J=1,NJY
```

```
      DO 25 K=1,NKZ
      P(J,K)=0.0
      PPL(J,K)=0.0
      U(J,K)=UE
      UP(J,K)=UE
      V(J,K)=0.0
      VP(J,K)=0.0
      W(J,K)=0.0
      WP(J,K)=0.0
      T(J,K)=TE
      TP(J,K)=TE
   25 CONTINUE
      DO 26 J=1,NY
      DO 26 K=1,NZ
      U(J,K)=1.0
      UP(J,K)=1.0
      T(J,K)=1.0
      TP(J,K)=1.0
   26 CONTINUE
      DELTAY=RY
      DELTAZ=RZ
      DELMIX=0.0
      IF(LORT .GT. 0.0) GO TO 54
      WRITE(6,58)
   58 FORMAT(/,10X,'LAMINAR JET CASE')
      AL1=2.0
      AL2=2.0
      BL1=2.0*ALPHA
      BL2=BL1
      GO TO 57
C
C   BEGINNING OF COMPUTATION LOOP
C
   54 WRITE (6,56)
   56 FORMAT(6X,'TURBULENT JET CASE')
   57 N=1
      KK=1
      IF(I .EQ. 0) YUHALF=DELTAY
      GO TO 67
C
C     READ IN INPUT DATA FROM DISC
C
 2000 CONTINUE
      READ(10) U,UP,V,VP,W,WP,T,TP,NY,NZ,XO,PPL,P,UE,UF,TE,TF,
     1VE,WE,LORT,USTART,AL1,AL2,BL1,BL2,DELXP,DELY,DELZ,RY,RZ,
     2DELTAY,DELTAZ,NJY,NKZ,NYI,NZI,NJY1,NKZ1,INDP,TC1,TC2,KK,
     3JCORE,RCOE,XCONV,UCONV,ECONV,PCONV,ANU,PRT,HTK,DENO,CP,
     4ALPHA,X,YUHALF,UVIN,I,NZK,NYJ,GCI,OMEGA,M
      CALL OUTPUT
   67 IF(U(1,1) .LT. USTART) GO TO 63
```

```
      GO TO 61
   63 IF(KK .EQ. 1) GO TO 77
      GO TO 61
   77 DIST=X*XCONV
      WRITE(6,62) DIST
   62 FORMAT(3X,'PREDICTED STARTING LENGTH =',G14.8)
      KK=KK+1
   61 CALL SDELX
      X=X+DELXP
      I=I+1
      IF(I .GT. 1) GO TO 141
      DELXM=DELXP
      NJY1=NJY-1
      NKZ1=NKZ-1
  141 CALL UVEL
      IF(I .EQ. 1) YUHALF=DELTAY
C
      ITER=0
      CALL VVELY
      CALL VVELZ
      CALL WVEL
C
C
C   PRESSURE CORRECTION--MAKE THE CORRECTION BEFORE PROCEEDING
C                TO THE NEXT STEP
C
C
  505 ITER=ITER+1
      DO 310 J=1,NJY
      DO 310 K=1,NKZ
  310 PPL(J,K)=0.0
      CALL PRESS
      DO 125 J=1,NYJ
      DO 125 K=1,NZK
      P(J,K)=P(J,K)+PPL(J,K)*OMEGA
  125 CONTINUE
      CALL VVELY
      CALL VVELZ
      CALL WVEL
      DO 162 K=1,NKZ
      DO 162 J=NY,NJY
  162 VP(J,K)=VP(NY,K)
      DO 164 J=1,NJY
      DO 164 K=NZ,NKZ
  164 WP(J,K)=WP(J,NZ)
      IF(UP(NY-1,NZ-1) .NE. UE) GO TO 1166
      VP(NY-1,NZ-1)=VP(NY,NZ-1)
      WP(NY-1,NZ-1)=WP(NY-1,NZ)
 1166 CONTINUE
      IF(ITER .LT. ITEND) GO TO 505
```

```
C
C    RESET THE BOUNDARY CONDITIONS FOR V AND W
C
      DO 160 J=1,NJY1
      VP(1,J)=0.0
 160  WP(J,1)=0.0
C
C    SOLVE TEMPERATURES
C
      CALL TEMP
      DO 60 J=1,NJY
      DO 60 K=1,NKZ
      U(J,K)=UP(J,K)
      V(J,K)=VP(J,K)
      W(J,K)=WP(J,K)
  60  T(J,K)=TP(J,K)
      REDELX=DELXP*XCONV
      WRITE(6,111) REDELX
 111  FORMAT(/,5X,'DELXP =',G14.7)
      IF(I .GT.  5) GO TO 55
      CALL OUTPUT
      GO TO 65
  55  II=IOUT*M
      IF(I .EQ. II) GO TO 122
      DIST=X*XCONV
      XBAR=X/RY/RY
      UCL=(U(1,1)-UE)/(USTART-UE)
      TCL=T(1,1)
      DDEY=DELTAY*XCONV
      RUHALF=YUHALF/RY
      WRITE (6,5200) I,DIST,XBAR,UCL,TCL,DDEY,RUHALF
 5200 FORMAT(5X,'I =',I4,5X,'X DISTANCE =',G12.5,5X,
     1'X VARIABLE =',G12.5/5X,'UCL =',G12.5,5X,'TCL =',G12.5,
     25X,'DELTAY =',G12.5,5X,'RUHALF =',G12.5)
      GO TO 68
 122  CALL OUTPUT
      M=M+1
  68  IF(NY .LE. 18) GO TO 65
      IN=0
      DO 5005 K=1,20,2
      IN=IN+1
      IM=0
      DO 5005 J=1,20,2
      IM=IM+1
      UP(IM,IN)=UP(J,K)
      U(IM,IN)=U(J,K)
      VP(IM,IN)=VP(J,K)
      V(IM,IN)=V(J,K)
      WP(IM,IN)=WP(J,K)
      W(IM,IN)=W(J,K)
```

```
      P(IM,IN)=P(J,K)
      TP(IM,IN)=TP(J,K)
      T(IM,IN)=T(J,K)
5005   CONTINUE
      DELY=DELY*2.0
      DELZ=DELZ*2.0
      NY=NY/2.0+1
      NZ=NZ/2.0+1
      NY2=NY+2
      NZ2=NZ+2
      NZ3=NZ+3
      DO 5006 K=1,NZ2
      DO 5006 J=NY2,NJY
      U(J,K)=UE
      UP(J,K)=UE
      V(J,K)=0.
      VP(J,K)=0.
      W(J,K)=0.
      WP(J,K)=0.
      P(J,K)=0.0
      T(J,K)=TE
      TP(J,K)=TE
5006  CONTINUE
      DO 5007 K=NZ3,NKZ
      DO 5007 J=1,NJY
      U(J,K)=UE
      UP(J,K)=UE
      V(J,K)=0.
      VP(J,K)=0.
      W(J,K)=0.
      WP(J,K)=0.
      P(J,K)=0.0
      T(J,K)=TE
      TP(J,K)=TE
5007  CONTINUE
  65   IF(I .LT. IEND) GO TO 67
       WRITE(11) U,UP,V,VP,W,WP,T,TP,NY,NZ,XO,PPL,P,UE,UF,TE,TF,
      1VE,WE,LORT,USTART,AL1,AL2,BL1,BL2,DELXP,DELY,DELZ,RY,RZ,
      2DELTAY,DELTAZ,NJY,NKZ,NYI,NZI,NJY1,NKZ1,INDP,TC1,TC2,KK,
      3JCORE,RCOE,XCONV,UCONV,ECONV,PCONV,ANU,PRT,HTK,DENO,CP,
      4ALPHA,X,YUHALF,UVIN,I,NZK,NYJ,GCI,OMEGA,M
       STOP
       END
```

```
      SUBROUTINE SDELX
      COMMON/A2/DELXP,DELY,DELZ,RY,RZ,DELTAY,DELTAZ,NJY,NKZ,
     1NYI,NZI,NJY1,NKZ1,INDP,TC1,TC2,JCORE,RCOE,XCONV,UCONV,
     2ECONV,PCONV
      COMMON/A7/SCOE
C
C     CALCULATE THE STREAMWISE STEP SIZE
C
      DELXP=SCOE*DELTAY
      RETURN
      END
```

```
      SUBROUTINE UVEL
      COMMON/A1/U(20,20),UP(20,20),V(20,20),VP(20,20),W(20,20)
     1,WP(20,20),T(20,20),TP(20,20),PPL(20,20),P(20,20),UE,UF,
     2TE,TF,VE,WE,LORT,USTART,AL1,AL2,BL1,BL2
      COMMON/A2/DELXP,DELY,DELZ,RY,RZ,DELTAY,DELTAZ,NJY,NKZ,
     1NYI,NZI,NJY1,NKZ1,INDP,TC1,TC2,JCORE,RCOE,XCONV,UCONV,
     2ECONV,PCONV
      COMMON/A3/ANU,PRT,HTK,DENO,CP,ALPHA,X,XO,YUHALF
      COMMON/A4/A(25),B(25),C(25),D(25),UVIN,I
      COMMON/A5/NY,NZ
      COMMON/A6/NZK,NYJ
      IIU=60
      IU=0
      NYJ=NY+2
      NZK=NZ+2
      UD=AL1/(2.0*DELY*DELY)
      UEE=AL1/(2.0*DELZ*DELZ)
300   IU=IU+1
      DO 210 K=1,NZK
      KJ=K
      DO 210 J=KJ,NYJ
      UA=U(J,K)/DELXP
      UB=V(J,K)/(2.0*DELY)
      UC=W(J,K)/(2.0*DELZ)
      CA=UA+2.0*UD+2.0*UEE
      C1=(UD-UB)/CA
      C2=(UD+UB)/CA
      C3=(UEE-UC)/CA
      C4=(UEE+UC)/CA
      C5=UA*U(J,K)/CA
      IF(K .EQ. 1) GO TO 282
      IF(J .NE. KJ) GO TO 260
      UP(J,K+1)=UP(J+1,K)
      UP(J-1,K)=UP(J,K-1)
260   UP(J,K)=C1*UP(J+1,K)+C2*UP(J-1,K)+C3*UP(J,K+1)+C4*UP(J,
     1K-1)+C5
      GO TO 210
282   IF(J .EQ. 1) GO TO 235
      UP(J,K)=C1*UP(J+1,K)+C2*UP(J-1,K)+(C3+C4)*UP(J,2)+C5
      GO TO 210
235   UP(1,1)=(C1+C2+C3+C4)*UP(2,1)+C5
210   CONTINUE
      UX=UP(NY,NZ)
      IF(IU .LT. 5) GO TO 280
      IF(IU .GT. IIU) GO TO 110
      IF(UX .EQ. 0.0) GO TO 300
      IF(ABS((UEND-UX)/UX) .LE. 0.0001) GO TO 110
280   UEND=UP(NY,NZ)
      GO TO 300
110   WRITE(6,216) IU
```

```
 216  FORMAT(3X,'IU =',I4)
      DO 310 K=2,NZK
      KJ=K-1
      DO 310 J=1,KJ
      UP(J,K)=UP(K,J)
 310  CONTINUE
C
C   CALCULATE YUHALF
      UPMEAN=(UP(1,1)+UE)/2.0
      DO 360 J=1,NJY
      IF(UP(J,1) .LE. UPMEAN) GO TO 42
 360  CONTINUE
  42  JJ=J
      JM=J-1
      YUHALF=JM*DELY+DELY*(UPMEAN-UP(JM,1))/(UP(JJ,1)-UP(JM,1))
      DO 361 J=1,NJY
      IF(UP(J,1) .LT. USTART) GO TO 24
 361  CONTINUE
  24  YCORE=(J-1)*DELY
      JCORE=J
C
C     CALCULATING JET HALF-WIDTH
C
      DO 90 J=1,NJY
      UTEST=(UP(1,1)-UP(J,1))/(UP(1,1)-UE)
      IF(UTEST .GE. UVIN) GO TO 27
  90  CONTINUE
  27  DELTAY=(J-1)*DELY
      NY=J
      NZ=J
C
C     RESET THE BOUNDARY CONDITIONS AT THE EDGE
C
      DO 601 K=1,NZK
      IF(UP(1,K) .LE. UE) GO TO 601
      DO 602 J=1,NYJ
      UTEST=(UP(1,K)-UP(J,K))/(UP(1,K)-UE)
      IF(UTEST .GE. UVIN) GO TO 627
 602  CONTINUE
 627  JB=J
      DO 605 J=JB,NYJ
 605  UP(J,K)=UE
 601  CONTINUE
      DO 608 K=2,NZK
      KJ=K-1
      DO 608 J=1,KJ
      UP(J,K)=UP(K,J)
 608  CONTINUE
 140  RETURN
      END
```

```
      SUBROUTINE  VVELY
      COMMON/A1/U(20,20),UP(20,20),V(20,20),VP(20,20),W(20,20)
     1,WP(20,20),T(20,20),TP(20,20),PPL(20,20),P(20,20),UE,UF,
     2TE,TF,VE,WE,LORT,USTART,AL1,AL2,BL1,BL2
      COMMON/A2/DELXP,DELY,DELZ,RY,RZ,DELTAY,DELTAZ,NJY,NKZ,
     1NYI,NZI,NJY1,NKZ1,INDP,TC1,TC2,JCORE,RCOE,XCONV,UCONV,
     2ECONV,PCONV
      COMMON/A3/ANU,PRT,HTK,DENO,CP,ALPHA,X,XO,YUHALF
      COMMON/A4/A(25),B(25),C(25),D(25),UVIN,I
      COMMON/A5/NY,NZ
      COMMON/A6/NZK,NYJ
      NYJ=NY
      NZK=NZ
      DO 15 K=1,NZK
      DO 5 J=2,NYJ
      IF(UP(J,K) .EQ. USTART) GO TO 55
25    UA=UP(J,K)/DELXP
      UB1=2.0*DELY*DELY
      UB=AL1/UB1
      UC=AL2/UB1
      UD=VP(J,K)/(2.0*DELY)
      B(J)=-UD-UC
      D(J)=UA+UB+UC
      A(J)=UD-UB
      DPDY=(P(J,K)-P(J-1,K))/DELY
      STAB=ABS(VP(J,K)*DELY/ANU)
      IF(STAB .LT. 2.0) GO TO 86
      IF(VP(J,K)  .GT. 0.0) GO TO 84
      B(J)=-UC
      D(J)=UA+UB+UC-2.0*UD
      A(J)=2.0*UD-UB
      GO TO 86
84    B(J)=-2.0*UD-UC
      D(J)=UA+UB+UC+2.0*UD
      A(J)=-UB
86    CONTINUE
      IF(K .NE. 1) GO TO 70
      C(J)=UA*V(J,1)-DPDY+AL1*(VP(J,2)-VP(J,1))/DELZ/DELZ
      GO TO 5
70    C(J)=UA*V(J,K)-WP(J,K)*(VP(J,K+1)-VP(J,K-1))/(2.0*DELZ)
     1+(AL1*(VP(J,K+1)-VP(J,K))-AL2*(VP(J,K)-VP(J,K-1)))/(2.*
     2DELZ*DELZ)-DPDY
      GO TO 5
55    B(J)=0.0
      D(J)=1.0
      A(J)=0.0
      C(J)=0.0
5     CONTINUE
      B(NYJ)=-UB-UC
      D(NYJ)=UP(NYJ,K)/DELXP+UB+UC
```

```
      CALL TRID2(A,B,C,D,NYJ)
      DO 52 J=2,NYJ
   52 VP(J,K)=C(J)
   15 CONTINUE
      DO 80 K=1,NKZ
      VP(K,NZ)=0.0
      VP(K,NZ+1)=0.0
      DO 80 J=NY,NJY
   80 VP(J,K)=VP(NY,K)
      RETURN
      END
```

```
      SUBROUTINE  VVELZ
      COMMON/A1/U(20,20),UP(20,20),V(20,20),VP(20,20),W(20,20)
     1,WP(20,20),T(20,20),TP(20,20),PPL(20,20),P(20,20),UE,UF,
     2TE,TF,VE,WE,LORT,USTART,AL1,AL2,BL1,BL2
      COMMON/A2/DELXP,DELY,DELZ,RY,RZ,DELTAY,DELTAZ,NJY,NKZ,
     1NYI,NZI,NJY1,NKZ1,INDP,TC1,TC2,JCORE,RCOE,XCONV,UCONV,
     2ECONV,PCONV
      COMMON/A3/ANU,PRT,HTK,DENO,CP,ALPHA,X,XO,YUHALF
      COMMON/A4/A(25),B(25),C(25),D(25),UVIN,I
      COMMON/AS/NY,NZ
      COMMON/A6/NZK,NYJ
      DO 15 J=2,NYJ
      DO 5 K=1,NZK
      IF(UP(J,K) .EQ. USTART) GO TO 56
25    UA=UP(J,K)/DELXP
      UBZ=2.0*DELZ*DELZ
      UB=AL1/UBZ
      UC=AL2/UBZ
      UD=WP(J,K)/(2.0*DELZ)
      B(K)=-UD-UC
      D(K)=UA+UB+UC
      A(K)=UD-UB
      DPDY=(P(J,K)-P(J-1,K))/DELY
      STAB=ABS(WP(J,K)*DELZ/ANU)
      IF(STAB .LT. 2.0) GO TO 86
      IF(WP(J,K)  .GT. 0.0) GO TO 84
      B(K)=-UC
      D(K)=UA+UB+UC-2.0*UD
      A(K)=2.0*UD-UB
      GO TO 86
84    B(K)=-2.0*UD-UC
      D(K)=UA+UB+UC+2.0*UD
      A(K)=-UB
86    CONTINUE
      IF(J .GE. NYJ) GO TO 55
      C(K)=UA*V(J,K)-VP(J,K)*(VP(J+1,K)-VP(J-1,K))/(2.*DELY)+
     1(AL1*(VP(J+1,K)-VP(J,K))-AL2*(VP(J,K)-VP(J-1,K)))/(2.0*
     2DELY*DELY)-DPDY
      GO TO 5
55    C(K)=UA*V(J,K)-DPDY
      GO TO 5
56    B(K)=0.0
      D(K)=1.0
      A(K)=0.0
      C(K)=0.0
5     CONTINUE
      IF(UP(J,1) .EQ. USTART) GO TO 60
      A(1)=-UB-UC
      D(1)=U(J,1)/DELXP+UB+UC
      B(1)=0.0
```

```
60  CONTINUE
    CALL TRIDIA(A,B,C,D,NZK)
    DO 52 K=1,NZK
52  VP(J,K)=C(K)
15  CONTINUE
    DO 80 K=1,NKZ
    VP(K,NZ)=0.0
    VP(K,NZ+1)=0.0
    DO 80 J=NY,NJY
80  VP(J,K)=VP(NY,K)
    RETURN
    END
```

```
      SUBROUTINE WVEL
      COMMON/A1/U(20,20),UP(20,20),V(20,20),VP(20,20),W(20,20)
     1,WP(20,20),T(20,20),TP(20,20),PPL(20,20),P(20,20),UE,UF,
     2TE,TF,VE,WE,LORT,USTART,AL1,AL2,BL1,BL2
      COMMON/A2/DELXP,DELY,DELZ,RY,RZ,DELTAY,DELTAZ,NJY,NKZ,
     1NYI,NZI,NJY1,NKZ1,INDP,TC1,TC2,JCORE,RCOE,XCONV,UCONV,
     2ECONV,PCONV
      COMMON/A3/ANU,PRT,HTK,DENO,CP,ALPHA,X,XO,YUHALF
      COMMON/A4/A(25),B(25),C(25),D(25),UVIN,I
      COMMON/A5/NY,NZ
      COMMON/A6/NZK,NYJ
      DO 100 K=1,NZK
      DO 100 J=1,NYJ
      WP(J,K)=VP(K,J)
100   CONTINUE
      RETURN
      END
```

```
      SUBROUTINE PRESS
      COMMON/A1/U(20,20),UP(20,20),V(20,20),VP(20,20),W(20,20)
     1,WP(20,20),T(20,20),TP(20,20),PPL(20,20),P(20,20),UE,UF,
     2TE,TF,VE,WE,LORT,USTART,AL1,AL2,BL1,BL2
      COMMON/A2/DELXP,DELY,DELZ,RY,RZ,DELTAY,DELTAZ,NJY,NKZ,
     1NYI,NZI,NJY1,NKZ1,INDP,TC1,TC2,JCORE,RCOE,XCONV,UCONV,
     2ECONV,PCONV
      COMMON/A3/ANU,PRT,HTK,DENO,CP,ALPHA,X,XO,YUHALF
      COMMON/A4/A(25),B(25),C(25),D(25),UVIN,I
      COMMON/A5/NY,NZ
      COMMON/A6/NZK,NYJ
C
C   PRESSURE CORRECTION
C
      IIP=150
      IP=0
      C1=1.0/DELY/DELY
      C2=1.0/DELZ/DELZ
      C3=2.0*(C1+C2)
      PC1=C1/C3
      PC2=C2/C3
      NY1=NY-1
      NZ1=NZ-1
      PB1=C1+2.0*C2
  100 IP=IP+1
      DO 15 K=1,NZ1
      IPC2=1
      KJ=K
      DO 10 J=KJ,NY1
      IF(UP(J,K) .EQ. USTART) GO TO 10
      CON=-((UP(J,K)-U(J,K))/DELXP+(VP(J+1,K)-VP(J,K))/DELY+
     1(WP(J,K+1)-WP(J,K))/DELZ)*XCONV/UCONV
      IF(UP(KJ,KJ) .LT. USTART) GO TO 25
      IF(IPC2 .GT. 1) GO TO 25
      IPC=J
      IPC2=2
   25 IF(J .EQ. IPC) GO TO 38
      IF(K .EQ. 1) GO TO 82
      IF(J .NE. KJ) GO TO 111
      PPL(J,K+1)=PPL(J+1,K)
      PPL(J-1,K)=PPL(J,K-1)
  111 CONTINUE
      PPL(J,K)=PC1*(PPL(J+1,K)+PPL(J-1,K))+PC2*(PPL(J,K+1)+PPL
     1(J,K-1))+CON/C3
      GO TO 10
   82 PPL(J,1)=PC1*(PPL(J+1,1)+PPL(J-1,1))+2.0*PC2*PPL(J,2)+
     1CON/C3
      GO TO 10
   38 IF(K .EQ. 1) GO TO 30
      IF(KJ .EQ. IPC) GO TO 85
```

```
      PPL(J,K)=C1/PB1*PPL(J+1,K)+C2/PB1*(PPL(J,K+1)+PPL(J,
     1K-1))+CON/PB1
      GO TO 10
   30 PPL(J,1)=C1/PB1*PPL(J+1,1)+2.0*C2/PB1*PPL(J,2)+CON/PB1
      GO TO 10
   85 PPL(J,K)=(PPL(J+1,K)+PPL(J,K-1))/2.0+CON/C3
   10 CONTINUE
      IF(UP(KJ,KJ) .LT. USTART) GO TO 15
      IPC1=IPC-1
      DO 310 J=KJ,IPC1
  310 PPL(J,K)=PPL(IPC,K)
   15 CONTINUE
      PX=PPL(NY1,NZ1)
      IF(IP .EQ. 1) GO TO 60
      IF(IP .GT. IIP) GO TO 110
      IF(PX .EQ. 0.0) GO TO 100
      IF(ABS((PEND-PX)/PX) .LE. 0.0001) GO TO 110
   60 PEND=PX
      GO TO 100
  110 WRITE(6,16) IP,PX
   16 FORMAT(3X,'ITERATION NO =',I5,5X,'PPL(NY1,NZ1) =',G15.5)
      DO 320 K=2,NZ1
      KJ=K-1
      DO 320 J=1,KJ
  320 PPL(J,K)=PPL(K,J)
      RETURN
      END
```

```
      SUBROUTINE TRIDIA (A,B,C,D,N)
      DIMENSION A(1),B(1),C(1),D(1)
      DO 10 I=2,N
      P=B(I)/D(I-1)
      D(I)= D(I)-P*A(I-1)
   10 C(I)=C(I)-P*C(I-1)
C  BACK SUBSTITUTION
      C(N)=C(N)/D(N)
      DO 20 I=2,N
      J=N-I+1
   20 C(J)=(C(J)-A(J)*C(J+1))/D(J)
      RETURN
      END
```

```
      SUBROUTINE TRID2 (A,B,C,D,N)
      DIMENSION A(1),B(1),C(1),D(1)
      DO 10 I=3,N
      P=B(I)/D(I-1)
      D(I)=D(I)-P*A(I-1)
   10 C(I)=C(I)-P*C(I-1)
C    BACK SUBSTITUTION
      C(N)=C(N)/D(N)
      N1=N-1
      DO 20 I=2,N1
      J=N-I+1
   20 C(J)=(C(J)-A(J)*C(J+1))/D(J)
      RETURN
      END
```

```
      SUBROUTINE TEMP
      COMMON/A1/U(20,20),UP(20,20),V(20,20),VP(20,20),W(20,20)
     1,WP(20,20),T(20,20),TP(20,20),PPL(20,20),P(20,20),UE,UF,
     2TE,TF,VE,WE,LORT,USTART,AL1,AL2,BL1,BL2
      COMMON/A2/DELXP,DELY,DELZ,RY,RZ,DELTAY,DELTAZ,NJY,NKZ,
     1NYI,NZI,NJY1,NKZ1,INDP,TC1,TC2,JCORE,RCOE,XCONV,UCONV,
     2ECONV,PCONV
      COMMON/A3/ANU,PRT,HTK,DENO,CP,ALPHA,X,XO,YUHALF
      COMMON/A4/A(25),B(25),C(25),D(25),UVIN,I
      COMMON/A5/NY,NZ
      COMMON/A6/NZK,NYJ
      IIT=60
      IT=0
      TD=BL1/(2.0*DELY*DELY)
      TEE=BL1/(2.0*DELZ*DELZ)
300   IT=IT+1
      DO 210 K=1,NZK
      KJ=K
      DO 210 J=KJ,NYJ
      TA=U(J,K)/DELXP
      TB=V(J,K)/(2.0*DELY)
      TC=W(J,K)/(2.0*DELZ)
      CA=TA+2.0*TD+2.0*TEE
      C1=(TD-TB)/CA
      C2=(TD+TB)/CA
      C3=(TEE-TC)/CA
      C4=(TEE+TC)/CA
      C5=TA*T(J,K)/CA
      IF(K .EQ. 1) GO TO 282
      IF(J .NE. KJ) GO TO 260
      TP(J,K+1)=TP(J+1,K)
      TP(J-1,K)=TP(J,K-1)
260   TP(J,K)=C1*TP(J+1,K)+C2*TP(J-1,K)+C3*TP(J,K+1)+C4*TP(J,
     1K-1)+C5
      GO TO 210
282   IF(J .EQ. 1) GO TO 235
      TP(J,K)=C1*TP(J+1,K)+C2*TP(J-1,K)+(C3+C4)*TP(J,2)+C5
      GO TO 210
235   TP(1,1)=(C1+C2+C3+C4)*TP(2,1)+C5
210   CONTINUE
      TX=TP(NY,NZ)
      IF(IT .LT. 5) GO TO 280
      IF(IT .GT. IIT) GO TO 110
      IF(TX .EQ. 0.0) GO TO 300
      IF(ABS((TEND-TX)/TX) .LE. 0.0001) GO TO 110
280   TEND=TP(NY,NZ)
      GO TO 300
110   WRITE(6,216) IT
216   FORMAT(3X,'IT =',I4)
      DO 310 K=2,NZK
```

```
      KJ=K-1
      DO 310 J=1,KJ
      TP(J,K)=TP(K,J)
310   CONTINUE
      DO 601 K=1,NZK
      IF(TP(1,K) .LE. TE) GO TO 601
      DO 602 J=1,NYJ
      TTEST=(TP(1,K)-TP(J,K))/(TP(1,K)-TE)
      IF(TTEST .GE. UVIN) GO TO 627
602   CONTINUE
627   JB=J
      DO 605 J=JB,NYJ
605   TP(J,K)=TE
601   CONTINUE
      DO 608 K=2,NZK
      KJ=K-1
      DO 608 J=1,KJ
      TP(J,K)=TP(K,J)
608   CONTINUE
      RETURN
      END
```

```
      SUBROUTINE OUTPUT
      COMMON/A1/U(20,20),UP(20,20),V(20,20),VP(20,20),W(20,20)
     1,WP(20,20),T(20,20),TP(20,20),PPL(20,20),P(20,20),UE,UF,
     2TE,TF,VE,WE,LORT,USTART,AL1,AL2,BL1,BL2
      COMMON/A2/DELXP,DELY,DELZ,RY,RZ,DELTAY,DELTAZ,NJY,NKZ,
     1NYI,NZI,NJY1,NKZ1,INDP,TC1,TC2,JCORE,RCOE,XCONV,UCONV,
     2ECONV,PCONV
      COMMON/A3/ANU,PRT,HTK,DENO,CP,ALPHA,X,XO,YUHALF
      COMMON/A4/A(25),B(25),C(25),D(25),UVIN,I
      COMMON/A5/NY,NZ
      COMMON/A6/NZK,NYJ
      DIMENSION CO(25)
      WRITE (6,10)
   10 FORMAT('0')
      DIST=X*XCONV
      XBAR=X/RY/RY
      UCL=(U(1,1)-UE)/(USTART-UE)
      TCL=T(1,1)
      DDEY=DELTAY*XCONV
      DDEZ=DELTAZ*XCONV
      RUHALF=YUHALF/RY
      WRITE (6,5200) I,DIST,XBAR,UCL,TCL,DDEY,RUHALF
 5200 FORMAT(5X,'I =',I4,5X,'X DISTANCE =',G12.5,5X,
     1'X VARIABLE =',G12.5/5X,'UCL =',G12.5,5X,'TCL =',G12.5,
     25X,'DELTAY =',G12.5,5X,'RUHALF =',G12.5)
      INPRO=1
      WRITE (6,25)
   25 FORMAT(///,2X,'U VELOCITY',3X,'(FT/SEC)',/)
      CALL PROFIL(UP,INPRO)
      WRITE (6,26)
   26 FORMAT(///,2X,'V VELOCITY',3X,'(FT/SEC)',/)
      CALL PROFIL(VP,INPRO)
      WRITE (6,27)
   27 FORMAT(///,2X,'W VELOCITY',3X,'(FT/SEC)',/)
      CALL PROFIL(WP,INPRO)
      INPRO=2
      WRITE (6,28)
   28 FORMAT(///,2X,'TEMPERATURE',3X,'(DEGREE F)',/)
      CALL PROFIL(TP,INPRO)
      INPRO=3
      WRITE(6,29)
   29 FORMAT(///,2X,'PRESSURE',3X,'(PSI)',/)
      CALL PROFIL(P,INPRO)
      WRITE(6,30)
   30 FORMAT(///,2X,'P  PL.',3X,'(PSI)',/)
      CALL PROFIL(PPL,INPRO)
      WRITE(6,32)
   32 FORMAT(///,2X,'SOURCE TERM ')
      DO 178 KK=1,NZK
      K=NZK-KK+1
```

```
      DO 176 J=1,NYJ
      CO(J)=((UP(J,K)-U(J,K))/DELXP+(VP(J+1,K)-VP(J,K))/DELY
     1+(WP(J,K+1)-WP(J,K))/DELZ)*UCONV/XCONV
176   CONTINUE
178   WRITE(6,167) (CO(J),J=1,NYJ)
167   FORMAT(10(1X,G11.4))
      RETURN
      END
```

```
      SUBROUTINE PROFIL (DXX,INPRO)
      COMMON/A1/U(20,20),UP(20,20),V(20,20),VP(20,20),W(20,20)
     1,WP(20,20),T(20,20),TP(20,20),PPL(20,20),P(20,20),UE,UF,
     2TE,TF,VE,WE,LORT,USTART,AL1,AL2,BL1,BL2
      COMMON/A2/DELXP,DELY,DELZ,RY,RZ,DELTAY,DELTAZ,NJY,NKZ,
     1NYI,NZI,NJY1,NKZ1,INDP,TC1,TC2,JCORE,RCOE,XCONV,UCONV,
     2ECONV,PCONV
      COMMON/A3/ANU,PRT,HTK,DENO,CP,ALPHA,X,XO,YUHALF
      COMMON/A4/A(25),B(25),C(25),D(25),UVIN,I
      COMMON/A5/NY,NZ
      COMMON/A6/NZK,NYJ
      DIMENSION DX(20,20),DXX(20,20)
      IF(INPRO .EQ. 2) GO TO 10
      IF(INPRO .EQ. 3) GO TO 20
      DO 40 K=1,NZK
      DO 40 J=1,NYJ
   40 DX(J,K)=DXX(J,K)*UCONV
      GO TO 100
   20 DO 45 K=1,NZK
      DO 45 J=1,NYJ
   45 DX(J,K)=DXX(J,K)*PCONV/32.174/144.0
      GO TO 100
   10 DO 50 K=1,NZK
      DO 50 J=1,NYJ
   50 DX(J,K)=DXX(J,K)*TC2+TC1
  100 DO 60 K=1,NZK
      KR=NZK-K+1
   60 WRITE(6,30) (DX(J,KR),J=1,NYJ)
   30 FORMAT(10(1X,G11.4))
      RETURN
      END
```